A PRELIMINARY STUDY OF $\delta^{18}O_{carb}$ AND $\delta^{13}C_{carb}$ IN *ODOCOILEUS VIRGINIANUS* TOOTH ENAMEL: PALEOCLIMATE AND DIET RECONSTRUCTION IN THE LOWER CHATTAHOOCHEE RIVER VALLEY AT THE ONSET OF THE LITTLE ICE AGE

By ALEXANDRA BONHAM

(Under the Direction of Suzanne Pilaar Birch)

ABSTRACT

Enamel $\delta^{18}O_{carb}$ and $\delta^{13}C_{carb}$ from white-tailed deer (*O. virginianus*) remain under-utilized in paleoenvironmental reconstructions despite their ubiquity in North American archaeological contexts. Paired M2 and M3 molars excavated from two midden contexts at Singer-Moye, a Mississippian Period site in the Lower Chattahoochee River Valley (LCRV) of Georgia, chronicle sub-annual variation of climate and deer diet at the onset of the Little Ice Age (LIA; 1300 – 1400 CE). Serially sampled enamel $\delta^{18}O$carb from Georgia deer reflect seasonality. Enamel $\delta^{13}C_{carb}$ elucidates maize abundance, a primary crop throughout the Mississippian Period. Results of nine modern and three archaeological serially sampled M2, M3 pairs reveal a positive mean $\delta^{18}O$ excursion (+ 3.9 ‰) between 1300 – 1400 C.E., suggesting an anomalously warm Atlantic Coastal Plain at the onset of the LIA. Mean $\delta^{13}C$ (~ -15 ‰) across both groups indicate C3 diets, though outliers suggest interaction with anthropogenic food sources in the modern deer.

INDEX WORDS: White-Tailed Deer, $\delta^{18}O_{carb}$, $\delta^{13}C_{carb}$, Paleoclimate, Georgia, Enamel, Seasonality, Little Ice Age, Mississippian

A PRELIMINARY STUDY OF $\delta^{18}O_{carb}$ AND $\delta^{13}C_{carb}$ IN *ODOCOILEUS VIRGINIANUS* TOOTH ENAMEL: PALEOCLIMATE AND DIET RECONSTRUCTION IN THE LOWER CHATTAHOOCHEE RIVER VALLEY AT THE ONSET OF THE LITTLE ICE AGE

by

ALEXANDRA BONHAM

B.S., Dalhousie University, Halifax, Canada, 2020

A Thesis Submitted to the Graduate Faculty of The University of Georgia in Partial Fulfillment of the Requirements for the Degree

MASTER OF SCIENCE

ATHENS, GEORGIA 2023

A PRELIMINARY STUDY OF $\delta^{18}O_{carb}$ AND $\delta^{13}C_{carb}$ IN *ODOCOILEUS VIRGINIANUS* TOOTH ENAMEL: PALEOCLIMATE AND DIET RECONSTRUCTION IN THE LOWER CHATTAHOOCHEE RIVER VALLEY AT THE ONSET OF THE LITTLE ICE

by

ALEXANDRA BONHAM

Major Professor: Suzanne Pilaar Birch

Committee: Ervan Garrison

David Patterson

Electronic Version Approved:

Ron Walcott

Vice Provost for Graduate Education and Dean of the Graduate School The University of Georgia

August 2023

DEDICATION

This work is dedicated to Sean Hartery, my partner, who was a source of limitless support and immeasurable love. Just as appreciably, this work is dedicated to all my friends from all the places I've ever called home. I am so grateful to be known by such a community – especially my maritimers. I carry you all with me everywhere I go. I also dedicate this work to my family, Mom, Dad, and Cayman – who fostered my love of science from an early age. Last, but not least, this thesis is dedicated to the deer whose teeth I used for science.

ACKNOWLEDGEMENTS

I would like to express the deepest appreciation to Dr. Suzie Pilaar Birch. Under Dr. Pilaar Birch's mentorship, my passion for research was reignited. Thank you to Dr. David Patterson for providing thoughtful feedback and discussions that significantly guided this research. Many thanks to Dr. Ervan Garrison for his expertise and support. I am enormously fortunate to have had such a wonderful committee whose supervision made this thesis possible.

I'd like to thank Dr. Amanda Thompson for providing ample support at the UGA Laboratory of Archaeology. Her kindness and willingness to help me find archaeological specimens went above and beyond. Thank you to RaeLynn A. Butler and the Historic and Cultural Preservation Department of the Muscogee Nation who approved my research proposal and allowed me to work with Muscogee zooarchaeological material. I extend my utmost appreciation.

I owe a debt of gratitude Jennifer Markett at Flint's Wild Game Processing in Fort Gaines, Georgia, who happily provided me with nine modern deer jaws upon request. This thesis would not have come into fruition without the addition of the modern samples; Thank you Flint's!

Thank you to the UGA Geology Department who provided me financial support through the Miriam Watts-Wheeler Fund and to Geological Society of America who provided travel funding to present this research. Special mention to Marjie, Laura, Lea, and Cade who kept me grounded, provided lightness and above all else, solidarity. Lastly, thank you to my cats - Briar, Pebble and Pangea, who kept me company during all those late nights in the office.

TABLE OF CONTENTS

LIST OF FIGURES

LIST OF TABLES

CHAPTER 1

INTRODUCTION

During the Mississippian Period (1000 – 1600 C.E.), Native Americans of the southeastern United States (US) constructed prominent earthen mounds, adorning river valleys. The mounds were often accompanied by plazas and served as significant cultural centers of Chiefdoms that prospered in the American southeast (Birch and Brannan 2016a). Their residents, broadly referred to as the Mississippians, were agriculturists who modified the landscape into a 'mosaic' of farm fields and gardens (Bowne, 2013; Pompeani et al., 2021; Scarry & Scarry, 2005; Willoughby, 2012). Though Mississippian settlements sustained large populations and flourished for centuries, many of the mound sites were significantly diminished in usage or completely abandoned by 1450 C.E., before European contact (Cobb and Butler, 2002; Willoughby, 2012; Meeks and Anderson, 2013). The drastic regional site abandonment coincides with the Little Ice Age (LIA; 1300 – 1850 C.E.), an interval of high climatic volatility that had resounding impacts on agriculturalist societies dependent on yearly crops (Williams, 1980). However, the timing of onset and effects of the LIA are not well understood, particularly in the context of continental, mid-latitude regions. A paucity of high-resolution paleoclimate proxies in the southeastern US compounds the difficulties in unraveling settlement histories at the end of the Mississippian Period. High-resolution paleoclimate reconstructions that capture the localized climate, of which there are few, are needed to resolve these questions (Cobb & Butler, 2002)

The paucity of high-resolution proxies for the Little Ice Age (LIA), especially records from low-latitude terrestrial sources, poses a significant challenge in climate models and reconstructions (Mayewski et al., 2004). The abandonment of Mississippian settlements coincides with the significant global cooling of the Little Ice Age (Bowne, 2013; Pompeani et al., 2021), yet, lower surface temperatures are not a regionally uniform trend (Mann et al., 2009). The onset and duration of the LIA are mainly constrained via marine sediment records and glacial proxies from high latitudes (Nesje & Dahl, 2003). It is not accurate to assume the degree and timing of cooling observed in Northern Europe and the North Atlantic presented similarly in the southeastern United States. Of the few high-resolution proxy records available in the SE US, fundamental disagreements persist regarding the onset and climate effects of the Little Ice Age (Nesje and Dahl, 2002). Speleothem records from Alabama indicate an increase in summer precipitation (Medina et al., 2022), whereas tree-ring records do not observe any centennial patterns of increased spring precipitation in the Southeast (Stahle and Cleaveland, 1994). A lake core from the largest Mississippian settlement, Cahokia, reveals a decrease in effective moisture and subsequent drying between 1200 – 1400 CE. Currently, the exact nature of seasonality and climate during the LIA in the Southeast remains unclear. It is thus challenging to determine the histories and relationship of Mississippian site abandonment without detailed proxy records from mid-latitude, terrestrial sources in the interior southeastern US.

Oxygen and carbon stable isotopes in mammalian, herbivore tooth enamel are established proxies for high-resolution climate and environmental reconstruction (Ben-David & Flaherty, 2012). Oxygen isotopes are present in the environmental waters. Physical processes such as evaporation, precipitation, and fractionation dictate their ratios ($\delta^{18}O$; Bowen & Wilkinson, 2002). Oxygen from meteoric sources are up taken by vegetation in the environment that then responds

to evapotranspiration. Herbivores that ingest water primarily through broad-leafed vegetation, convey changes in precipitation amount, humidity gradient, and temperature (Cormie & Schwarcz, 1994). Carbon isotopes ($\delta^{13}C$) originate in the environment's flora and fauna and can be used to reconstruct their diet (Koch et al., 1994). $\delta^{13}C$ values reflect the proportion of plants ingested with either C_3 or C_4 photosynthesis pathways (Cormie & Schwarcz, 1994; Harrison & Katzenberg, 2003). In proximity to Mississippian chiefdoms of the Southeast, a majority of vegetation is C_3 with the exception of maize and grasses (Rivera-Araya & Pilaar Birch, 2018). Thus, $\delta^{13}C$ values in herbivore tooth enamel can illuminate maize availability and consumption. Tooth enamel archives sub-annual variation in $\delta^{18}O$ and $\delta^{13}C$ amounts across the period of tooth formation (Morris, 2015). When serially sampled perpendicular to the growth axis of the tooth, these values can be interpreted as a time series.

White-tailed deer are ubiquitous herbivores in the southern and eastern US and were a primary resource for the Mississippian Peoples (Bowne, 2013; Willoughby, 2012). In the Lower Chattahoochee River Valley of Georgia, Mississippian mound sites host dense middens containing preserved molar pairs of white-tailed deer (Brannan and Birch, 2017). Despite their concentration in North American archaeological contexts, white-tailed deer (*Odocoileus virginianus*) tooth enamel remains under-utilized as a proxy in paleoclimate and paleoenvironmental reconstructions.

This thesis seeks to reveal seasonality, climate and maize availability at the onset of the Little Ice Age in the Southeast using $\delta^{18}O$ and $\delta^{13}C$ of white-tailed deer enamel (*Odocoileus virginianus;* herein synonymous with 'deer'). The Lower Chattahoochee River Valley was chosen as the area of focus for this research because of its high density of Mississippian sites inhabited at the onset of the LIA. In addition, this thesis will add to a growing body of literature on white-tailed deer enamel in Georgia. To date, there are four published studies on stable isotopes in deer enamel.

Two of these are concerned with modern populations from Georgia (Malasek et al., 2023; Rivera-Araya & Pilaar Birch, 2018). Two additional studies have successfully applied deer enamel $\delta^{18}O$ and $\delta^{13}C$ analyses to zooarchaeological contexts for the late Prehistoric Period outside of Georgia (Morris, 2015; Rivera-Araya et al., 2019). In this study, I add to the breadth of Georgia deer enamel studies by examining $\delta^{18}O$ and $\delta^{13}C$ in modern and archaeological populations from a defined micro-region (LCRV). In this thesis, I validate $\delta^{18}O$ and $\delta^{13}C$ values from modern deer against available climate data of the region for insights into archaeological enamel $\delta^{18}O$ and $\delta^{13}C$ values from the onset of the Little Ice Age.

1.1 Research Objectives

This thesis uses two sample groups of deer, modern and archaeological, from the LCRV to elucidate climate and seasonality, as well as maize availability, at the onset of the LIA. Modern deer teeth were obtained from a deer processor within the LCRV. Archaeological teeth are from middens at a nearby Mississippian mound site, Singer-Moye. When referenced in text, samples from Singer-Moye mound site are shortened to 'archaeological'.

I first look to validate the relationships between modern climate variables against $\delta^{18}O$ from modern deer enamel in the LCRV. This has been previously done by Rivera-Araya and Pilaar Birch (2018) and Malasek (2023) for known aged, modern deer from the Georgia Piedmont region. In this thesis, I am expanding upon these relationships in the context of the Lower Chattahoochee River Valley. Following the validation of modern climate variables and modern deer, the archaeological deer enamel $\delta^{18}O$ is examined and compared. $\delta^{13}C$ between both modern and

archaeological groups are compared to elucidate diets between the archaeological and modern deer in the LCRV.

My research objectives are as follows:

1. To validate the relationship between climate variables (precipitation, temperature) and stable isotopes captured by modern deer enamel in the context of the Lower Chattahoochee River Valley, GA
2. Elucidate differences in climate (seasonality, precipitation, temperature) between the onset of the Little Ice Age and modern day in the Lower Chattahoochee River Valley by investigating differences in $\delta^{18}O$ trends, means and amplitude between the two sample groups.
3. Assess differences in $\delta^{13}C$ trends, means and amplitude to illuminate maize proportionality in deer diet in both sample groups.
4. Expand the body of literature on deer enamel in Georgia (Rivera-Araya and Pilaar Birch, 2019; Malasek, 2021) to the archaeological record; specifically, the Mississippian Period of the southeastern US.

In the following chapter, I present the Lower Chattahoochee River Valley (LCRV) as a region of interest in Georgia. I then introduce Singer-Moye, a Mississippian mound site located within the LCRV that acts as the source locale of the zooarchaeological samples used in this study.

1.2 Study area

Lower Chattahoochee River Valley

The Lower Chattahoochee River Valley (LCRV) lies on the westernmost extent of the Georgia Coastal Plain. The valley encompasses the Georgia-Alabama border, extending to the Fall Line northward, and is bounded to the south by the Florida panhandle (Figure 1). The coastal plain and the LCRV have been host to human activity since the early Holocene and remain so today (Blitz & Lorenz, 2006; Brannan, 2018). During the Mississippian Period the Lower Chattahoochee River acted as a resource reservoir and a highway to the Gulf. Trade, connections, and chiefdom relationships were fostered by transportation along the river while associated floodplains provided lush fertile soil for domestic crops like maize (Willoughby, 2012)..

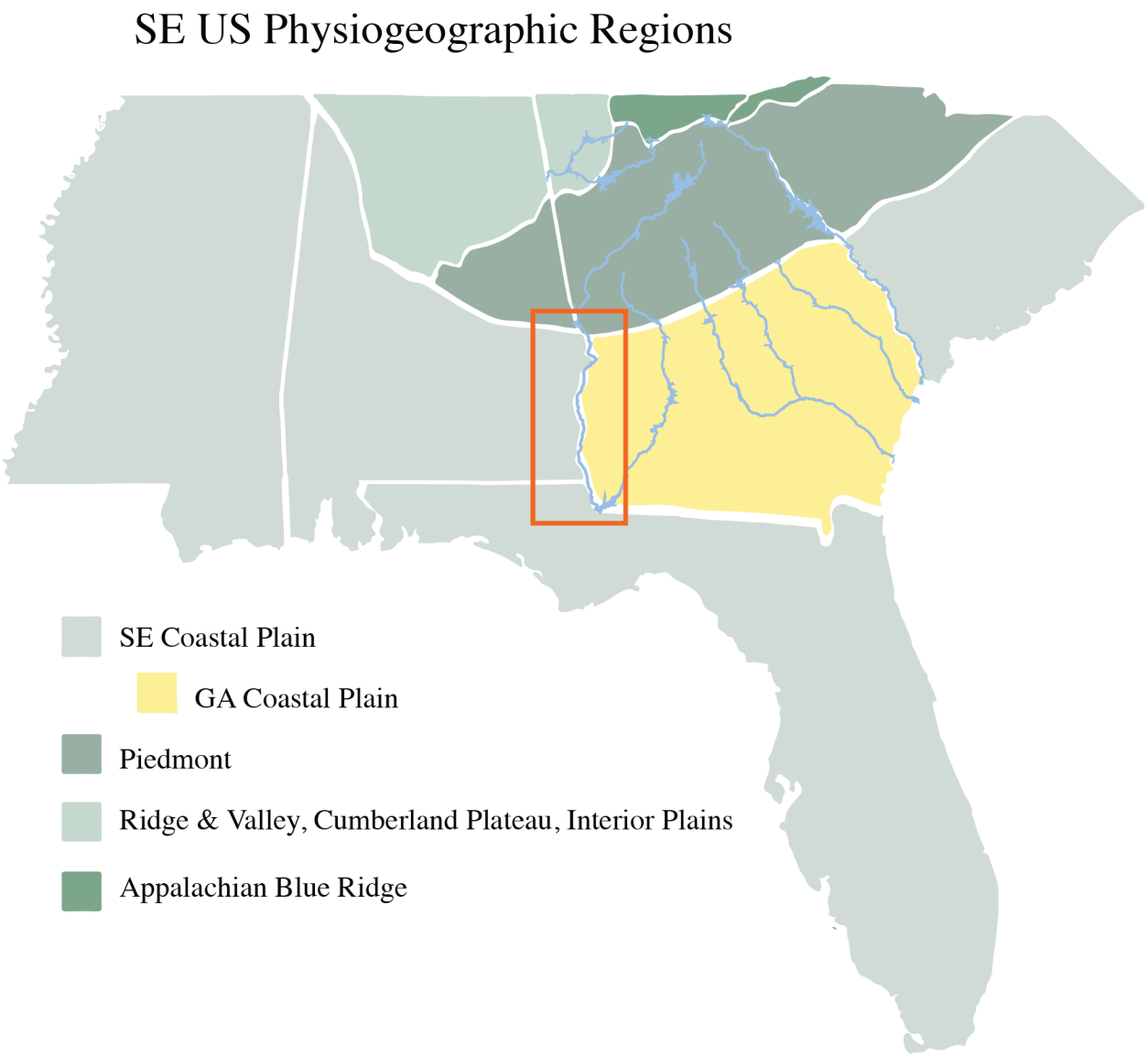

Figure 1: Map of Lower Chattahoochee River Valley (red box) on the Georgia Coastal Plain (yellow). Chattahoochee River Basin map modified from Willoughby, 2012. Physio-geographic regions of the Southeast figure modified from Dunbar, 2016 and Thomson, 1960.

The LCRV is part of the mid-latitude, sub-tropical climate regime of the Southeast US. The regional hydroclimate is defined by advective moisture from the subtropical North Atlantic, Mexican Caribbean, and Gulf of Mexico. The interaction between the Gulf Stream, Caribbean Air, and dry inner-continental air leaves this region vulnerable to climate feedback caused by changes in atmospheric and oceanic circulation (Medina-Elizalde et al., 2022). Archaeological records and

ethnographic accounts reveal rich interactions between the environment, people, and their response to climate change in the LCRV (Anderson et al., 1994; Blitz & Lorenz, 2006; Cook Hale & Sanger, 2020; Kellett & Jones, 2017; Stahle & Cleaveland, 1994). The human-environment interactions in this region cannot be fully understood due to the lack of high-resolution terrestrial proxies available for climate reconstruction.

Singer-Moye

The Lower Chattahoochee River Valley houses several Mississippian sites from the Late Woodland Period with faunal remains (Blitz & Lorenz, 2006). This study uses archaeological material from Singer-Moye - a Late-Mississippian Muscogee mound site in Stewart County, Georgia, located 150 miles interior the Gulf of Mexico on the Alabama and Georgia border. Middens contain a high density of well-preserved faunal material due to geochemical buffering that bone and shell provide against the acidic Georgia soils (Smith and McGrath, 2011). Though, not all sites share the equipotential of preservation. Archaeological faunal materials are more susceptible to diagenesis and weathering in coastal ecosystems as opposed to woodland (Behrensmeyer, 1978; Kendall et al., 2018). For this study, archaeological samples were sourced from the interior of the Atlantic Coastal Plain to minimize taphonomic concerns.

Following the hunter-gathering culture of the Woodland Peoples (Figure 2; 350 – 1000 C.E.), Mississippian cultures emerged in the Southeast as the dominant culture (1000 and 1500 C.E.) (Brannan, 2018). The Mississippian culture is discernable by their settlement style, composed of earthen mounds, plazas, and agricultural fields (Anderson et al., 1994; Bowne, 2013; Willoughby, 2012). The Lower Chattahoochee River Valley (LCRV) served as a rich cultural locus for the Mississippian Peoples (Willoughby, 2012, Blitz and Lorenz, 2006). Within the river valley,

a total of 330 sites have been identified that demonstrate evidence of occupation during the Mississippian Period (Brannan, 2018). Singer-Moye is one of the few sites to have multiple mounds constructed. The settlement and occupation of Singer-Moye spanned the late Woodland Period from 1100 – 1450 C.E. (Blitz & Lorenz, 2006). Singer-Moye is typical of large Late Woodland Mississippian sites, in that it contains flat-top and domed mounds, and two plazas (Figure 3 Brannan, 2018). Singer-Moye is the only major mound-bearing Mississippian settlement in the LCRV that is not situated on the main trunk of the Chattahoochee River. Instead, Singer-Moye is located upon Patuala Creek, a tributary of the Chattahoochee River. The mound site straddles two watersheds, the Flint and Chattahoochee River.

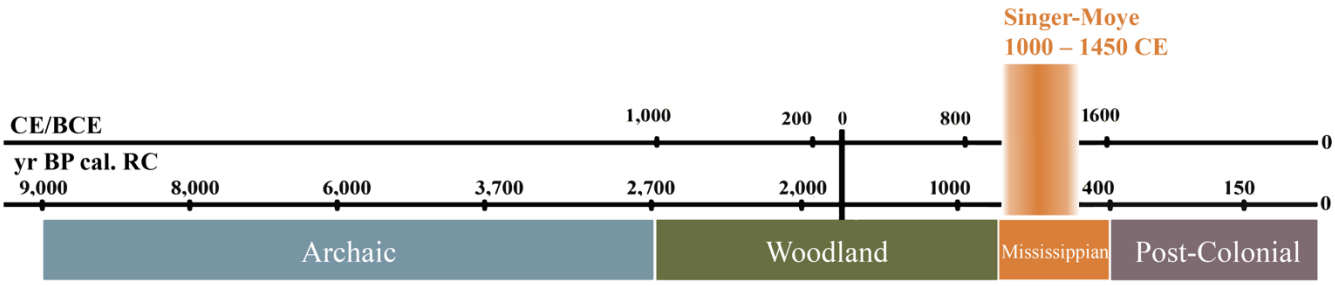

Figure 2: Singer-Moye occupation timeline. Occupation (orange) placed in the context of Eastern Woodland archaeological periods. Two timelines illustrated above, before Common Era (CE/BCE) and radiocarbon years before present (year BP cal. RC).

In addition to straddling two watersheds, Singer-Moye is located on the boundary between two ecotones (Figure 4; Griffith et al., 2001). The Hilly Gulf Coastal Plain and Coastal Plain Red Uplands differ in vegetation cover. The former is predominantly oak-hickory pine forest with minimal mixed forest, while the latter is dominated by mixed forest with sparse oak-hickory pine. Access to diverse forest cover and vegetation types was likely advantageous from a resource standpoint for the occupants of Singer-Moye (Brannan and Birch, 2016a). Additionally, Singer-Moye is located just beneath the Fall Line that is reputed to have been seasonally visited for

securing deer and oak mast in the autumn by hunter-gatherers in the Archaic (Anderson and Hanson, 1988).

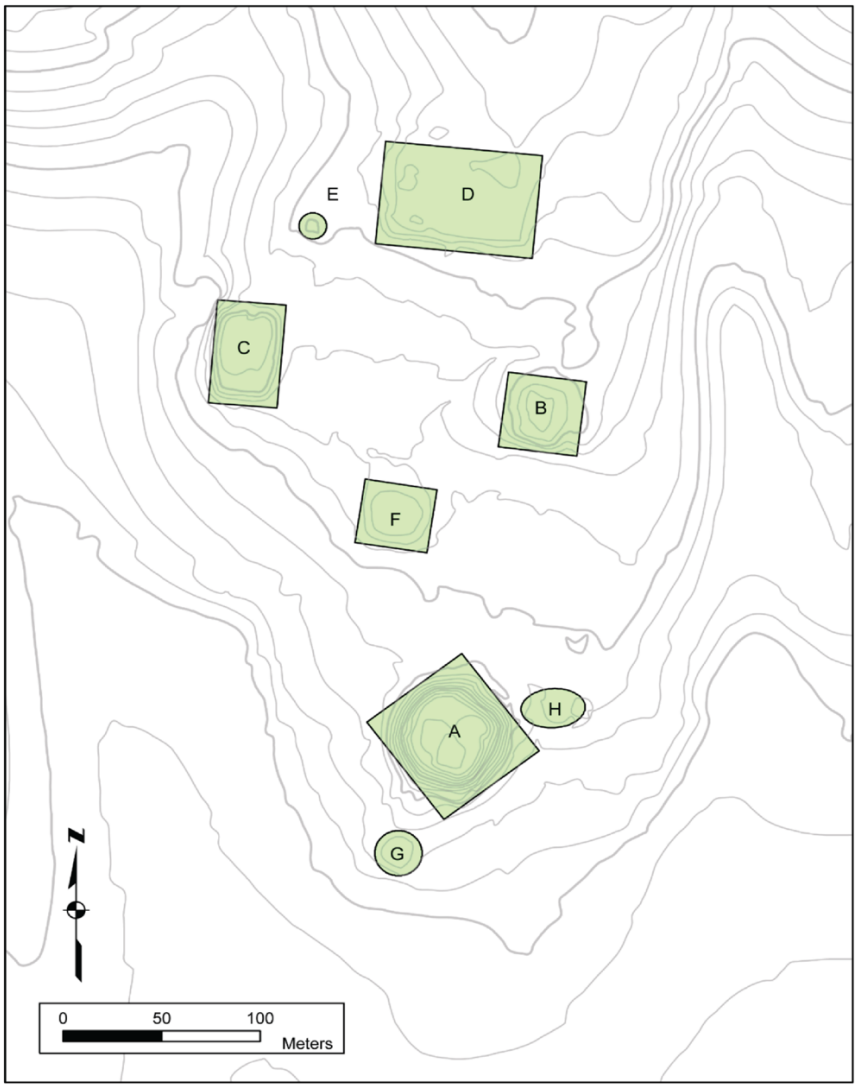

Figure 3: Map of Singer-Moye. Figure reprinted from Brannan, 2018.

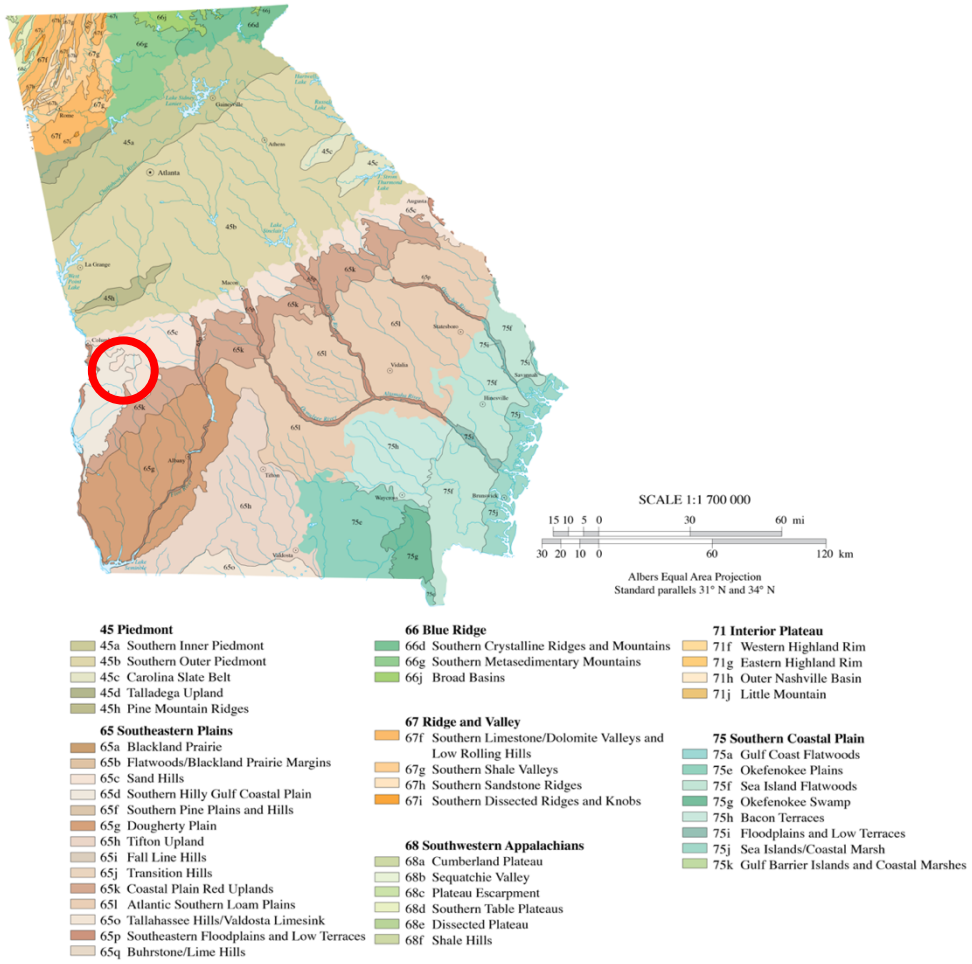

Figure 4: Location of Singer-Moye in the context of Georgia ecoregions. Singer-Moye site location approximated by red circle. Note the site location straddles two ecoregions (65k, 65d) on the Georgia Coastal Plain: The Coastal Plain Red Uplands and Southern Hilly Gulf Coastal Plain. Map adapted from Griffith et al., 2001.

The role of maize in Mississippian cultures

Mississippian settlements have been described as a 'mosaic' of fields and food-bearing floras. Alongside various types of corn, Mississippian Peoples cultivated squash and beans in a relationship colloquially known as 'the three sisters'. Historical ethnographic accounts from the 1700s describe large fields in the lowland floodplains with individual homes placed upon terraced grounds, accompanied by smaller gardens. Corn harvesting was done in the summer and was associated with ritual celebrations among the Lower Creek Peoples (Willoughby, 2012). Nonetheless, the availability of corn was likely year-round, as farmsteads and fields housed individual and communal corn granaries (Scarry & Scarry, 2005).

The cultivation of maize was deeply significant to Mississippian cultures (Willoughby, 2012). Maize appears in other diet proxy records as a dominant presence in Mississippian agriculture as early as 1000 C.E. (Emerson et al., 2020; Willoughby, 2012). At Greater Cahokia, the largest mound site of the Eastern Woodlands, $\delta^{13}C$ values in human tooth enamel and bone collagen reveal the widespread adoption of maize coinciding with swift and significant population growth (Emerson et al., 2020). There is little doubt that the transition to year-round agricultural sustenance is linked to higher population capacities at Mississippian settlements. Thus, reconstructions of deer diets offer insight into maize availability and the correlated population capacity.

Settlement timeline at Singer-Moye

The occupation history of Singer-Moye can be broadly categorized into three main intervals. Singer-Moye is one of many Mississippian Chiefdoms that experienced growth during the Medieval Warm Period (MWP;~800 – 1300 CE), which directly preceded the LIA (Bowne,

2013; Hughes & Diaz, 1994). From 1100 – 1300 C.E., Singer-Moye transitioned from seasonal occupation to a pioneering settlement. Between 1200 and 1400 C.E., Singer-Moye experienced a settlement size increase by a factor of five (Brannan, 2014). During the interval of the maximum occupancy, 1300 – 1400 C.E., the site was a large, aggregated town (Birch and Brannan, 2017). Following 1450 C.E. Singer-Moye is speculated to have been nearly all but abandoned with potential, intermittent site re-use (Brannan, 2018).

The underlying causes of the collapse of the Moundville Chiefdom at Singer-Moye are elusive, but examination of contemporaneous Mississippian sites exposes a similar temporal pattern of depopulation. The term 'Vacant Quarter' has been applied to the apparent abandonment of large inland mound centers in the interior eastern US (North of the LCRV) during the Little Ice Age, between 1450 C.E. and 1550 C.E. (Meeks & Anderson, 2013). Outside of the inland eastern US, coastal settlements in Florida are also posited to have been abandoned in part due to the climatic instability of the Little Ice Age (Holland-Lulewicz & Thompson, 2021). Collapse at Cemococheebee and Roods Landing, two large contemporaneous mound sites in the LCRV, in the early 1500s is thought to have been triggered by disease following contact with Hernando de Soto and the Spaniards (Willoughby, 2012). Settlement patterns are complex, and a combination of factors contributes to the dispersal of population centers. Nevertheless, recent paleoclimate reconstructions have supported an intrinsic link between the onset of the Little Ice Age and the Mississippian settlement abandonment (Holland-Lulewicz & Thompson, 2021; Pompeani et al., 2021; Meeks and Anderson, 2013). At Singer-Moye, and within the LCRV, paleoclimate reconstructions, timing, and effects of the LIA remain to be resolved (Brannan, 2018).

History of Singer-Moye archaeological investigations

The property that Singer-Moye is located on was owned by the Columbus Museum of Georgia from 1953 until 2008. Excavations were carried out by the Columbus Museum between 1967 and 2007 with principal interest in Mounds A, C, D, E, and H. Unfortunately, the excavations were not properly backfilled and are too damaged to provide any meaningful context (Brannan, 2018). The University of Georgia acquired the site in 2008 and an additional 102 adjacent acres in 2011 to be managed by the Georgia Museum of Natural History (Brannan, 2014).

Under UGA's management, dense deposits of faunal material containing contain deer bone and teeth were uncovered at Singer-Moye between 2013 – 2018 (Brannan, 2018). The excavations were overseen by Dr. Jennifer Birch and Dr. Stefan Brannan with the UGA archaeological field school Singer-Moye Archaeological Settlement History (SMASH) project.

Following a series of fruitful shovel tests in 2012 and 2013, three 2x2m units were excavated (2013_XU1, 2013_XU2, 2013_XU3) southeast of Mound A. The third unit, XU3, contained the densest faunal material, including bivalves, gastropods, turtles, bird, fish, and white-tailed deer (Little, 2013). Unique to LCRV midden deposits was the presence of rare taxa at Singer-Moye, such as the passenger pigeon and a saltwater clam (Little, 2013). In 2016, three more units were excavated to the east of the 2013_XU block and revealed the dense midden deposit. Faunal analysis of the 2013 unit's materials was carried out by UGA graduate student Maran Little. Ceramic seriation was compared against Brannan's (2017) chronology which confirmed the ages of 2013_XU3 unit fall between 1300 and 1400 CE. This period coincides with Singer-Moye's maximum occupation (Brannan and Birch, 2016b).

In 2016, a 1x6m unit was excavated south of Mound A and H based on a brief geophysical survey that suggested a possible house-like structure (Brannan and Birch, 2016b). The southern portion of an L-shaped trench was broken up into an east (2016_XU1_E) and west (2016_XU1_W)

component. A hearth feature and wall posts were revealed alongside a midden in the eastern portion that extended 80cm into the sub-surface – originally thought to be part of a house structure. At the base of the midden, large mammal bone fragments and shells were particularly dense. The previously hypothesized house structure was never located. Instead, a series of posts were uncovered. The posts indicated an area of high-status access related to Mound A, reminiscent of a nearby palisade excavation. The seriation of ceramics dated the entire midden deposit to 1300 – 1400, the same as the midden in unit 2013_XU3 (Brannan and Birch, 2016b). Thus, materials from the 2016 unit fall within the same temporal bounds as the 2013-unit Faunal analysis of the 2016 unit was carried out by SMASH research associate Kimi Swisher, which was completed in June 2022 and accessioned into the UGALA.

Both units reveal the unique and continuous usage of the area surrounding the largest mound, A, from the inception of the Mississippian settlement to its eventual abandonment (Birch and Brannan, 2017). A wall trench found just beneath the 2016_XU1_E midden was dated to be among the earliest zones of occupation at Singer-Moye from 1150 – 1300 CE (Birch and Brannan, 2017). In contrast, pottery shards found on Mound A's summit and flank were carbon dated as 1294 – 1440 C.E., but the style of the pottery is post-dated 1300 CE., suggesting the construction of Mound A's summit is closer to 1400-1450 CE (Brannan, 2014). The area of provenance for all the archaeological teeth in this study, to the south and east of Mound A and Mound H, was likely a locale for the elite and their specialized activities such as crafting and feasting (Brannan and Birch, 2017).

CHAPTER 2

LITERATURE REVIEW

This chapter comprises a literature review through four topics. I begin by discussing the use of stable isotopes in enamel carbonate as paleoenvironmental proxies. In this first section, I focus on prior investigations using white-tailed deer enamel, physiological controls on enamel mineralization, as well as environmental sources of oxygen and carbon isotopes in white-tailed deer enamel. In the second section of this chapter, I consider white-tailed deer behavior, ecology, and diet. I then summarize climate trends, variables, and controls relevant to the LCRV. Lastly, I review available proxy records nearby that capture the Little Ice Age in the southeast US.

2.1 Stable isotopes in enamel carbonate as paleoenvironment proxies

High-resolution temperature, precipitation, and seasonality reconstructions in the southeast US are principally based on dendrochronology and speleothems in the region (Stahle and Cleaveland, 1994; Mann et al., 2008; Medina-Elizalde et al., 2022). Tree rings provide inter-annual to decadal resolution of precipitation and temperature (Hughes, 2011; Meeks & Anderson, 2013; Stahle & Cleaveland, 1994). However, sub-annual variation is not discernible in tree rings. Speleothem records are more commonly used for high-resolution paleoclimate reconstruction, though, unfortunately, their records are not widely available due to the rare conditions required for formation. Stable isotopes from freshwater mollusks, (i.e. bivalves) can also provide intra-annual resolution for seasonality reconstruction proximal to terrestrial locations. There are difficulties in

using bivalves in zooarchaeological contexts for paleoclimate reconstruction – firstly, access to articulate, well-preserved specimens that have not been altered by groundwater causing a diagenetic overprint. Bivalves are common in coastal archaeological settings (i.e. shell middens) but are rarer in inland river-valley settings. Bivalves also reflect the water temperature during their interval of growth and fluctuations therein and are not directly indicative of surface air temperatures, precipitation amounts, or humidity. Bivalves also are prone to growth cessation and may lack a continuous record (Goodwin et al., 2003).

Tooth enamel is regarded as structurally stable, resistant to diagenesis and widely available in archaeological contexts (Koch et al., 1997; Zazzo et al., 2004). Because of these reasons, numerous studies have employed the use of stable isotopes in tooth enamel to reconstruct diet, mobility, and environment (e.g. Britton et al., 2009; Hoppe, 2006; Koch et al., 1994; Pellegrini et al., 2008; Pilaar Birch et al., 2016; Sponheimer & Lee-Thorp, 1999). Horizontal, serial sampling in a transect parallel to the growth axis of the tooth captures intra-tooth variations that may then be interpreted as a time series (Balasse, 2003). Stable oxygen isotopes in enamel carbonate provide valuable insight into seasonality and environmental conditions while stable carbon isotopes are reflective of diet across the interval of tooth mineralization (Fraser et al., 2021a; Morris, 2015; Noble et al., 2020).

Of the abundant herbivorous ungulates in North America, the white-tailed deer has yet to be utilized in many paleoclimate or environment reconstructions (Rivera-Araya & Pilaar Birch, 2018). Much of the previous work with *O. virginianus* has focused on stable isotopes in bone collagen to elucidate deer diet and climatic variables like precipitation (Morris, 2015; Bergh, 2012). Carbon and nitrogen isotope ratios examined in deer bone collagen are derived from an ingested protein in their diet, and are not reflective of C_3, C_4 vegetation availability (Cormie &

Schwarcz, 1994). Moreover, bone collagen lacks the temporal resolution of tooth enamel, which mineralizes sequentially and is more resistant to diagenesis (Balasse, 2002; Koch, 1998; Morris, 2015). Isotopic analyses of archaeological enamel from members of the family Cervidae and Bovidae, such as goat, horse, sheep, bison and elk, have been successfully utilized in paleoclimate reconstructions (Blumenthal et al., 2019; Bocherens et al., 2001; Drucker et al., 2001; Fraser et al., 2021; Julien et al., 2012, Waite and Pilaar Birch, 2023). The exceptional preservation potential of tooth enamel underscores the potentiality of archaeological and fossil specimens in paleoclimate reconstructions.

Tooth enamel mineralization

Deer teeth are made up of three hard tissues: dentin, enamel, and cementum (Hillson, 2005). Enamel is the least porous and most durable of the three mineralized tissues (Kendall et al., 2018). The chemical make-up of enamel is two-fold, primarily bio-hydroxyapatite phosphate, and minor amounts of structural carbonate (Miller et al., 2018). Structural carbonate is approximately 3% per weight of the total enamel. Both the carbonate and phosphate from tooth enamel have been used in isotopic enamel studies, but for the purpose of this study, I am focused on the structural carbonate (Zazzo et al., 2004).

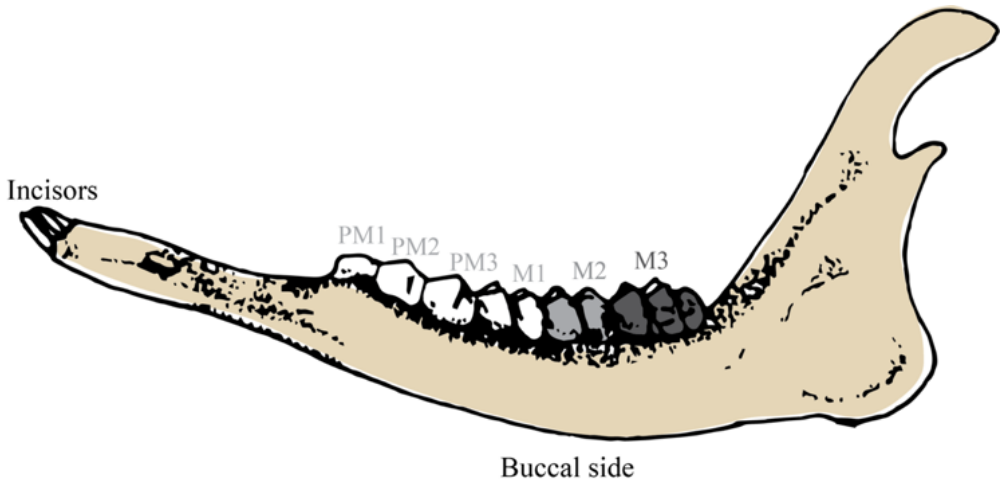

Figure 5: Lower left deer mandible with incisors, premolars (PM) and molars (M) labeled. This study used M2 and M3 pairs for stable isotopic analyses. Figure modified from Smith, 1991. Original drawing by K. M. Endres.

White-tailed deer have three premolars and three permanent molars on each hemimandible. (Figure 5). The crown mineralizes first, sequentially adding layers at the enamel-root junction. Tooth eruption occurs after the enamel finalizes formation (Severinghaus, 1949). When fawns approach two months of age, they begin mineralizing their M2 molar, with eruption occurring by five or six months. Third molars (M3) mineralize next, between five and ten months of age. White-tailed deer breed in autumn and their gestation averages approximately 200 days. This results in an average birth date between May and June (Smith, 1991). Thus, M2 and M3 record the duration of late summer to early spring in stable isotopic variation of their environment (~ July – March; Morris, 2015).

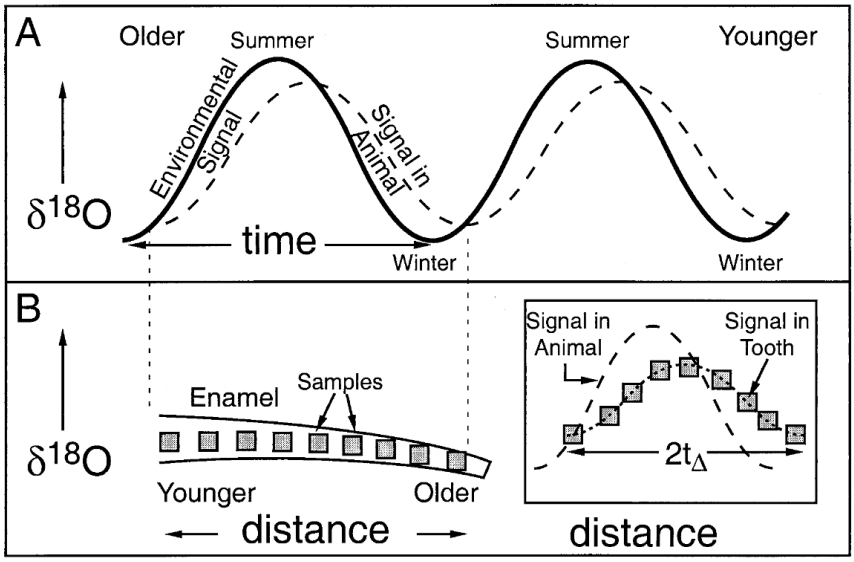

Figure 6: Damping and offset of isotopic time series during enamel maturation. The amplitude of serially sampled isotopes plots a sinusoidal curve (A), reflecting enamel material (B). Figure reprinted from Kohn, 2004.

The process of enamel mineralization takes place in two steps. First, a primary layer is laid down and then a secondary maturation phase occurs. During mineralization, isotopic signatures are time averaged across a gradual, but finite, maturation phase. This results in a damping effect, or attenuation, of isotopes during amelogenesis (Figure 6; Passey & Cerling, 2002). The timing of enamel maturation and damping effect of isotopic variation differs between taxa (Kohn, 2004). Estimations of maturation time and damping are only known for a select few species including cattle, bison, sheep, elk, goat, and horses (Fricke et al., 1998; Fricke & O'Neil, 1996; Kohn, 2004; Zazzo et al., 2005; Morris, 2015). In the case of large cervids like elk, maturation is thought to take six months with an overall 50% damping of isotopic signal (Kohn, 2004). This assumption cannot be uniformly applied across the *Cervidae* family, though, since enamel maturation rates are highly correlated to body mass. A close approximation may be conjectured by considering ungulates of similar body mass. For example, antelope undergo a secondary enamel maturation phase over the course of one month, and the resultant damping of the primary isotopic signature

by 10% (Zazzo, 2002). In this study, I assume that overall body size is the more critical factor in controlling enamel maturation rates and damping, versus genetic proximity. Thus, this study assumes a maturation phase closer to 1 month and a damping of 50%. This translates into an offset and potential error in plotting isotopic values against a time series of a month. Since M2 and M3 capture a ~10-month interval, shifting the placement of maxima and minima in the generated curve of isotopic values by +/- 1 month does not significantly impede interpretations of seasonality. No matter the offset of maturation time, deer teeth still record a near-complete annual cycle of seasons. Both diet and source water change throughout the seasons, which is expected to be reflected in the sub-sampled isotopic curves. Figure 7 summarizes the relationship between environmental variables, tooth formation, and generated isotopic curves.

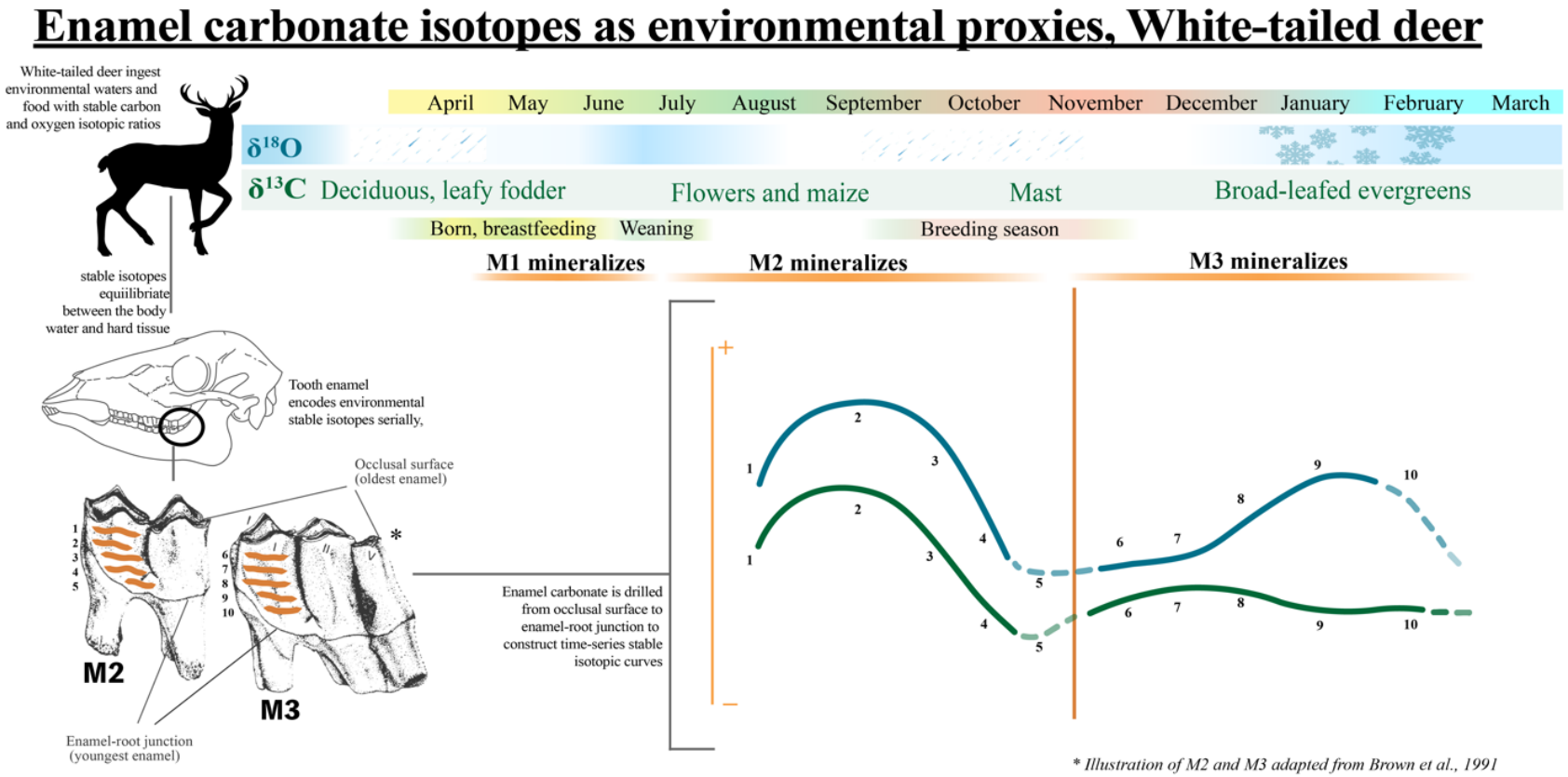

Figure 7: Schematic representation of environmental sources of $\delta^{18}O$ and $\delta^{13}C$, enamel timing, and relationship to generated seasonality curves. Note the timing of deer's M2 and M3 molar formation, July – November and November – March, respectively. $\delta^{13}C$ is ingested via foodstuffs (green bar). $\delta^{18}O$ is ingested via leaf water and environmental waters (blue bar).

Oxygen

Deer imbibe water and ingest foodstuffs from their local environment that contain differing ratios of lighter oxygen (^{16}O) to heavier oxygen (^{18}O). The primary sources of $\delta^{18}O$ in deer enamel are leaf water and surface waters, though deer can facultatively drink from ponds, and puddles, and eat snow (Smith, 1991). Deer prefer liquid water over snow. Water requirements vary among climate conditions, food availability, ontogeny, and metabolic costs. For example, pregnant deer in captivity have been shown to drink two the three times the amount of water relative to dry material (Downing and McGinnes, 1976). The ratio of oxygen isotopes is then integrated into their body water, and further incorporated into hard tissues, i.e. enamel. Enamel carbonate fractionates in isotopic equilibrium with body water (Kohn, 1996; Luz et al., 1984). Fricke et al. (1998) demonstrated that cattle given tap water displayed little to no intra-tooth variation in $\delta^{18}O$. Additionally. Rivera-Araya and Pilaar Birch (2018) showed similar results for non-wild deer kept at the Whitehall Forest research facility in GA. Hence, it is assumed that a primary source of $\delta^{18}O$ variation in enamel is environmental variation during tooth formation that reflects precipitation, humidity, and precipitation amount (Balasse, 2002; Fraser et al., 2021a; Fricke et al., 1998; Rivera-Araya & Pilaar Birch, 2018).

The physiogeographic distribution of oxygen isotopes depends on the amount of precipitation and temperature that are a function of latitude, elevation, and continentality, (Akers et al., 2017; Bowen & Wilkinson, 2002). Typically, high temperatures that entail higher evapotranspiration are associated with high (relatively more positive) $\delta^{18}O$ ratios, whereas colder temperatures reflect lower (relatively more negative) $\delta^{18}O$ ratios. In the southeastern US, the correlation between surface temperature and $\delta^{18}O$ precipitation is insignificant ($r^2 = 0.2$; Akers et al., 2017). Controls on $\delta^{18}O$ may be attributed primarily to the amount effect and moisture

recycling in the humid sub-tropical SE US. The amount effect is the amount of precipitation received and will result in a lowering of $\delta^{18}O$ ratios in hot, humid climates that are subjected to a lot of precipitation (Dansgaard, 1964; Akers et al., 2017). The amount effect is dominant in tropical to subtropical regions, while temperature mainly controls $\delta^{18}O$ in mid to high latitudes (Akers et al., 2017; Bowen, 2008; Dansgaard, 1964). Because Georgia's climate is humid year-round, we can expect a depletion of $\delta^{18}O$ during periods of increased precipitation.

The ratio of ^{18}O to ^{16}O measured in a sample is divided by the ratio of ^{18}O to ^{16}O of a standard to obtain δ (also noted as $\delta^{18}O$; Equation 1).

Equation 1.

$$\delta = \frac{\left(\frac{^{18}O_{sample}}{^{16}O_{sample}}\right)}{\left(\frac{^{18}O_{standard}}{^{16}O_{standard}}\right)} - 1$$

Carbon

Stable carbon isotope ratios can be utilized to infer dietary regimes, and thus environmental reconstruction, in archaeological and paleontological contexts (Cerling et al., 2015, Thorp and Van der Merwe, 1987). Deer ingest foodstuffs containing ratios of lighter carbon (^{12}C) and heavier carbon (^{13}C) isotopes (Cormie & Schwarcz, 1994). Because photosynthetic pathways fractionate carbon differently, the $\delta^{13}C$ signature in deer enamel can be used to infer the ratio of ingested C_3 and C_4 plant types. Plants with C_3 photosynthesis pathways reflect relatively more negative $\delta^{13}C$

values, ranging from ~ –35‰ to –27‰, while C_4 plants exhibit more positive $\delta^{13}C$ values, ~ –13‰ to –9‰ (Van Der Merwe & Vogel, 1978). In ungulates, $\delta^{13}C$ enrichment from source (diet) to enamel is 14‰ (Cerling and Harris, 1999). $\delta^{13}C$ in deer enamel, thus, should fall between –21‰ and –13‰ for diets if consuming C3 plants. Deer forage to meet their metabolic needs and prefer high-nutrient C_3 plants such as mast, fodder, fruits, and acorns (McCullough, 1984). The exception to this preference is the consumption of grasses, a C_4 plant, commonly eaten in the spring and early summer (Smith, 1991). The most common grass deer ingest is maize, a widely abundant C_4 plant cultivated near both contemporary and ancient human settlements (Cormie & Schwarcz, 1994; Van Der Merwe & Vogel, 1978).

Stable carbon isotopes in bone collagen reveal that some deer reflect overall more agricultural diets (Cormie & Schwarcz, 1994; Rivera-Araya & Pilaar Birch, 2018). Bone collagen largely reflects the protein component of an individual's diet (Harrison & Katzenberg, 2003) and, in addition, bone collagen exhibits time-averaging of carbon isotopes as the turn over rate is on the scale of years (Van Der Merwe & Vogel, 1978). In contrast, enamel-stable carbon isotopes are more likely to elucidate seasonal shifts in maize consumption due to the sequential capture of isotope ratios over the year. If deer supplement their diet with maize during the time of tooth formation, the $\delta^{13}C$ of enamel carbonate will become more enriched. Determining whether deer are consuming large quantities of maize, the main crop of eastern Woodland societies (Willoughby, 2012), is particularly useful in answering questions regarding settlement and agricultural history in North America.

Carbon isotope signatures are also influenced by the pre-weaning stage in fawns. Consequently, M1 enamel is enriched in fatty acids from the mother's milk and has been shown to exhibit more negative $\delta^{13}C$ than in M2 and M3 enamel (Malasek et al., 2023). As a result, M1

does not reflect a direct source of environmental vegetation. This study only considers the M2 and M3.

The ratio of ^{13}C to ^{12}C measured in a sample is divided by the ratio of ^{13}C to ^{12}C in a standard to obtain δ (also noted as $\delta^{13}C$; Equation 2).

Equation 2.

$$\delta = \frac{\left(\frac{^{13}C_{sample}}{^{12}C_{sample}}\right)}{\left(\frac{^{13}C_{standard}}{^{12}C_{standard}}\right)} - 1$$

2.2 White-tailed deer ecology

White-tailed deer (*Odocoileus virginianus*; Zimmerman 1780) are an abundant hoofed and antlered browser, belonging to the family *Cervidae*. They are the most common cervid member found in North America (Morris, 2015). They prosper across equatorial, sub-tropical, and mid-latitudes, ranging from their southern extent in Bolivia to northern extremes on the Canadian Shield (Smith, 1991; Morris, 2015; Heffelfinger, 2011). Because of their widespread distribution across the new world, deer are ubiquitous in archaeological site contexts (see Morris, 2015 and references therein).

White-tailed deer are not known to migrate annually, movement is controlled by access to food (Smith, 1991). On the SE Coastal Plain, deer are not limited by food due to the year-round

mild, humid climate that supports ample vegetation (Newsom, 1984). Estimates of their home radius vary from 3.5 km^2 (Marchinton et al., 1994) to 5km^2 (Smith, 1991). Regardless, white-tailed deer in the SE are highly localized, making them excellent reflections of the local environment.

Diet

White-tailed deer are specialists in times of food abundance, capable of maximizing their nutritional intake, but will adapt to more generalist feeding behavior in times of scarcity (Hesselton and Hesselton, 1982). Deer prefer areas of increased agriculture where crop resources and forest clearings support higher populations (Smith, 1991). The relationship between deer and proximity to human agriculture is long-standing. Archaeological evidence of deer-human cohabitation and mutualism has been observed at Neotropical sites where a practice of unharvested maize was intently left at field margins to divert deer from feeding on the primary plots (Sugiyama et al., 2020). In modern populations, crops from agricultural areas provide up to three-quarters of their total diet by mass (Smith, 1991). Deer will select the most nutrient-dense food in their foraging behavior, switching from forbs in the spring and summer to mast in the autumn (Figure 7). Acorns dominate their diet in the autumn during hormonal changes associated with energy-intensive activities like rutting and mating. These activities require caloric-rich foods that such as acorns and mast (Morris, 2015). Concurrent is the inclusion of maize, with some estimates close to 70% of the total diet during the autumn (Morris, 2015; Smith, 1991). During winter, white-tailed deer browse on evergreens and dried leaves. Sedges, grasses, and fungi are common supplements to their winter diet (Smith, 1991; Geist, 1998)

2.3 The Medieval Warm Period and Little Ice Age

The Medieval Warm Period and Little Ice Age are the most recent of six episodes of rapid climate change to occur during the Holocene (11,500 cal. yr BP; Mayewski et al., 2004). The two climate periods accompanied major events in human settlements and cultures, nevertheless – neither are well constrained in their timing, and regional variation leaves much to be resolved (Mann et al., 2009).

Anthropogenic climate change due to modern greenhouse gas emissions parallels the global climate during the Medieval Warm Period (MWP; ~950 – 1250 C.E) not in intensity but in trends (Mann et al., 2009; Hughes & Diaz, 1994). The Medieval Warm Period was characterized by glacier retreat in the Northern Hemisphere, allowing for greater human exploration and settlement, including the seafaring Norse who expanded their range into the North Atlantic at this time (Hughes and Diaz, 1994). Arid events were also characteristic of the MWP. Droughts punctuated the 14th century, with at least three major arid events recorded in tree ring records of the mid-continental US (Meeks & Anderson, 2013). The MWP was not uniform in warming across different regions. Although some regions experienced a similar degree to that of the current anthropogenic climate change, the warming trend was not as significant globally.

Following the MWP, a period of rapid cooling bore glacial advance once more during the Little Ice Age. The Little Ice Age was a period of anomalously cold winters and mild summers, between ~1300 – 1850 CE. The exact onset is undefined due to regional variability, much like the MWP. For example, disputes over the beginning of the period range from 1250 C.E. to 1550 C.E amongst Scandinavian glacial proxy records. The bulk of proxy evidence for the Little Ice

Age originates from higher latitudes, comprised of ice and sediment cores from the North Atlantic and Western Europe (Nesje & Dahl, 2003). Proxy data for mid-latitude regions, such as the southeastern US, is highly reliant on tree rings to detect the beginning of the Little Ice Age and its duration (Grimm et al., 1993; Stahle & Cleaveland, 1994).

Despite the trend of global cooling in the LIA, surface temperatures are estimated to have been anomalously high and even drought-inducing in micro-regions. Environmental variability on the Southeast Coast has been captured in tree ring records dated to the onset of the LIA (Napora and Jantzi, 2020). Modeled surface temperatures based on composite proxies unveil a temperature excursion on the Southern Coastal Plain region encompassing Georgia and Alabama (Figure 8). Deviation from mean surface temperatures during the LIA is estimated to be upwards of + 1.4º C along the Georgia and Alabama coastal plain (Mann et al., 2009). Evidence of significant periods of food-stressed years triggered by droughts between 1288 – 1308, 1385 – 1413, 1449 – 1458, and 1483 – 1492 are observed in the Vacant Quarter, which includes western Kentucky and Tennessee (Meeks and Anderson, 2013). Supporting the theory of hot, dry temperatures are lake sediments from the largest Mississippian mound site, Cahokia. There, sediment proxy records indicate low-effective moisture leading up to the abandonment of the site in 1450 C.E. (Pompeani et al., 2021).

In contrast to the evidence for hot, dry LIA conditions in the southeastern continental US, recent speleothem proxy records from Alabama reveal a negative isotope excursion during the onset and duration of the LIA (Medina et al., 2022). In opposition to the modeled surface temperature findings of Mann et al. (2009), this excursion would signify a cooling in the region – instead, the authors instead interpret the negative oxygen isotope excursion to be a result of increased summer precipitation (i.e. the amount effect; Medina Elizalde et al., 2022).

Reconciling the speleothem records of increased precipitation, and low effective moisture in the southeastern US highlights the need to add high-resolution proxy data from continental sources.

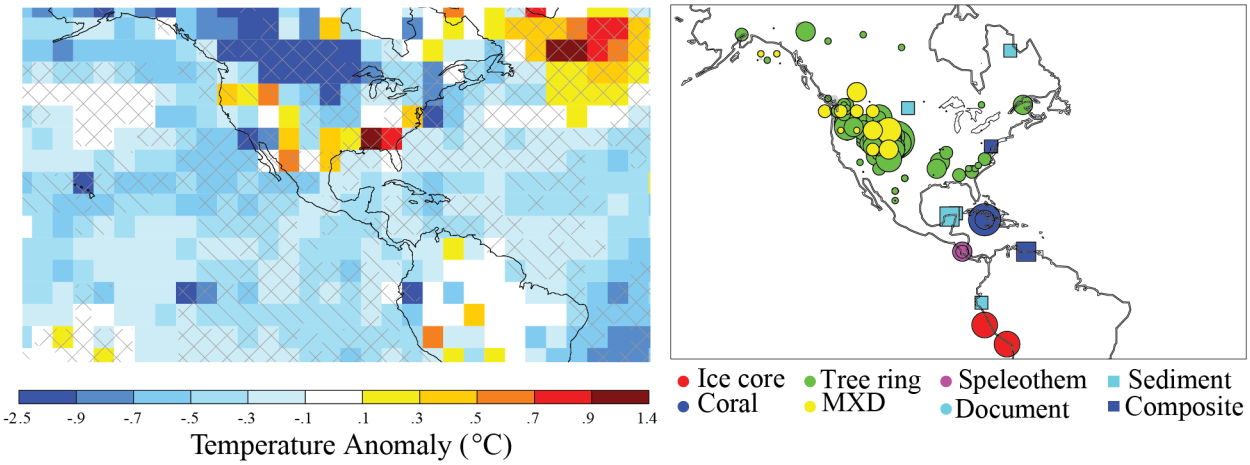

Figure 8: Mean surface temperature anomaly based on proxy modeling for North America by Mann et al., 2009. Available proxy records used in the model are denoted on the right, with symbol sizes indicating relative weighting in the model.

CHAPTER 3

METHODS

To address my research objectives, I sampled both modern and archaeological white-tailed deer M2/M3 pairs from the Lower Chattahoochee River Valley. Nine modern deer mandibles were obtained from Flint's Wild Game Processing in Fort Gaines, Georgia. Three archaeological M2/M3 pairs were located within the Singer-Moye faunal collection at the University of Georgia Laboratory of Archaeology (UGALA). Modern and archaeological teeth were serially sub-sampled for enamel carbonate that was then pre-treated at the UGA Quaternary Isotope Paleoecology (QUIP) Laboratory. Stable isotopic analyses of the treated enamel powder were carried out at the Center for Applied Isotope Studies (CAIS) at UGA. In total, three pairs of archaeological M2/M3 teeth yielded 24 measurements of $\delta^{18}O$ and $\delta^{13}C$. Nine pairs of modern M2/M3 teeth yielded 88 measurements of $\delta^{18}O$ and $\delta^{13}C$.

Chapter three comprises four sections. First, I discuss the modern group of deer and their ages. Next, I discuss the archaeological group of deer and their provenience. I follow with laboratory methods and finally, I outline the data analysis used in the interpretation of the stable isotope results.

3.1 Modern deer

To validate the relationship between climate variables and white-tailed deer enamel in the context of the Lower Chattahoochee River Valley, nine modern mandibles were retrieved from

Flint's Wild Game Processing in Fort Gaines, Georgia in January of 2023. Flint's is located directly in the heart of the LCRV (Figure 9). The nine jaws represent individual deer (n=9) killed during the 2022 hunting season, from late October to early January in Georgia. Deer processors are abundant in southern Georgia, so while verification of each deer's life history prior to death cannot be ascertained, the deer processed at Flint's are likely to be local to the LCRV. The on-site processors asserted that their clientele hunt locally. Georgia hunting laws regulate the transportation of deer from Alabama across the border, thus, even non-local deer are likely from the interior Georgia coastal plain. Additionally, when considering the roaming ranges of white-tailed deer (0.5 – 5 km^2; Smith, 1991), the modern deer from Flint's are almost certainly representative of the Lower Chattahoochee River Valley.

The modern jaws remained frozen until retrieval for preparation in January 2023. Initial preparation included macerating the remaining soft tissue from the jawbone between soaking baths of warm water and unscented Dawn dish detergent. To avoid altering the original enamel carbonate composition, the jaws were never exposed to solution temperatures above 65º C. In bioapatite, structural carbonate preserves its original isotopic value to thresholds of 225º C (Munro et al., 2008). Following 'de-greasing', the jaws were photographed (APPENDIX A) and M2/M3 pairs were extracted from each left mandible at the QUIP Laboratory.

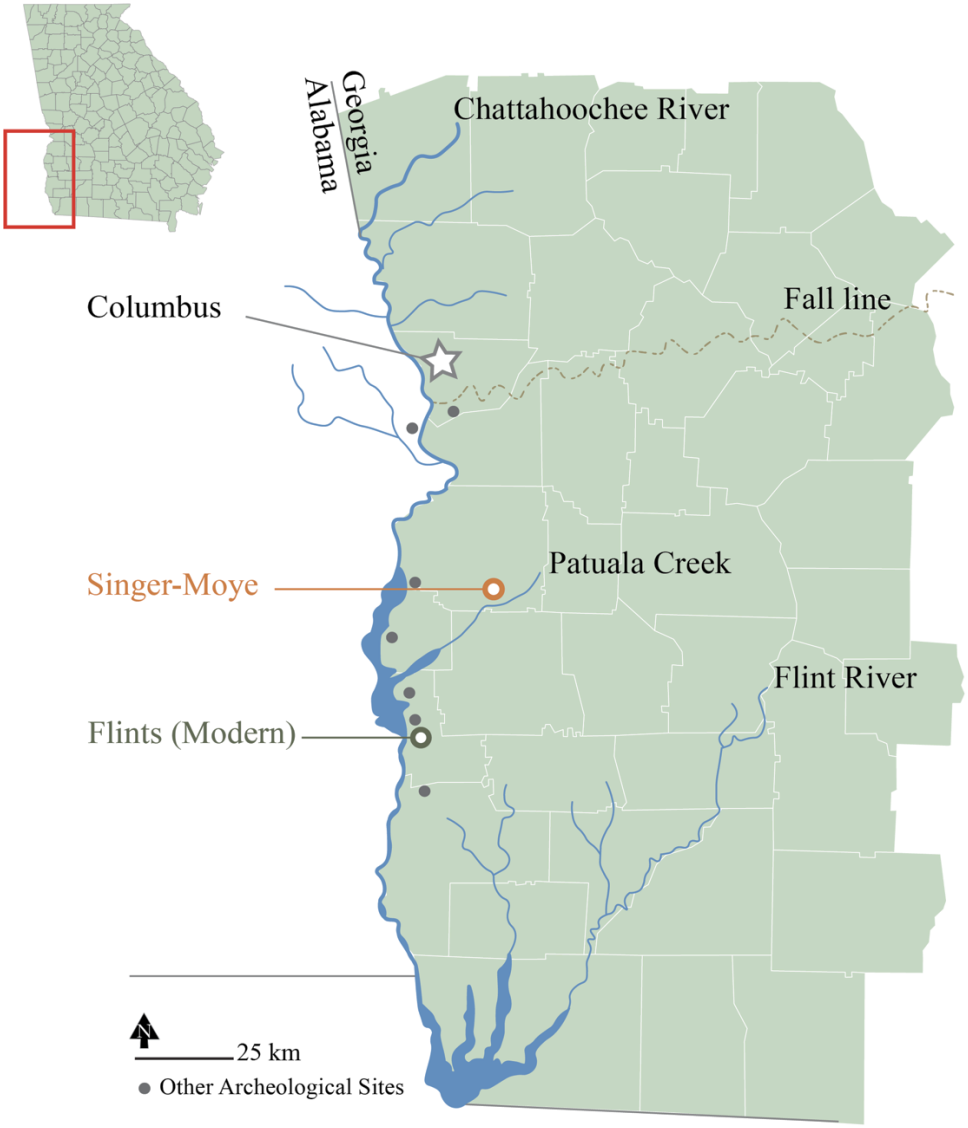

Figure 9: Location of sourced modern and archaeological deer molars. Flint's Wild Game Processing is labeled in green. Singer-Moye mound site is labeled in orange. Both sites lie within the Lower Chattahoochee River Valley. Image adapted from Willoughby, 2012.

Table 1: Context and measurements of modern teeth selected for isotopic analysis

Deer ID	QUIP Lab ID	Tooth	Length (mm)	Breadth (mm)	Crown Height (mm)	Estimated Age		Estimated captured interval of M2 + M3
						TWR	CA	
D1	SM8	M2	16.0	10.5	8.6	3 – 3.5	3.5	Summer 2019 – Spring 2020
	SM9	M3	18.8	9.9	9.7			
D2	SM10	M2	15.6	10.1	7.7	4.5 – 5	4.5	Summer 2018 – Spring 2019
	SM11	M3	21.4	9.9	8.4			
D3	SM12	M2	14.5	10.0	11.5	3.5	3.5 – 4	Summer 2019 – Spring 2020
	SM13	M3	17.7	8.9	10.8			
D4	SM14	M2	16.9	10.4	12.2	2.5 – 3	3	Summer 2020 – Spring 2021
	SM15	M3	19.4	11.0	13.0			
D5	SM16	M2	16.2	11.0	9.8	4 – 4.5	4.5	Summer 2018 – Spring 2019
	SM17	M3	20.4	10.6	9.5			
D6	SM18	M2	15.7	10.1	9.8	2.5 – 3	2.5	Summer 2020 – Spring 2021
	SM19	M3	19.7	9.5	10.4			
D7	SM20	M2	14.0	10.1	9.7	2.5 – 3	3	Summer 2020 – Spring 2021
	SM21	M3	19.6	9.9	10.8			
D8	SM22	M2	16.8	10.9	10.2	2.5	3	Summer 2020 – Spring 2021
	SM23	M3	21.7	10.7	10.1			
D9	SM24	M2	15.9	10.6	10.4	3.5	3.5	Summer 2019 – Spring 2020
	SM25	M3	24.8	10.2	11.0			

**TWR, teeth wear replacement*
**CA, cementum annuli*

3.1.1 Ages

In order to contextualize the relationship of modern deer enamel isotopes to climate variables at the time of formation, a known deer age is required. The M2 and M3 record approximately 10 months of climatic and environmental variables, beginning approximately two months following birth (Morris, 2015). Hence, the age of the deer at time of death can be used to back-calculate the year and seasons of M2 and M3 formation. The ages of the modern deer were estimated using two methods, tooth wear replacement (TWR; Severinghaus, 1949) and cementum annuli (Adams & Blanchong, 2020; Gilbert, 1966; Kay, 1974). Misclassification of age is common. Demonstrable error in age estimation is much greater in deer two years or older after all teeth have erupted (Adams & Blanchong, 2020). Thus, to make estimates of the modern deer ages I took a two-pronged approach - firstly approximated the TWR based on Severinghaus (1949) and then selected M1s from their associated jaws for cementum annuli analysis (Kay, 1974).

Thin sections of M1 teeth were sliced using a diamond Dremel wheel, with continuous inspection of the enamel-root junction location as to maximize exposure of cementum annuli perpendicular to the molar front. The thin slices of M1s and their cementum annuli were examined under a dissecting scope at random to prevent confirmation bias with prior determined TWR ages. Thin section photos and cementum annuli estimations are depicted in Appendix C. My age estimates between both methods are agreeable within 6 months. The results of both methods were taken into consideration and averaged before being assigned an interval of tooth formation. Age estimate results are presented in Table 1.

.

Table 2: Context and measurements of archaeological teeth selected for isotopic analysis

UGA Archaeology Laboratory Context	Unit Strata Level	Deer ID	QUIP Lab ID	Tooth	Length (mm)	Breadth (mm)	Crown Height (mm)
Lot 1580 Box #03048	Unit: 2016_XU1_E Strata: 3 Level: 7	AD1	SM1	Left M_2	18.1	8.4	8.1
			SM2	Left M_3	17.8	9.6	7.8
Lot 2108 Box #03151	Unit: 2013_XU3 Strata: trans. 2/ 3 Level: 8	AD2	SM3	Left M_2	16.1	10.5	7.8
			SM4	Left M_3	22.2	10.6	8.1
Lot 1587 Box #03049	Unit: 2016_XU1_E Strata: 3 Level: 9	AD3	SM5	Right M_2	15.6	10.1	8.9
			SM6	Right M_3	19.7	8.8	9.3

3.2 Archaeological deer

Three pairs of archaeological deer molars dated between 1300 and 1400 CE were chosen from the Singer-Moye collection at the UGALA under the supervision of Operations Director, Amanda Thompson. Molars were selected based on overall preservation (i.e. minimal fractures, percent completeness, occlusal surface wear) and those seated within a mandible were preferential. Unassociated pairs of M2 and M3s from the same excavation unit strata and level, but not seated together in a mandible, were also considered for analyses. Table 3 outlines the final selection of molar pairs and associated UGALA contexts. Appendix B contains images of the archaeological teeth. In general, upper molars were over-represented in the available collection relative to lower molars and many of the lower molars were too fragmented for sampling. These constraints on material availability and selection could be overcome by considering upper molars in future work

and further midden excavation at Singer-Moye. To maintain consistency with prior deer enamel studies I elected to exclude upper molars.

Isotopic analysis of enamel is a destructive process. While in this case, zooarchaeological material from Singer-Moye does not fall under the jurisdiction of the Native American Graves Protection and Repatriation Act (NAGPRA; Department of Interior, 1995), the UGALA engages with tribal consultation to foster relations with descendant communities. In compliance with UGALA protocol for non-NAGPRA contexts, tribal consultation with the Muscogee (Creek) Nation was carried out and mediated by Dr. Amanda Roberts Thompson. In June 2022, permission for destructive analysis of the archaeological specimens was granted by the Muscogee Nation with the agreement that all findings and data be shared with the Muscogee Nation.

Provenience and context

The Singer-Moye faunal material in the UGALA collection is a result of excavations carried out by the UGA Archaeological Field School. Faunal analysis following the excavations in 2013 were completed by Maran E. Little under the supervision of Dr. Elizabeth Reitz. Faunal analysis from the 2016 and 2017 field seasons was done by Kimi Swisher. All archaeological teeth (SM1 – SM6) were collected southeast of the largest flat-topped mound at Singer-Moye, A, and a smaller dome-shaped mound, H (Figure 10). SM3 and SM4 (individual AD2) are from unit 2013_XU3 and SM1, SM2 (AD1), SM5 and SM6 (AD3) are the result of the 2016 excavation of unit XU1. Both units intersect midden features that date to the same interval based on ceramic seriation chronology (1300 – 1400 CE) but vary in precise contexts (Brannan, 2017). The dates associated with the archaeological teeth fall within the onset of the LIA (~1250 – 1850 C.E.).

Teeth from AD1 and AD2 represent two pairs that were each seated in mandibles. An assumption about the relationship between SM5 and SM6 was made based on the stratigraphic association and level. The two teeth were not seated in a mandible so an exact relationship cannot be ascertained as to whether they represent a single individual. Nevertheless, because they were recovered from a contemporaneous layer with no other mandible fragments and are both lower right in position – I have presumed that they are 1.) from the same individual whose mandible either was never deposited or 2.) from a mandible that deteriorated post-deposition. Thus, in this study, SM5 and SM6 are labeled as AD3 and assumed to serve as representatives of a concomitant time-series for that strata and level.

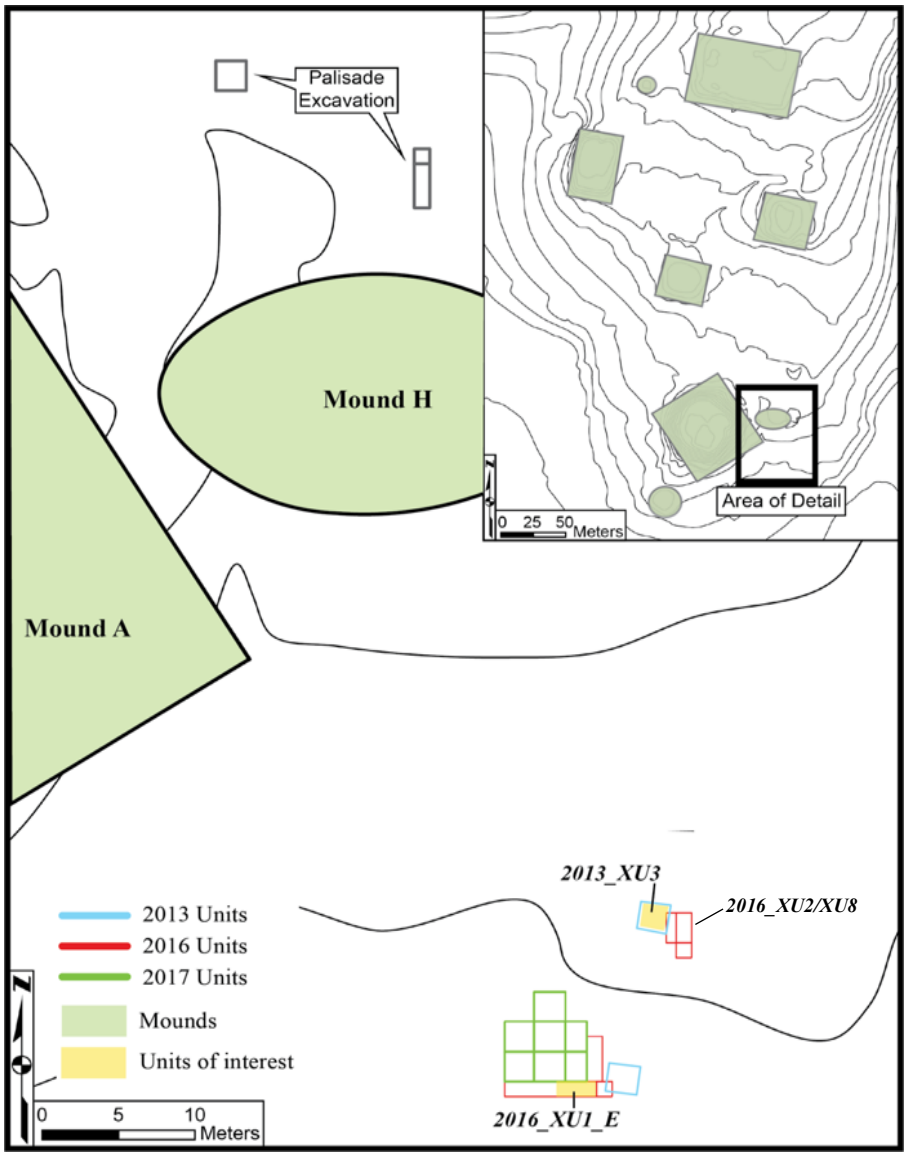

Figure 10: Location of relevant 2013, 2016 and 2017 excavations southeast of Mound A and H at Singer-Moye. Excavations were carried out during the UGA archaeological field school SMASH project. Both 2016_XU1_E and 2013_XU3 units intersect dense midden structures. Adapted from Brannan and Birch, 2016; Birch and Brannan, 2017.

3.3 Laboratory analyses

Sampling and preparation of the enamel carbonate for isotopic analysis was carried out at the Quaternary Isotope Paleoecology Laboratory at UGA. Serial samples were taken using a Dremel Microdrill fitted with a 0.5 mm diamond-tipped drill bit. Samples were taken parallel to the growth axis, beginning at the crown, and ending at the root-enamel junction. The minimum enamel powder weight required for stable isotopic analyses (5 – 6 mg) was the limiting factor in the possible number of serial samples per tooth. As a result, approximately five samples were drilled per tooth. Between each sample, the drill bit was sequentially submerged in three baths of Type 1 filtered water and dried to ensure no cross-contamination of enamel powder.

Pretreatment was applied to both modern and archaeological batches to maintain consistency between comparisons. After drilling the enamel powder, a solution of 0.5 – 1 mL of 3% sodium hypochlorite was added, agitated, and left for 24 hours to ensure the dissolution of organic matter. The enamel carbonate was rinsed three times with Type 1 water and decanted between each rinse cycle. Following the removal of sodium hypochlorite, 0.1 M acetic acid was applied for 4 hours to remove exogenous carbonate (Balasse, 2002). Three more rinses were applied to the enamel powder before final decantation and loading into a desiccator for 24 hours. In total, 30 archaeological and 88 modern enamel powder samples were submitted in two batches. In each batch, four standards were submitted: two samples of archaeological bovine (LRM3) and two samples of modern bovine (LRM2).

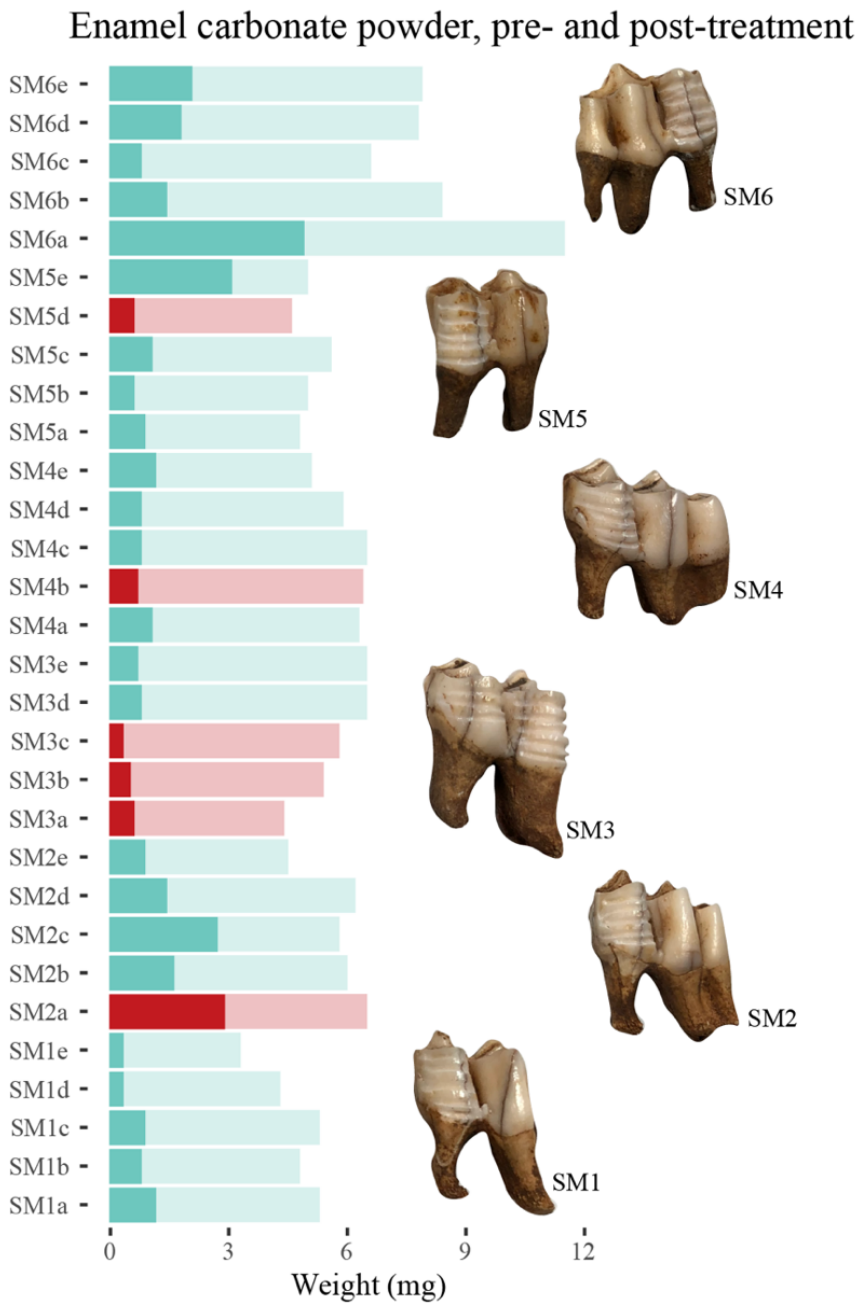

Figure 11: Pre-treated enamel powder weights in milligrams noted in the light shaded boxes. Saturated boxes denote final weight in milligrams following pre-treatment procedure outlined in section 3.3. Blue boxes were successfully analyzed at Center for Applied Isotopes on the IRMS. Red shaded boxes represent failed samples due to carbonate amounts below the detection limit.

All enamel powder samples were sent to CAIS at UGA for isotopic analysis with the Thermo Gas Bench and Delta V Isotope Ratio Mass Spectrometry (IRSM), coupled with GC Pal auto-sampler. A weight of 1 mg of each sample was reacted with phosphoric acid at 70°C in

exetainers to convert solid $CaCO_3$ to gaseous CO_2. The CO_2 was then concentrated through a liquid nitrogen bath, known as a preconcentration technique, a method useful for small powder weights. Even with the preconcentration technique, pretreatment at QUIP rendered six of the archaeological samples insufficient in total weight for processing at CAIS (Figure 11). Of the 30 archaeological samples submitted, 24 were run successfully. Of the modern group, 88 total samples were submitted, and all samples met the detection limit at CAIS and were run successfully. Results are reported in reference to the international standard Vienna Pee Dee Belemnite (VPDB).

3.4 Data analyses

Elucidating climate using deer enamel $\delta^{18}O_{carb}$

The following assumptions are made in the process of comparing enamel isotopic values as paleoenvironmental proxies: chiefly, that enamel carbonate encodes environmental stable isotopic ratios in equilibrium and in sequence (Balasse, 2002). Second, the primary control on stable oxygen values is a combination of relative humidity, amount of precipitation, and more indirectly, temperature, in sub-tropical latitudes (Akers et al., 2017; Dansgaard, 1964; Fricke & O'Neil, 1996; Pederzani & Britton, 2019). Third, seasonality can be inferred from the relative amplitude (range) of the serially sampled enamel stable oxygen values (Kohn et al., 1998; Fraser et al., 2021). To determine if seasonality has increased, decreased, or stayed the same between modern day and the onset of the LIA in the LCRV, individual curves were plotted, and relative amplitudes were assessed. Because M2/M3 pairs record approximately 10 months of environmental variation, seasonal variability is captured. Sinusoidal curve structures are indicative of a higher degree of seasonality. $\delta^{18}O$ curves with horizontal trends are suggestive of low seasonality.

Diet reconstruction using enamel $\delta^{13}C_{carb}$

In paleoenvironmental studies, carbon isotopes principally come from ingested foodstuffs (Balasse & H. Ambrose, 2005; Cormie & Schwarcz, 1994; K. A. Hoppe et al., 2004). I applied similar assumptions to $\delta^{13}C$ as I did $\delta^{18}O$, mainly that the captured ratio of carbon isotopes in deer enamel is an authentic reflection of ingested foodstuffs. Seasonality can also be inferred from $\delta^{13}C$ through seasonal shifts in food availability and behaviorally driven selections food across seasons. The most relevant signal in stable carbon isotopes is the dietary preference towards plants with C_3 of C_4 photosynthetic pathways (Balasse, 2002). Potential sources for C_4 plants in deer diets include grasses during resource-scarce intervals, but more typical is the consumption of maize, a type of C_4 grass. Positive shifts in $\delta^{13}C$ values for both modern and archaeological deer may be interpreted as an increase in ingestion of maize due to proximity to agriculture.

Statistical tests

With these assumptions in mind, oxygen, and carbon curves for each deer's M2/M3 pair were plotted, as well as composite curves to assess relative seasonality. Each tooth's sequence of measurements were then pooled for comparison of means to assess for statistical differences across time intervals and tooth type. A box-and-whisker plot of median $\delta^{18}O$ and $\delta^{13}C$ values for each M2 and M3 tooth across both time intervals was used to determine the skewedness of the distribution. Differences between pooled means across tooth type and time interval was tested using a Wilcoxon-Rank-Sum test at the $p < 0.05$ alpha level, where sample sizes were not normally distributed, nor were the same size. A paired t-test was used to compare intra-individual means of $\delta^{18}O$ and $\delta^{13}C$ between tooth type where sample sizes were the same and normally distributed. The statistical power of the non-parametric Wilcoxon Rank Sum test is particularly low due to the

disparity in sample sizes - nine modern individuals versus three archaeological individuals. The results of statistics are discussed with caveats in Chapter 4.

Contextualizing modern enamel $\delta^{18}O$

To interpret $\delta^{18}O$ values from the archaeological deer enamel, I first sought to validate the relationship between $\delta^{18}O$ in modern deer enamel and known and modeled climate variables at the time of formation. I compiled three figures of climate data in the context of the Lower Chattahoochee River Valley – predicted regional $\delta^{18}O$ precipitation values, local river surface water $\delta^{18}O$, and monthly temperature and precipitation – herein I describe below.

1. I determined the predicted monthly $\delta^{18}O$ values for the Singer-Moye region using the Online Isotope Precipitation Calculator via waterisotopes.org (Bowen et al., 2023).
2. I constructed a curve of monthly measured surface water $\delta^{18}O$ from two nearby rivers, the Flint and Chattahoochee, using the Global Network of Isotopes in Rivers GNIR to determine minima, maxima, ranges and means of environmental surface water $\delta^{18}O$ values in the modern LCRV (IAEA/WMO, 2023).
3. I compiled temperature and precipitation amounts at daily and monthly scales for the duration of the modern deer's respective enamel formation to compare trends in enamel $\delta^{18}O$ seasonality to concurrent climate variables using NOAA's Global Historical Climatology Network.

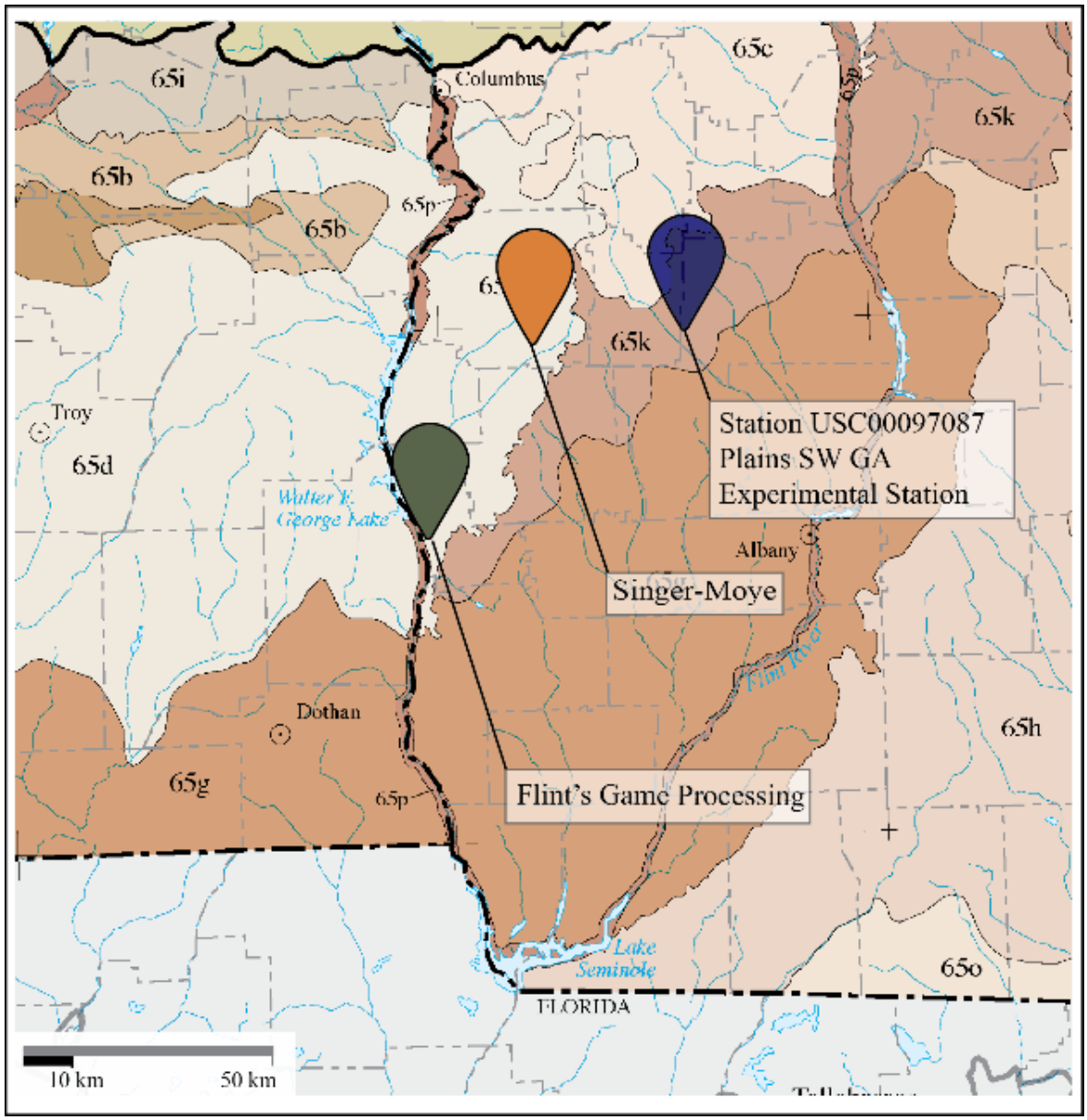

Figure 12: Location of NOAA climate monitoring station #USC00097087 in reference to Singer-Moye and Flint's Game Processor. Note that all three locations fall within the Southeastern Plains ecoregion designation (65). Map modified from Griffith et al., 2001.

Daily temperature and precipitation data to accompany modern deer teeth were accessed via NOAA NCEI Data Access tool. The data is part of the Global Historical Climatology Network – Daily, version 3 (GHCN-Daily) (Menne et al., 2012). Station # USC00097087 was chosen as the closest available Georgia data station to Flint's and Singer-Moye, (Figure 12).

In addition to the measured climate variables, I also compiled a figure to compare the means and ranges of various Georgia environmental $\delta^{18}O$ sources, summarized from waterisotopes.org. against measured deer enamel $\delta^{18}O$. To contextualize the archaeological and modern deer $\delta^{18}O$ against environmental $\delta^{18}O$, all deer enamel $\delta^{18}O$ values were converted to a VSMOW precipitation equivalent via the methods outlined in Rivera-Araya and Pilaar Birch, 2017.

CHAPTER 4

RESULTS

In this chapter, I present the means, minima, maxima, amplitude, and trends in $\delta^{18}O$ and $\delta^{13}C$ between the group of modern deer and archaeological deer from the LCRV. First, I briefly discuss the results of laboratory standards between the two batch submissions to CAIS. Then, individual $\delta^{18}O$ and $\delta^{13}C$ curves of each modern deer are introduced. I discuss $\delta^{18}O$ and $\delta^{13}C$ means, data spread, and associated ranges for both groups of deer. I also construct a composite curve of total $\delta^{18}O$ and $\delta^{13}C$ data points plotted as a time series to look for overall trends in amplitude and seasonality. I then expound upon $\delta^{18}O$ and $\delta^{13}C$ values between M2 and M3 teeth and variation therein through non-parametric Wilcoxon Rank Sum statistical analysis where data is non-normally distributed. Where normally distributed, a paired t-test is used. Finally, I conclude this chapter by contextualizing $\delta^{18}O$ environmental sources for the Singer-Moye deer and modern LCRV deer through the conversion of deer enamel $\delta^{18}O$ VPDB to equivalent meteoric $\delta^{18}O$ VSMOW.

A note of caution is necessary regarding the small sample size of Singer-Moye deer, before interpreting the following data (number of individuals = 3, NISP = 6). While similar archaeological studies use small sample sizes, the ideal number of individuals is likely closer to 6 (Fraser et al., 2021). Small sample sizes and non-normal distribution of archaeological $\delta^{18}O$ values require the use of a low-power statistical test. Conversely, Benfer (1968) has argued that small sample sizes are not undesirable in anthropology, as they deter the impact of 'lurking'

variables. The ramifications of the statistical methods used in this study are discussed further in Chapter 5.

4.1 Standards

Following stable isotopic analysis on the IRMS, the means and confidence intervals for each group of standards, archaeological bovine (LRM3) and modern bovine (LRM2), were calculated and plotted (Figure 13). All standards plot within the confidence intervals (C.I. 95%), indicating similar precision levels between batches at CAIS. Ruling out cross-contamination or significant analytical measurement error, the results of the two analyses follow.

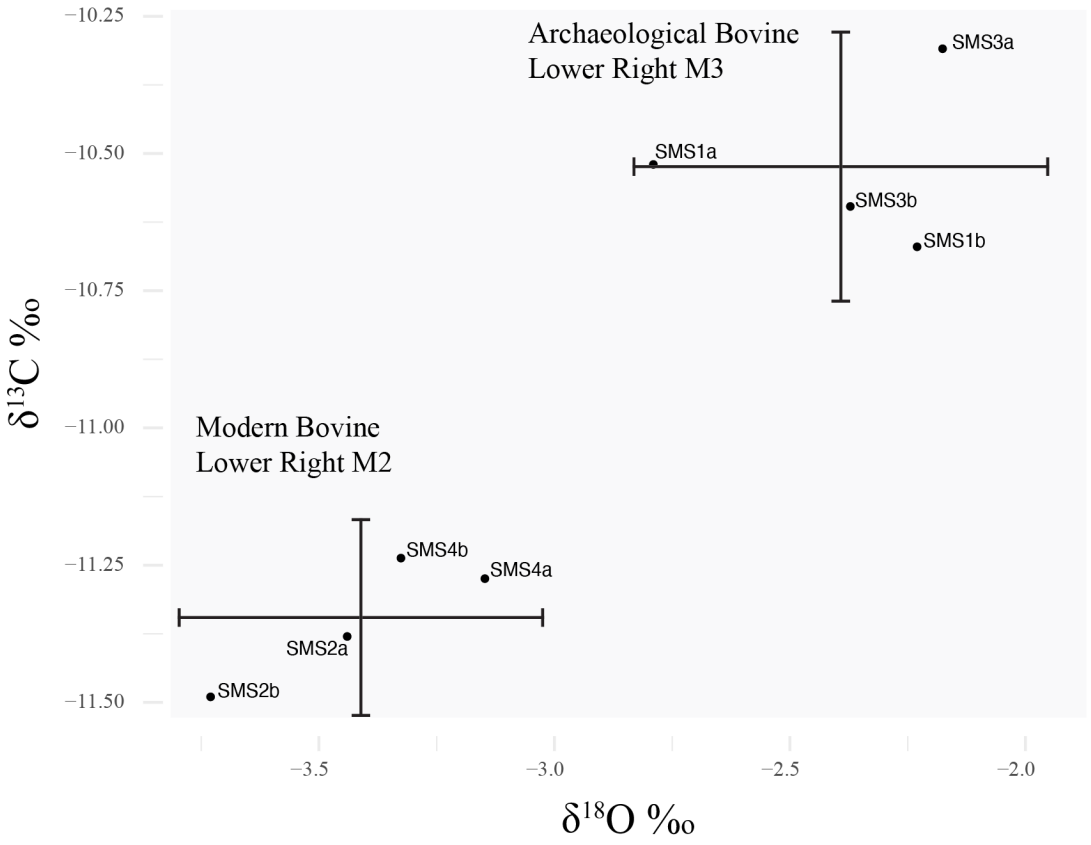

Figure 13: QUIP laboratory standards, two samples of archaeological bovine (LRM3) and two samples of modern bovine (LRM2), $\delta^{18}O$ and $\delta^{13}C$ values for two different batch submissions to the Center for Applied Isotopes. 95% confidence intervals plotted with all values occurring within the intervals, indicating no significant difference between batch runs.

4.2 Modern deer

M2, M3 pairs from nine modern deer (D1 – D9) left hemimandibles were submitted to CAIS for stable isotopic analysis of $\delta^{18}O$ and $\delta^{13}C$. Table 3 outlines the minima, maxima, ranges, means and standard deviations of each modern tooth. Figure 14 depicts the individual modern curves.

Modern deer enamel $\delta^{18}O$ has a mean of -1.6 ‰. Generally, the individual modern deer curves display their minimum in the M2 and maxima in the M3 (Figure 14). Variability in shape and trend is high across the entire sample group. For instance, D2 illustrates a highly seasonal curve, and D4 a significantly damped curve. In D2, the sinusoidal pattern is well defined with a minimum in M2 and a maximum in M3 separated by a 6‰ difference. D4 depicts no picture of seasonality, maintaining a near-horizontal trend. Oxygen curve amplitude is damped in individuals D4, D6, and D9. The highest amplitudes in oxygen curves are displayed in D1, D2, D5, and D7.

The primary drivers of $\delta^{18}O$ values in the modern dataset are environmental water sources; leaf water, standing water, surface waters, and anthropogenic water sources. This may explain why D2 exhibits a strongly negative $\delta^{18}O$ excursion in M2. Ostensibly, that individual's source water is depleted in ^{18}O isotopes. In Rivera-Araya and Pilaar Birch (2018), a control group of nonwild deer at the Whitehall Facility have similar values (-5 ‰). The deer at Whitehall were not capturing isotopes from their environment, but rather a controlled one in captivity with access to constant municipal water. In this study, similar variables could influence D2's M2 $\delta^{18}O$ values, for example, drinking regularly from a town reservoir or agricultural stock watering hole.

The average $\delta^{13}C$ value for the modern deer is -15.4 ‰, reflecting a primarily C_3 diet. Carbon curves for the modern group tend to exhibit damped curves, except for D3 and D4. The

variability in total carbon values for the modern deer seem driven by outliers from these two individuals. Both D3 and D4 display positive excursions, upwards to -10 ‰.

Table 3: Minima, maxima, ranges, means and standard deviation of $\delta^{18}O$ and $\delta^{13}C$ from modern white-tailed deer teeth. All δ values reported in per mil VPDB.

				$\delta^{18}O$ ‰ VPDB					**$\delta^{13}C$ ‰ VPDB**				
	Individual	Lab ID	Tooth	Min	Max	Range	Mean	Std	Min	Max	Range	Mean	Std
Modern	D1	SM8	LM2	-4.5	-2.7	1.9	-3.5	0.8	-16.0	-14.9	1.1	-15.1	0.5
		SM9	LM3	-1.0	1.7	2.7	0.0	1.1	-16.2	-15.5	0.8	-15.9	0.3
	D2	SM10	LM2	-5.9	-2.4	3.5	-3.5	1.6	-15.3	-14.7	0.6	-15.0	0.3
		SM11	LM3	-1.5	0.1	1.5	-0.7	0.6	-15.8	-14.3	1.5	-15.1	0.7
	D3	SM12	LM2	-3.7	-2.0	1.8	-3.0	0.7	-10.2	-9.5	0.7	-9.8	0.3
		SM13	LM3	-3.7	-0.3	3.3	-1.8	1.4	-14.6	-12.4	2.3	-13.7	0.9
	D4	SM14	LM2	-2.9	-1.5	1.5	-2.1	0.5	-16.8	-16.1	0.8	-16.3	0.3
		SM15	LM3	-1.8	-0.3	1.5	-1.0	0.7	-17.3	-16.7	0.6	-17.0	0.3
	D5	SM16	LM2	-3.7	-2.7	1.0	-3.1	0.4	-17.6	-17.0	0.6	-17.3	0.2
		SM17	LM3	-2.0	0.4	2.4	-0.3	1.1	-17.4	-16.6	0.7	-17.0	0.3
	D6	SM18	LM2	-3.1	-2.5	0.7	-2.7	0.3	-14.7	-14.1	0.6	-14.4	0.3
		SM19	LM3	-1.2	0.4	1.6	-0.2	0.6	-16.7	-16.3	0.4	-16.5	0.1
	D7	SM20	LM2	-2.6	-1.6	1.0	-2.3	0.4	-19.1	-18.5	0.6	-18.7	0.2
		SM21	LM3	-1.5	0.9	2.3	0.1	0.9	-18.9	-16.9	2.0	-17.7	0.8
	D8	SM22	LM2	-2.8	-1.5	1.2	-2.0	0.5	-14.6	-13.5	1.1	-13.9	0.5
		SM23	LM3	-0.9	0.7	1.6	0.0	0.6	-15.4	-15.1	0.3	-15.3	0.1
	D9	SM24	LM2	-3.0	-2.8	0.2	-2.9	0.1	-13.6	-12.4	1.2	-12.8	0.5
		SM25	LM3	-1.5	-0.4	1.1	-1.0	0.5	-15.8	-15.2	0.6	-15.5	0.2

LCRV, Modern deer (2023 C.E.)

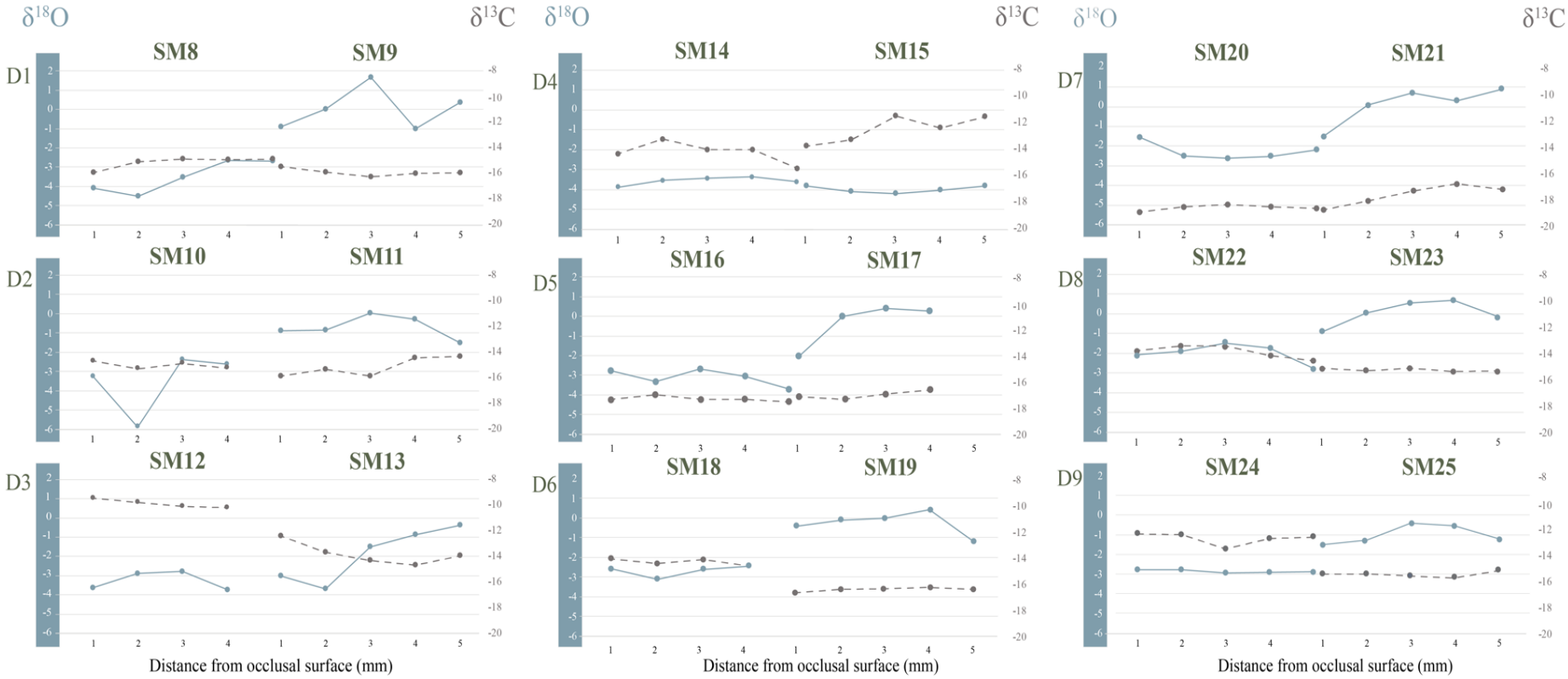

Figure 14: Oxygen and carbon curves for M2 and M3 pairs from nine modern deer, D1 – D9. Solid blue line represents $\delta^{18}O$, plotted on the primary Y axis. Dashed grey line represents $\delta^{13}C$. plotted on the secondary axis. Note that Y axis scale for the oxygen is 2 to -6.

4.3 Archaeological deer

Six teeth, representing at least 3 individual deer, were recovered from midden contexts at Singer-Moye and analyzed for $\delta^{18}O$ and $\delta^{13}C$. Figure 15 illustrates the oxygen and carbon curves for each individual deer. Table 4 outlines the minima, maxima, ranges, means and standard deviations of each archaeological deer, designated AD1, AD2 and AD3.

The archaeological deer present three scenarios: intensely seasonal oxygen curves in AD1, moderately seasonal in AD2, and damped seasonality in AD3. AD1 has the most extreme amplitude, showing a maximum in each molar, of 7.3 ‰ and 6.3 ‰, correspondingly. AD1's oxygen curve for just the M2 has a range of 9.6‰, the largest out of any single individual curve in this study. The secondary peak at the end of M3 is coeval with a peak in the carbon curve. A maximum value of 6.5‰ is also present at the terminus of M3. Data is missing from M2 due to unsuccessful laboratory analysis. Whether AD2 has a maximum in M2 like AD1 cannot be determined. The amplitude of the curve is 5‰, which is considerably high given the maximum amplitude from any modern deer is 3.5‰. AD3 diverges in trend from AD1 and AD2 by presenting a damped curve with a small range of 1.8‰, more similar to that of modern deer. The maxima and minima locations resemble that of AD1, though. Both M2 and M3 for AD3 end in peaks.

Singer-Moye mean $\delta^{13}C$ averages -13.7 ‰. The range in the amplitude of carbon curves differs widely from those of the modern. Deer from Singer-Moye display tightly concentrated carbon values with minimal spread. Carbon values have a range of 3‰, with a minimum and maximum of -14.74 ‰ and -11.76 ‰, respectively. In contrast, the modern $\delta^{13}C$ values have a spread of >10 ‰, between -19.05 ‰ and -9.46 ‰.

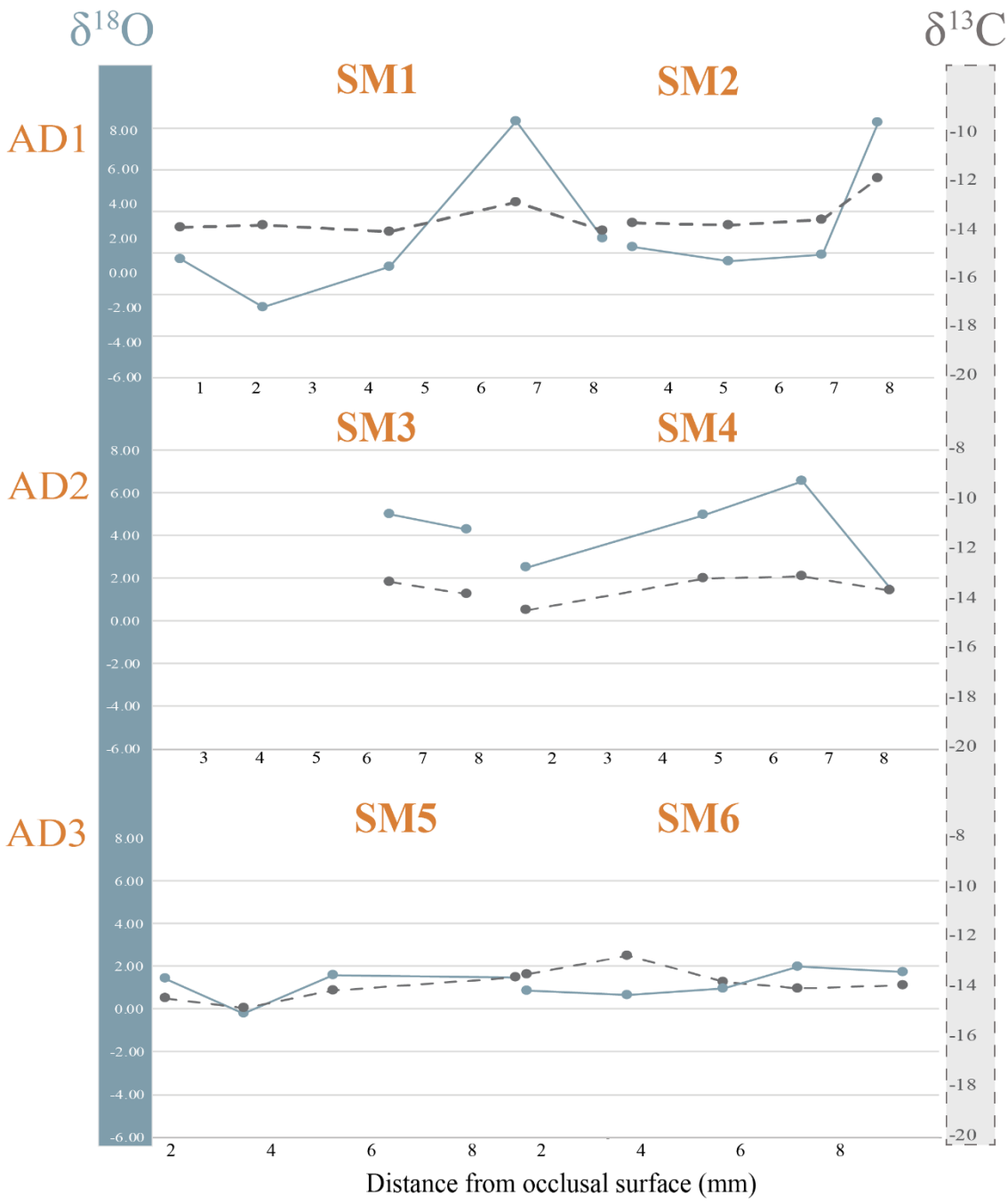

Figure 15: Oxygen and carbon curves for individual M2 and M3 pairs from archaeological deer of Singer-Moye, AD1 – AD3. Dashed grey line represents carbon, blue solid line represents oxygen. Note that Y axis scale for Oxygen is 8 to -6.

Table 4: Minima, maxima, ranges, means and standard deviation values of $\delta^{18}O$ and $\delta^{13}C$ from archaeological white-tailed deer teeth. All values reported in VPDB

				$\delta^{18}O$ ‰ VPDB					**$\delta^{13}C$ ‰ VPDB**				
	Individual	Lab ID	Tooth	Min	Max	Range	Mean	Std	Min	Max	Range	Mean	Std
Archaeological	AD1	SM1	LM2	-2.3	7.3	9.6	1.2	4.2	-14.0	-12.8	1.2	-13.6	0.5
		SM2	LM3	-0.4	6.3	6.7	1.5	2.8	-13.9	-11.8	2.2	-13.3	0.9
	AD2	SM3	LM2	4.2	5.0	0.7	4.6	0.5	-13.8	-13.3	0.4	-13.6	0.3
		SM4	LM3	1.5	6.5	5.0	3.9	2.3	-14.4	-13.1	1.4	-13.6	0.6
	AD3	SM5	RM2	-0.2	1.6	1.8	1.1	0.9	-14.7	-13.5	1.2	-14.2	0.5
		SM6	RM3	1.0	2.5	1.5	1.5	0.6	-14.3	-13.2	1.1	-13.8	0.5

4.4 $\delta^{18}O$ and $\delta^{13}C$ composite curves and comparisons

A regression was calculated to test whether oxygen and carbon isotopes are independent of each other. The correlation between oxygen and carbon stable isotopes for the modern and archeological groups is expressed by a weak r^2 value, 0.11 and 0.34, respectively. The assumption that different processes control the ratio of stable carbon and oxygen isotopes is validated in this study by the presence of a weak, insignificant correlation (Figure 16).

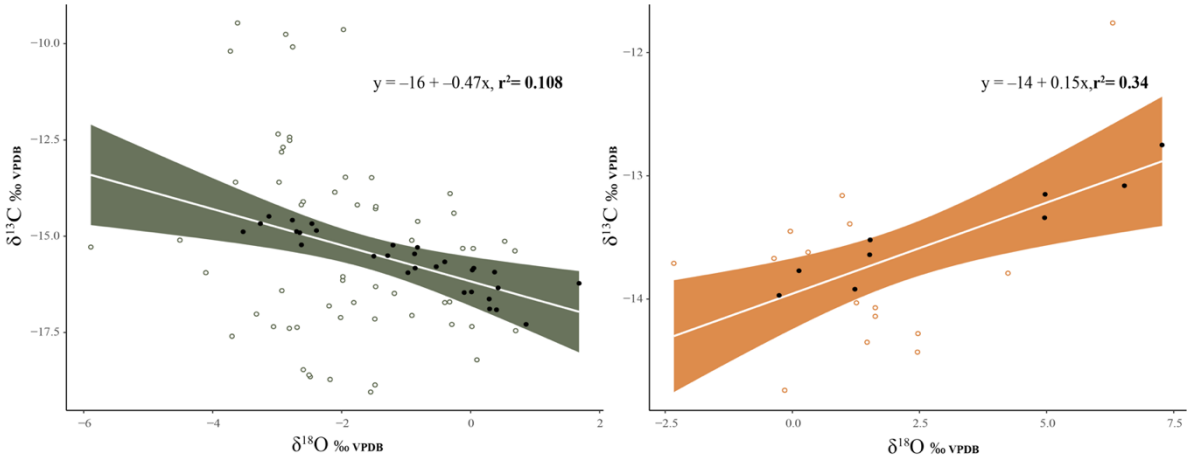

Figure 16: Correlation between $\delta^{18}O$ and $\delta^{13}C$ values for modern(left) and archeological(right) groups. Spread is diffuse and there is a weak, insignificant relationship.

Values were then pooled in all M2 and M3 to obtain an overall mean of $\delta^{18}O$ and $\delta^{13}C$ per group. The mean of the pooled values for both groups, along with maximum, minimum, standard deviation, and range, are outlined in Table 5. The pooled means are also presented in a boxplot (Figure 17), Finally, all values were also plotted in a time series as composite curves (Figure 18).

Table 5: Means, maximum, minimum, standard deviation and ranges for pooled $\delta^{18}O$ and $\delta^{13}C$ values for archaeological and modern enamel carbonate.

		Mean	Maximum	Minimum	Std	Range
$\delta^{18}O$	Modern	-1.6	1.7	-5.9	1.3	7.6
	Singer-Moye	2.3	7.3	-2.3	1.5	9.6
$\delta^{13}C$	Modern	-15.4	-9.5	-19.1	2.1	9.6
	Singer-Moye	-13.7	-11.8	-14.7	0.3	3.0

**all values reported VPDB*

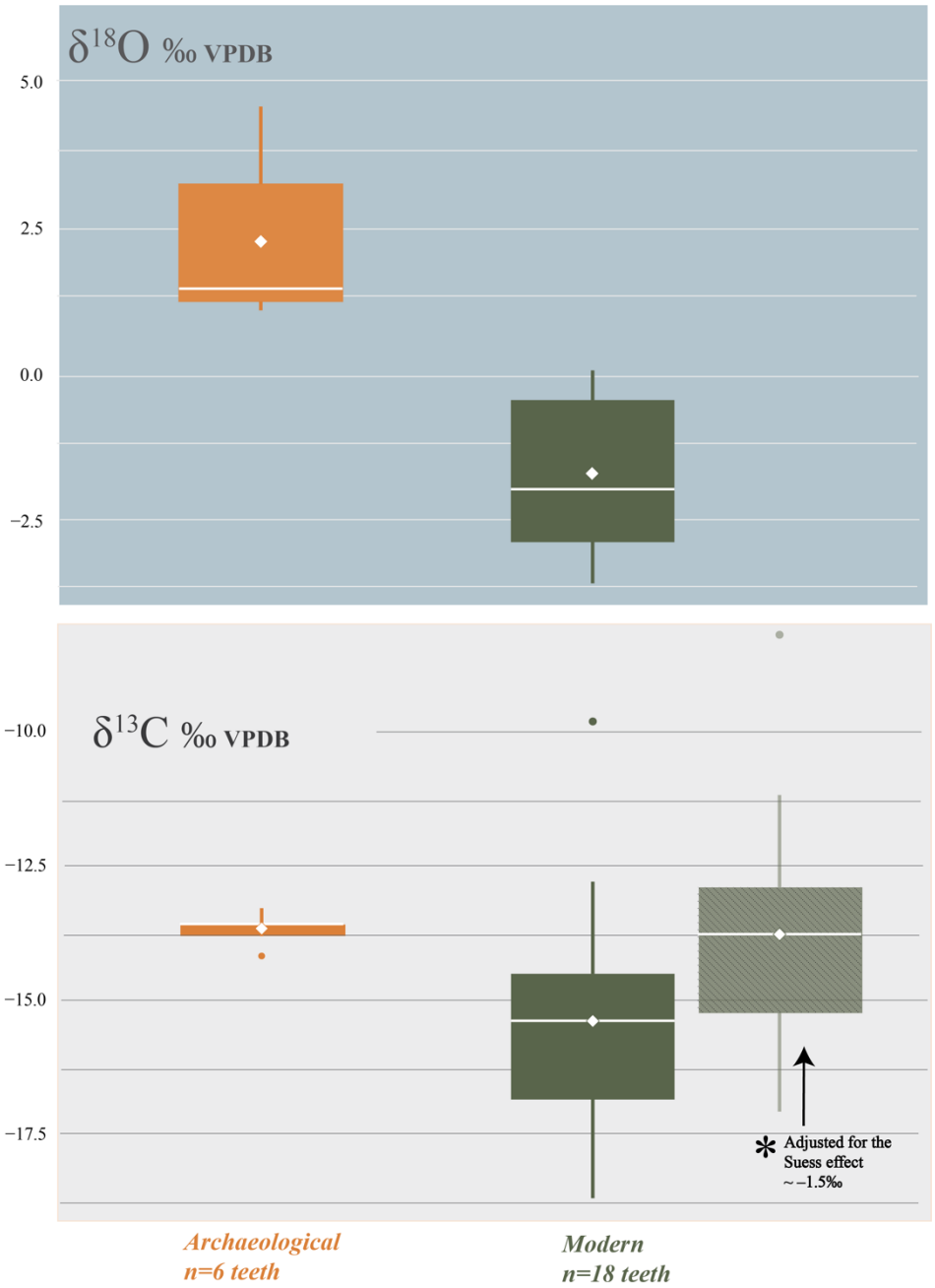

Figure 17: Combined total M2, M3 median values of $\delta^{18}O$ and $\delta^{13}C$ for archaeological (Singer-Moye, n=6) and modern (n=18) groups. White diamond denotes median value of distribution. Shaded boxes comprise 2nd and 3rd interquartile ranges, whiskers are 1st and 4th interquartile ranges. Outliers are dots that fall outside the whiskers. Note the modern $\delta^{13}C$ are depleted by an average of 1.5‰ – 2‰ due to Suess effect. All δ values reported in ‰ VPDB.

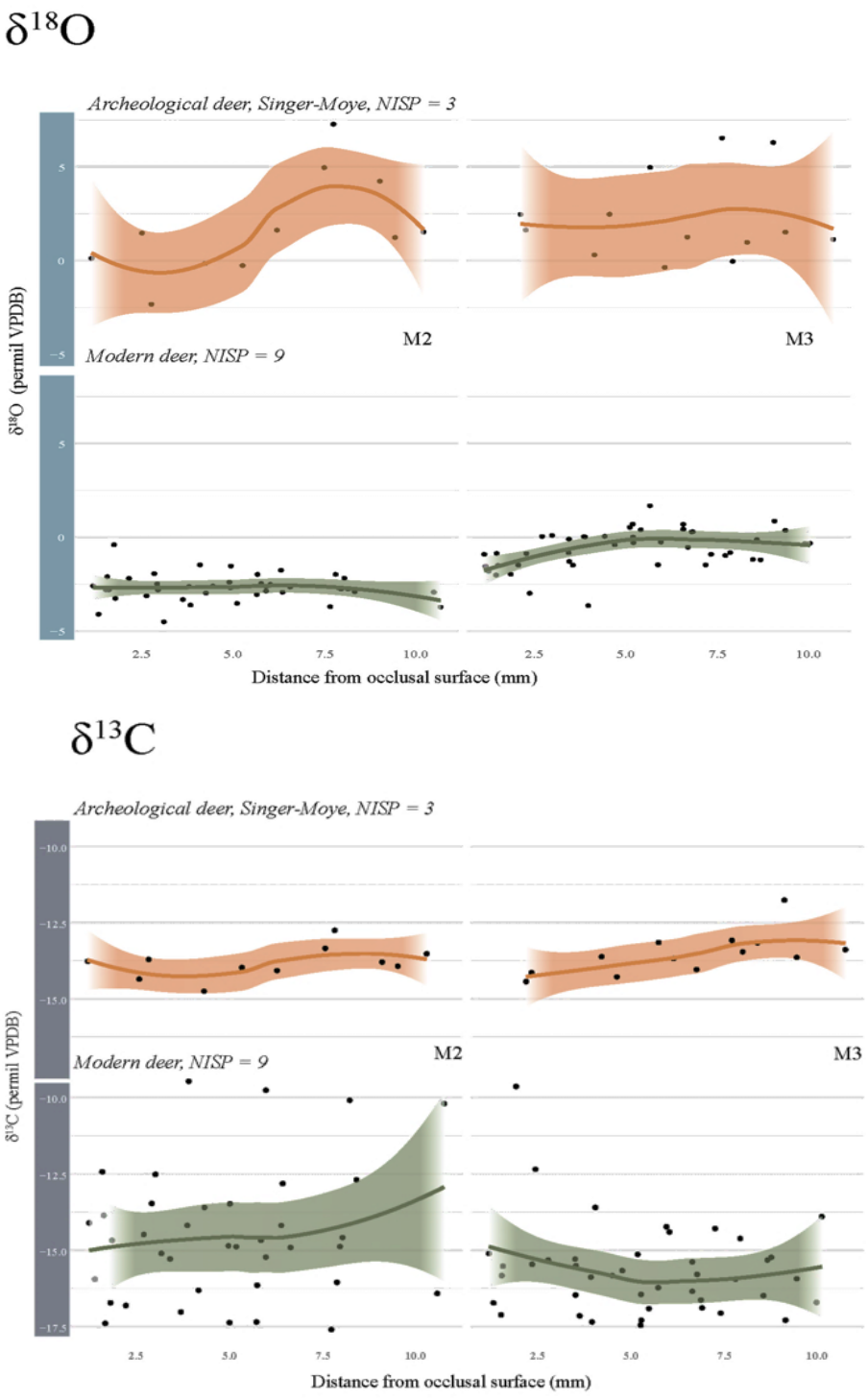

Figure 18: Composite curves of $\delta^{18}O$ and $\delta^{13}C$ values across M2 and M3, plotted as a time series. Time increases to the right. The average line was generated using a linear regression function, geom_smooth, in R package, ggplot2. Shaded relief represents a 95% confidence interval of composite values.

Carbon and the Suess effect

The modern $\delta^{13}C$ values are significantly lower than the archaeological values. A value of – 15.4‰ is calculated for the modern pooled $\delta^{13}C$ means. Compared to the archaeological pooled average of – 13.7‰, the difference of 2‰ can be explained by the Suess effect. In carbon stable isotope studies, a correction must be applied to measurements made after the industrial revolution. Enrichment of atmospheric CO_2 from the burning fossil fuels accounts for at least a 1.5‰ to 2‰ enrichment of $\delta^{13}C$ in modern samples (Dombrosky, 2019). When the modern mean value is corrected for the Suess effect, the two $\delta^{13}C$ mean values are negligibly different (Modern – 15.4‰, Archaeological -15.4‰ – 15.7‰). These averages suggest that white-tailed deer are ingesting similar ratios of C_3 to C_4 plants in both populations, across both time intervals.

Although the pooled $\delta^{13}C$ means are indistinguishable, the range and curve shape are distinctly at odds (Figure 18). Modern deer exhibit high spread of $\delta^{13}C$ values and high amplitudes. The archaeological samples in this study act in opposition with a tight spread and minimal amplitude. The variation in curve shape may be driven by behavioral differences between the sampled populations.

Inter-tooth variation: M2 and M3

To assess whether the median values of oxygen and carbon are significantly different between the archaeological and modern samples, the non-parametric Wilcoxon Rank Sum test is used in place of a t-test. This is to account for the small sample size (number of individuals=3, NISP=6) of archaeological values. I compared stable oxygen, and stable carbon in M2s and then again in M3s across archaeological and modern sample groups. Table 6 summarizes the results of these statistical comparisons.

Based on the Wilcoxon Rank Sum Test and a significance value of p=0.05, neither oxygen or carbon means for archaeological samples significantly differ across M2 and M3 (p=0.66; p=0.21). A paired t-test reveals a detectable difference between oxygen means across M2 and M3 in the modern samples (p=2.7e-5), but not in the carbon means (p=0.06).

When comparing means from specific molars (M2, M3) across time intervals, all combinations resulted in detectable differences between means except for M2 carbon values. Thus, M2 oxygen and carbon means from the Singer-Moye deer are significantly different than modern deer and M3 oxygen means in the Singer-Moye samples are significantly different than modern samples. However, because all four combinations pooled means were of different sample sizes and not normally distributed, the Wilcoxon Rank Sum test offers little statistical power.

Table 6: Summary of statistical tests comparing inter-tooth and inter-group $\delta^{18}O$ and $\delta^{13}C$

Value	Comparison	Test	Statistic, df	p value	H_o
Modern $\delta^{18}O$	M2 vs M3	Paired t-test	t = –8.5 df = 8	2.7 e-05	Reject
Modern $\delta^{13}C$	M2 vs M3	Paired t-test	t = 2.2 df = 8	0.06	Fail to reject
Archaeo $\delta^{18}O$	M2 vs M3	Wilcoxon Rank Sum	W = 3	0.66	Fail to reject
Archaeo $\delta^{13}C$,	M2 vs M3	Wilcoxon Rank Sum	t = -1.9 df = 2	0.21	Fail to reject
M2 $\delta^{18}O$	Archaeological vs. Modern	Wilcoxon Rank Sum	W = 0	0.01	Reject
M3 $\delta^{18}O$	Archaeological vs. Modern	Wilcoxon Rank Sum	W = 0	0.02	Reject
M2 $\delta^{13}C$	Archaeological vs. Modern	Wilcoxon Rank Sum	W = 7	0.28	Fail to reject
M3 $\delta^{13}C$	Archaeological vs. Modern	Wilcoxon Rank Sum	W = 1	0.02	Reject

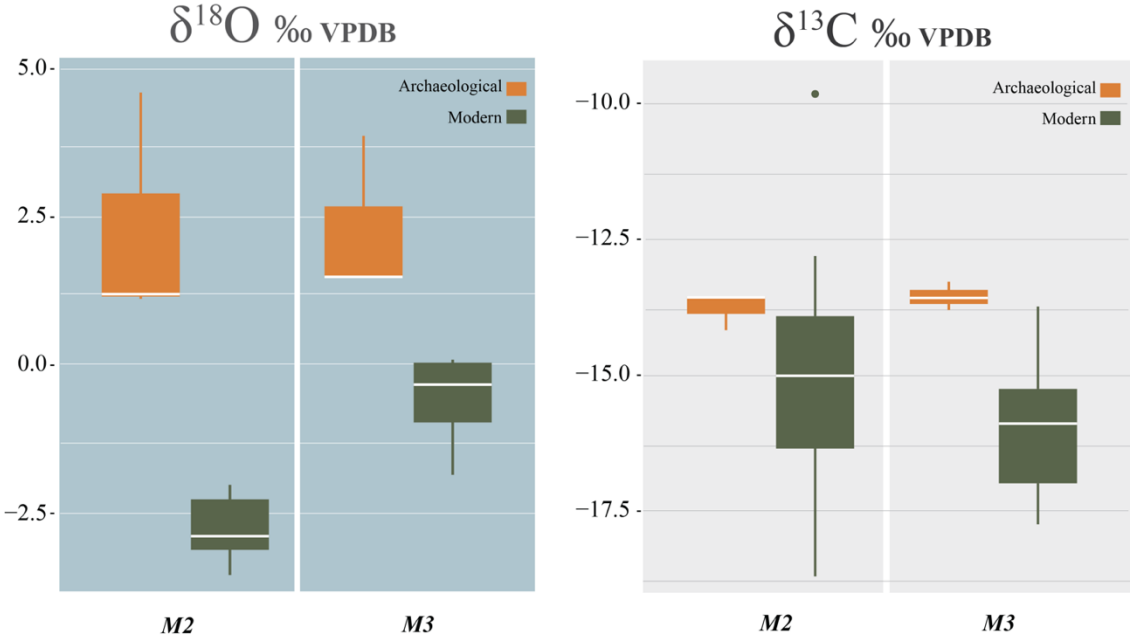

Figure 19: Inter-tooth, M2 and M3, distributions of $\delta^{18}O$ and $\delta^{13}C$ between archaeological and modern white-tailed deer enamel. Plots displays median, 1st and 2nd interquartile, and ranges for $\delta^{18}O$ and $\delta^{13}C$ values, respectively. The white bisector line in each box represents the median value for group.

Figure 19 summarizes the relationships outlined in Table 6 by plotting individual M2 and M3 pooled means of $\delta^{18}O$ and $\delta^{13}C$ for both archaeological and modern samples. In Figure 19, the M2 modern $\delta^{18}O$ values fall entirely outside the M3 modern $\delta^{18}O$ range. Archaeological $\delta^{18}O$ values overlap in ranges across M2 and M3 and share a similar skewed distribution across molar type.

The $\delta^{13}C$ boxplot in Figure 19 shows a near-inverted relationship between M2 and M3 across modern and archaeological samples. Carbon values for M2 and M3 of the modern group have a wide range of values while the archaeological ranges are much more constrained. In the case of $\delta^{13}C$, both modern and archaeological sample groups do not show considerable differences

in the medians but do in their distribution. Because the archaeological group is small in sample size, we'd expect less variation – whereas the large sample size of the modern group should capture more variation. This supports the fidelity of the archaeological samples and the assumption that outliers are not the driving the variation in the sample group.

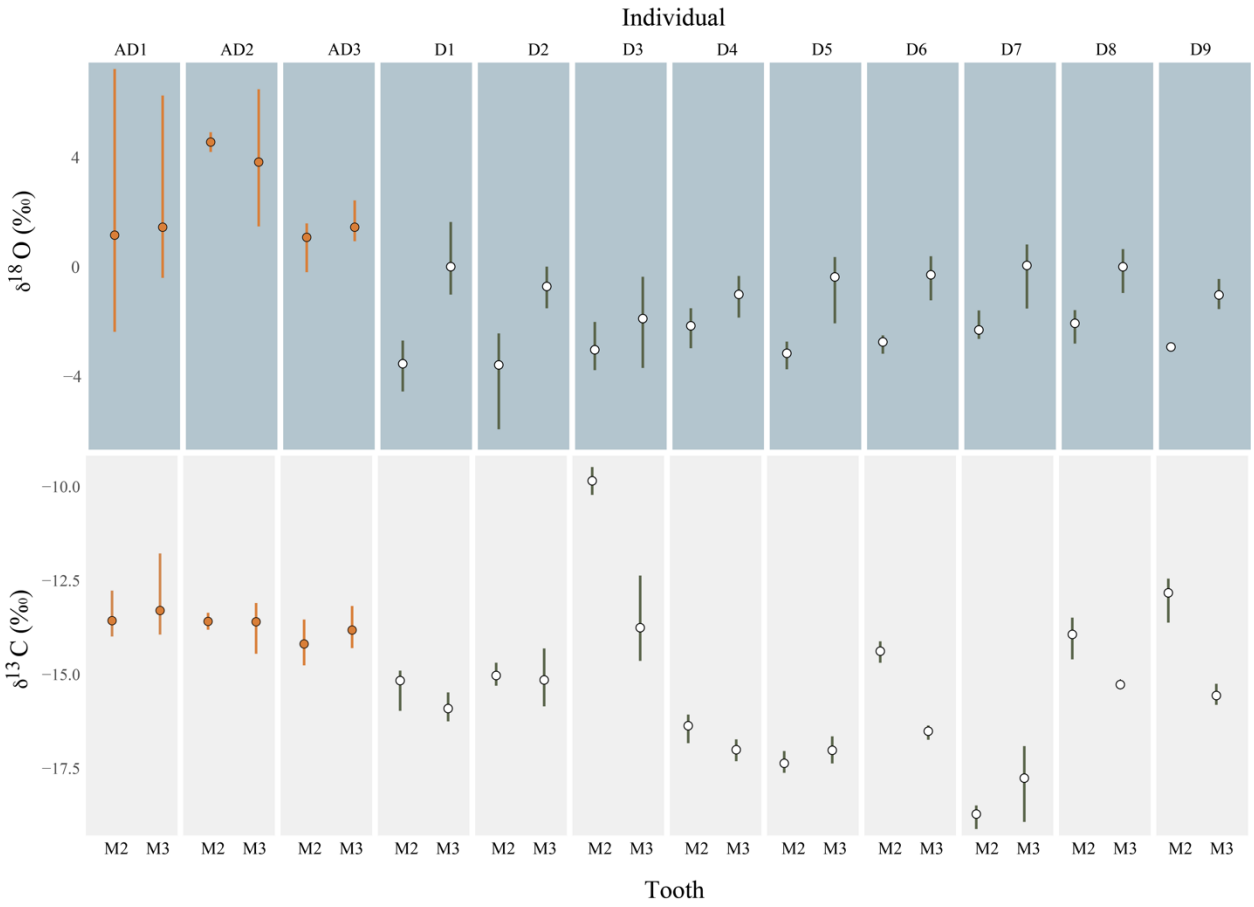

Figure 20: Inter-tooth means and ranges of $\delta^{18}O$ and $\delta^{13}C$ for all deer. Archaeological individuals in orange (AD1, AD2, AD3), and modern individuals in green (D1 – D9).

The inversion of spread between oxygen and carbon across the archaeological and modern groups is notable in Figure 20. In the oxygen ranges, archaeological samples have large spreads – which is interpreted as large amplitudes – versus the modern samples that display

restrained ranges and generally much more negative means. Conversely, the carbon values for archaeological samples are narrowly constrained and overlap with high precision. The modern carbon values show no discernable pattern in ranges or means – and seem to be composed of significant outliers.

4.5 Contextualizing modern enamel $\delta^{18}O$

To contextualize the $\delta^{18}O$ enamel values in the environment from where they are sourced, I compiled a summary of compare modeled precipitation, surface waters, meteoric waters and known deer enamel $\delta^{18}O$ in Figure 21. All the modern deer $\delta^{18}O$ values, this study, Rivera-Araya and Birch (2018) and Malasek et al., (2021), overlap with the average Georgia precipitation $\delta^{18}O$ VSMOW range. The archaeological samples from Singer-Moye overlap slightly, but the mean value falls well outside the average precipitation range.

Modeled oxygen isotope values for Singer-Moye from wateriosotopes.org (Figure 22) show a minimum in February, presumably a combination of cold temperatures, low evapo-transpirative potential, and increased precipitation. This minimum is also seen in the measured $\delta^{18}O$ values of surface water at both Flint River and Lower Chattahoochee (Figure 23).

The modern deer can be grouped into three distinct intervals of captured climate and environmental data based on when they were born: 2019-2020, 2020-2021, and 2021-2020. In each interval, the assumptions remains that deer are born in late spring and enamel in M2 begins forming between summer and late autumn and M3 forms between winter and early spring, capturing nearly 10 months of time (Morris, 2015).

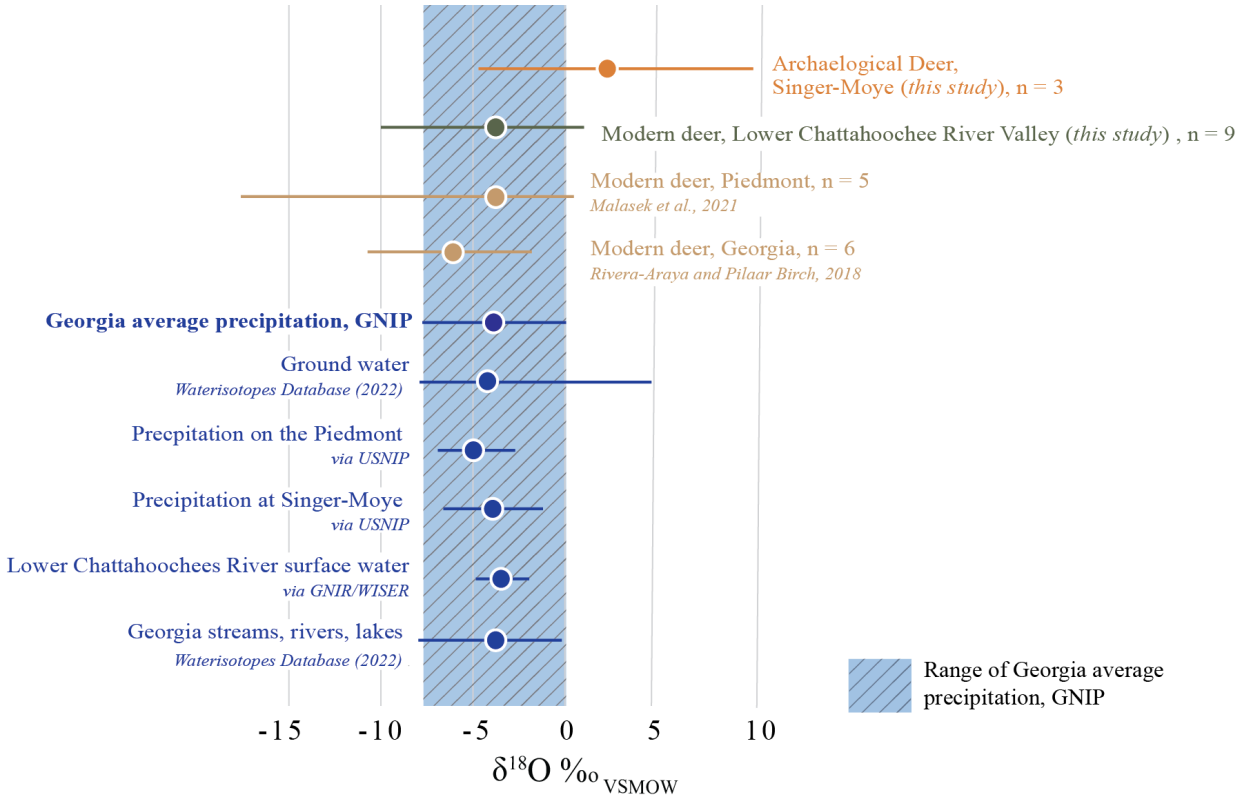

Figure 21: Comparison of $\delta^{18}O$ values, enamel versus environmental sources. Both archaeological and modern deer sample groups converted to equivalent enamel VSMOW meteoric $\delta^{18}O$. Plotted against measured and modeled source of $\delta^{18}O$ in Georgia environment. The mean value of each source is indicated by a point with range bars. The blue box bounds the range of precipitation $\delta^{18}O$ VSMOW value for Georgia based on GNIP measurements. Mean value for Archaeological, Singer-Moye deer (this study; orange) plot outside the range of average GA precipitation $\delta^{18}O$ VSMOW. Modern, LCRV deer (this study; green) and two additional modern Georgia studies (gold) plot within range of average GA precipitation $\delta^{18}O$ VSMOW.

Temperature and precipitation data from the corresponding intervals of environmental capture by the modern deer's enamel was compiled via NOAA's Global Historical Climatology Network. Daily data did not reveal any distinctive patterns in seasonality for precipitation. There is moderate seasonality noted in temperature (Figure 24). To further explore the relationship

between climate variables and seasonality in the LCRV, I aggregated the daily data into monthly averages and then replotted the curves against the individual modern deer who correspond to the interval (Figure 25). In all instances, precipitation is a year-round phenomenon, with a modest peak in the winter months.

A Bartlett's Test of Homogeneity of Variances was applied to test whether variances between the three years of climate intervals captured by the modern deer were significantly different from one another. Temperature across the three time periods captured by the modern sample of teeth does not show any significant variance ($K^2 = 0.005, df=2, p=0.10$). Precipitation displays significantly different variance but only between the 2019-2020 and 2020-2021 periods ($F = 6.6463, df = 10, p= 0.006$). However, when all three time periods are considered, there are no significant differences in mean values of precipitation amount and temperature ($p > 0.05$).

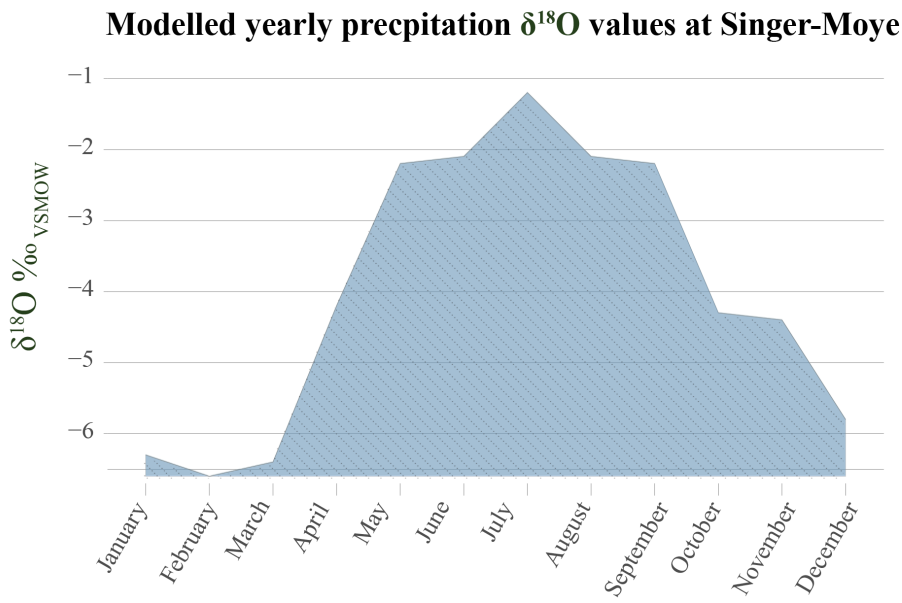

Figure 22: Interpolated average monthly meteoric $\delta^{18}O$ VSMOW for Singer-Moye area from waterisotopes.org (2023).

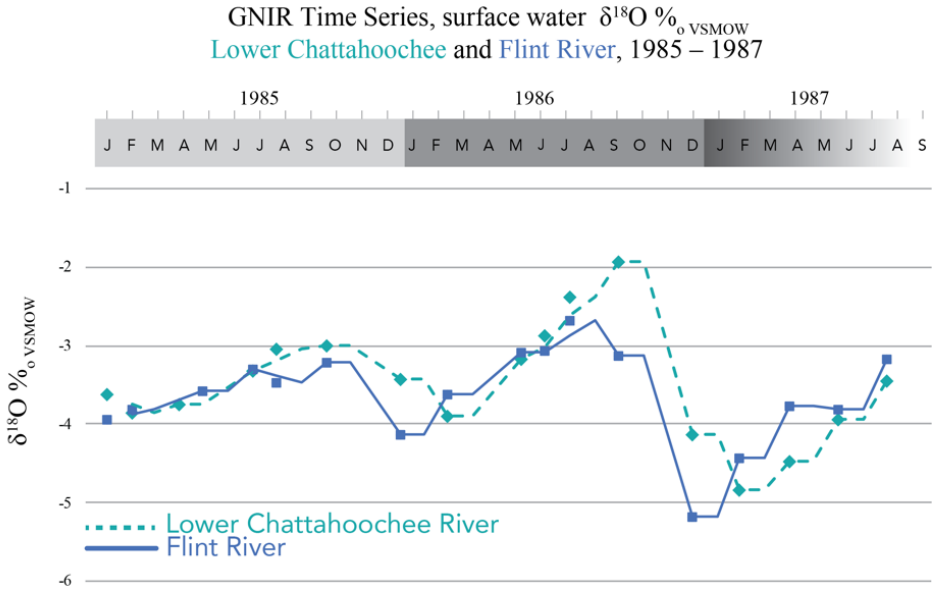

Figure 23: $\delta^{18}O$ measurements for surface water of the Lower Chattahoochee and Flint River, 1985 – 1987 Coplen and Kendall, 2000).

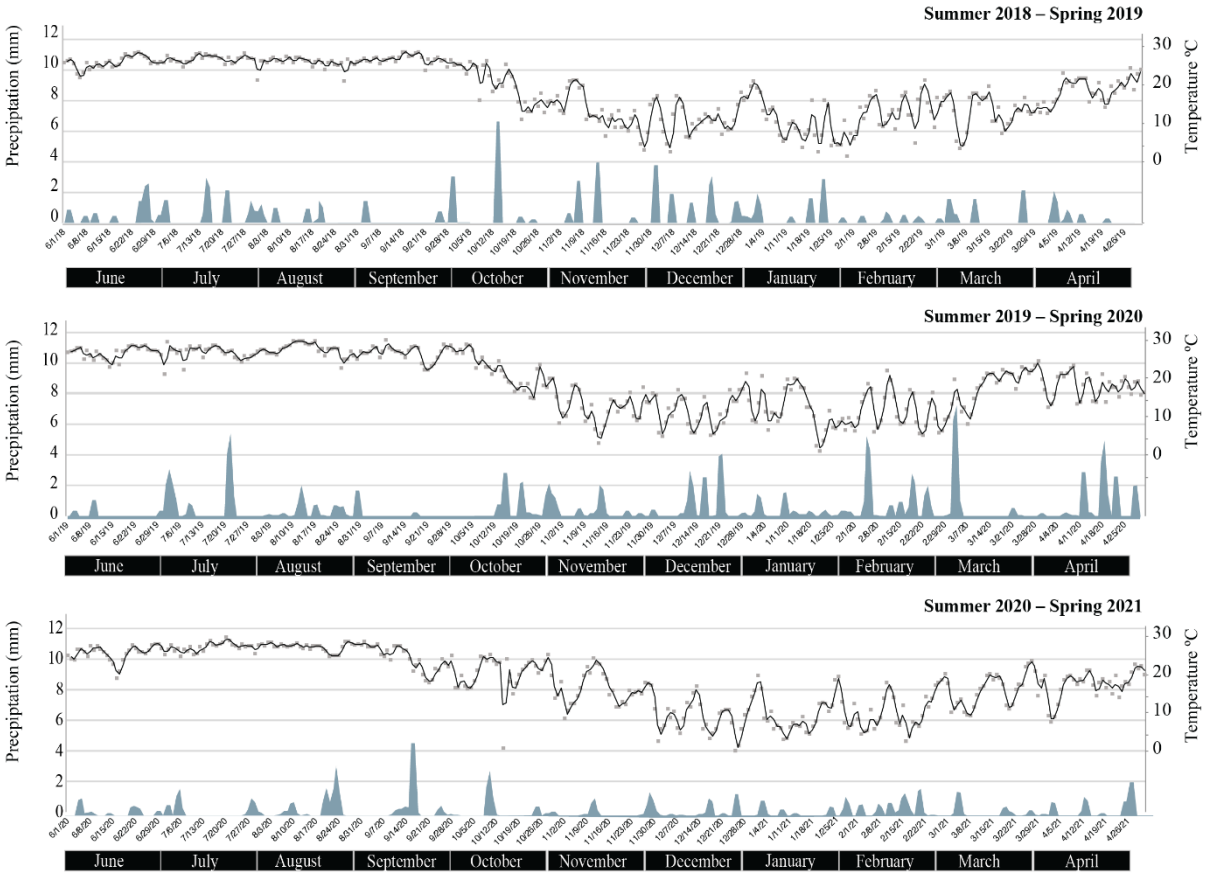

Figure 24: Daily temperature and precipitation values from station #USC00097087, Menne et al., 2012.

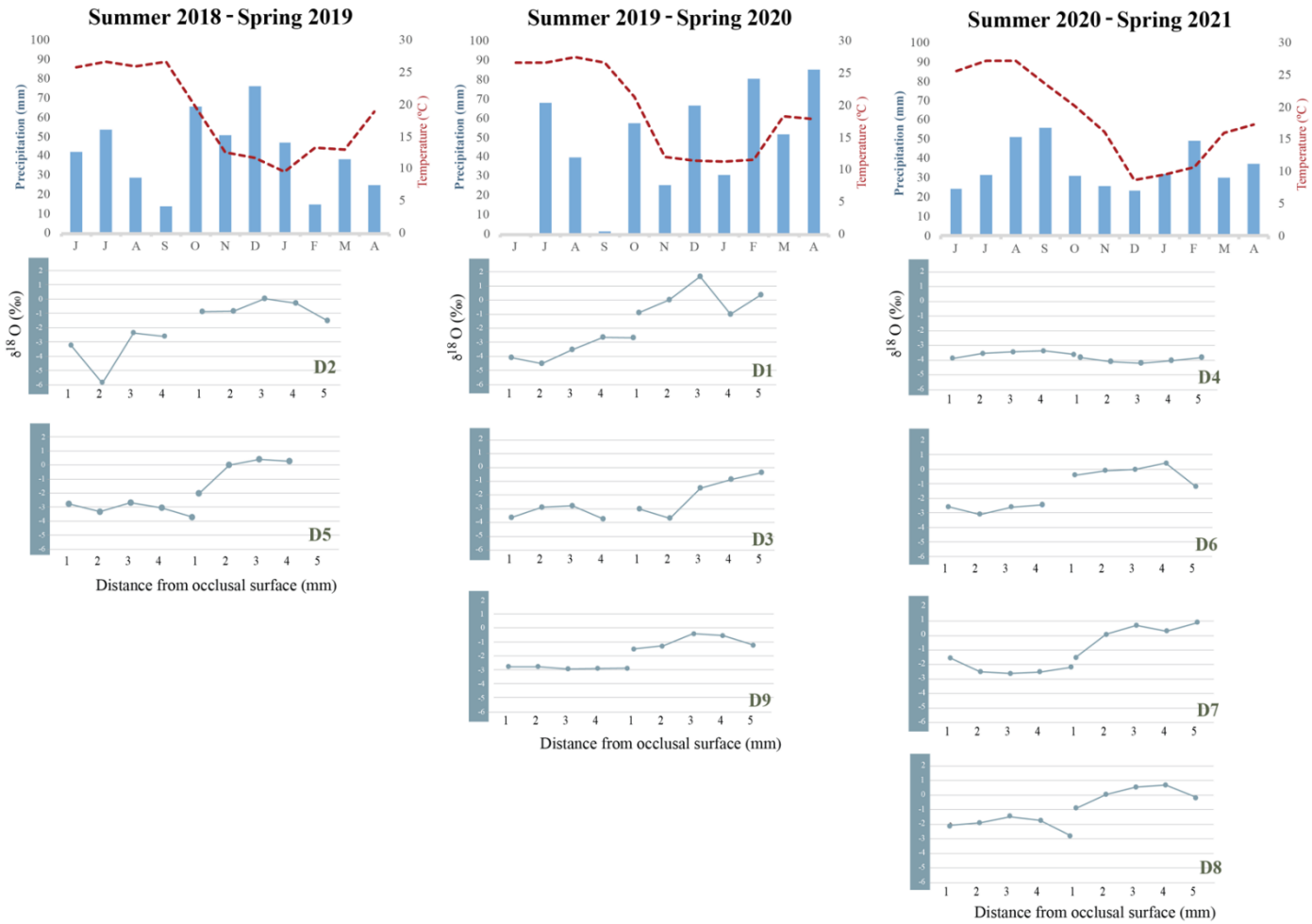

Figure 25: Aggregated monthly averages in temperature and precipitation for the LCRV with the associated group of modern deer. Note the x-axis scale for climate data (top graphs) ranges from June to April.

CHAPTER 5

DISCUSSION

In this chapter, I discuss the implications of the stable isotope results for paleoclimate and paleodiet interpretations at the onset of the Little Ice Age in the LCRV. I contextualize my findings in the broader literature and compare to two other studies of Georgia deer enamel.

5.1 Methodological considerations

Sample size and resolution

A physical constraint in using enamel carbonate, as opposed to enamel phosphate, is the weight percentage of carbonate in tooth enamel and the size of deer molars. The detection limit of the Thermo Gas Bench and Delta V IRMS requires a minimum 1 - 2 mg of material per sample. Because carbonate makes up 3% weight of total enamel material, serial sampling resolution is coarse – approximately 5 or 6 subsamples per tooth. The nature of deer molars, too, sets this physical limit. Deer are browsers, and their low-crowned molars average ~10mm in height. In high-crowned grazer teeth, like those of the pronghorn sheep for example, upwards of 14 sub-samples are possible per cheek tooth transect (Fraser et al., 2021). Herbivores with larger teeth may exhibit significant damping of primary isotopic signals as observed in elk (Kohn, 2004). It can be difficult to balance the potential loss of primary signal with sampling resolution, though deer offer a decent compromise.

Small sample sizes in ungulate enamel studies are not uncommon, often ranging from 4 to 10 individuals (Fraser et al., 2021). It is important to maintain caution when interpolating broad-

scale vegetation and climatic patterns when sample sizes are less than five (Malasek et al., 2023). While more archaeological teeth from Singer-Moye would have proven ideal for this study, the six teeth from three individuals will provide an initial basis for interpretation into the paleoenvironment and climate of the LCRV. Consideration of the spatial-temporal scale of my research objectives guides the interpretations in Chapter 4, where individual snapshots into seasonality from the three archaeological specimens are not interpolated across the entirety of the 1300 – 1400 CE window but rather offer insight into the variation and means as compared with the modern sample set.

Validity of primary isotopic signature

In this study, I assume that the isotopic measurements from the archaeological enamel represent a primary environmental signature and have not been altered or compromised. One benefit of using enamel structural carbonate is its resistant nature to diagenesis and secondary alteration, thus concern for isotopic disequilibrium is minor. Swisher noted in her faunal analysis that the midden's faunal material was burned at various strata (Birch and Brannan, 2016b). If the archaeological deer enamel was heated significantly, the integrity of structural carbonate may be compromised and thus be more susceptible to diagenesis. Post-mortem processing of the deer skulls may have compromised the fidelity of the enamel isotopic signature. The First Nations of Iroquoian Ontario, for example, commonly boiled entire deer skulls for feasting events (Morris, 2015). The diagenetic impact can be assessed by calculating the spacing between carbonate and phosphate values of enamel $\delta^{18}O$ (Koch et al., 1997). If a similar practice was applied by the Mississippian peoples at Singer-Moye, the alteration would remain an unlikely scenario, as structural carbonate is stable up to 225 º C for up to 4 hours (Munroe et al., 2008).

Deer Age and Sex

Aging deer using eruption timing and tooth wear replacement (TWR) are well-established methods in hunting and processing communities but misclassification is common (Adams & Blanchong, 2020). Eruption of permanent molars occurs in known intervals that bracket age classes broadly to below a year and a half of age (fawn) or above (yearling). After a year and a half of age, TWR is required to further age the deer. Severinghaus (1949) systematically assessed qualitative occlusal surface wear to determine stages and associated age classes. When applying Severinghaus' method, variations in regional diets must be taken into consideration. Generally, deer lose about 1 mm of height on their crown per year of wear (Sauer, 1984). In the Northeast U.S. where soft winter vegetation is sparse, woody branch buds and hard mast have a greater impact on enamel wear. In contrast, deer in sub-tropical environments with access to soft forbs and herbs will experience considerably less enamel wear and, as a result, skew younger in age classifications.

Another method to assess deer age is to examine the cementum annuli. The accreting layers of collagen fibers beneath the enamel-root junction amass as a dark and dense layer during the winter months and a light band in the summer (Sauer, 1984). Cementum annuli can be counted for either incisors or molars that have been mounted on a thin section (Gilbert, 1966; Kay, 1974). Both methods, TWR and cementum annuli are susceptible to misclassification, especially to an untrained eye. Because I do not consider myself experienced with deer aging, the possibility of misclassification of my modern samples is something to contend with. Regardless of their age classification, the modern deer in this study represent - with certainty - climatic intervals over the last three years. As observed in the daily and monthly temperature and precipitation values in

Chapter 4, climate variability between the three years is minimal. In future work, strontium should be considered to elucidate age class if it is not known in modern groups (Schultz & Flyger, 1965).

Sex was not known for either archaeological or modern specimens in this study. Sexual dimorphism in deer is observed in behavior and diet, particularly, when and where they feed and the ecological range they inhabit (Smith, 1991). For example, males tend to wander farther during rutting and mating seasons. In my modern samples, some of the carbon outliers could be explained by rutting males deviating from group behavior and seeking unique food sources.

Assigning the sex of white-tail deer requires noting the absence or presence of antlers, or examination of the frontal and pelvic bone (Purdue, 1983; Thompson, 1958). Attempts to sex deer based on mandibular physiology and teeth are inconclusive if age is not well constrained (Rees, 1969, 1971). Deer are sexually dimorphic in physiology, with males being larger, and thus significant differences can be determined between bone measurement means. When applying this method to a small sample size, problems and uncertainty arise due to bias in sampling, and large overlaps between mean values (Purdue, 1983). These problems can be remedied with extensive comparison to a modern faunal collection that share the same lineage (Martínez-Polanco & Cooke, 2019; Purdue, 1983). Unfortunately, towards the end of the 19th century, Georgia's native deer were almost entirely eradicated, reaching their lowest populations in 1920 (Newsom, 1984). Deer from Texas and Wisconsin were used to restock Georgia populations (Jeffries, 1975). Modern Georgia collections may not, then, serve as a direct comparison to the archaeological populations. If sex was known, possible variation in the $\delta^{13}C$ variation from the modern deer may very well be explained.

5.2 Interpretations of paleoclimate and paleodiet

Amount effect and $\delta^{18}O$

Typically, when temperatures are high and humidity is low, oxygen stable isotope ratios become more positive – or enriched. In low ambient temperatures and highly humid conditions, oxygen isotope ratios become depleted. Thus, we would expect M2, which forms in the peak temperatures of Georgia summer and early autumn, to be enriched relative to the M3. This is not the case in this study as the M3 stable oxygen values are more positive than those of the M2s in each individual deer, modern and archaeological, which contradicts expected trends.

The median of pooled $\delta^{18}O$ values indicates a 2‰ enrichment of M3 relative to M2 in the modern group. A paired t-test reveals significant differences between $\delta^{18}O$ in M2 and M3 in the modern group (*t=-8.54, df=8, p= 2.7e-05*). In contrast, the archaeological deer display the same trend but to a much lesser degree. Differences between median oxygen values from M2 to M3 in AD1 and AD3 are less than 0.5‰. In AD2, there is greater depletion in oxygen values from M2 to M3 by ~ 1‰ but this is likely a byproduct of data loss and the incompleteness of AD2's M2 curve.

Malasek et al. (2023) observed the same unusual M2 depletion for a group of modern wild Georgia deer. The authors posit that the M3 is not enriched, but the M2 is depleted relative to the M3 due to the amount effect. The amount effect is the dominant control on stable oxygen isotope ratios in warm, humid environments (Akers et al., 2017). Since precipitation amounts show a negligible difference in amounts year-round, the M2 enamel is capturing a warm, humid climate with high amounts of precipitation, reflecting an enriched $\delta^{18}O$ in the summer and autumn months. Akers (2017) found that the correlation between surface temperatures and stable oxygen isotope ratios is insignificant on the Atlantic coastal plain ($r^2 = 0.1 – 0.2$). Oxygen ratios

are then likely to be explained by the amount effect in Georgia's subhumid climate instead of temperature that dictates ratios in higher latitudes.

The difference in spacing between overall M2 and M3 $\delta^{18}O$ values reflects differing seasonality between the archaeological and modern groups. The mean value of $\delta^{18}O$ between M2s and M3s in the archaeological samples is negligibly different. The M2 is not depleted significantly relative to the M3. This may be indicative of higher summer temperatures and drier summer conditions leading to a decreased amount effect captured by the M2. This supports the Mann et al. (2009) proxy model results of a high-temperature excursion on the Southeastern coastal plain. Arid events are noted elsewhere in the eastern US during the Little Ice Age, causing droughts that brought on food stress years in the 13th through 15th centuries (Meeks and Anderson). This result is also in agreeance with those paleoenvironmental reconstructions from the Vacant Quarter during the same interval (1300 – 1400 C.E.).

The combined mean oxygen values in the archeological deer agree that overall hotter conditions may be the underlying cause. High temperatures would lead to increased evapotranspiration and concentration of heavy isotopes in leaves and surface waters where deer subsequently record more positive oxygen ratios. The availability of effective moisture declined considerably between 1200-1400 A.D. in the mid-continental mound site of Cahokia (Pompeani et al., 2021). Drought conditions would have had profound impacts on the agriculturally dependent Mississippian societies. The Mississippian Chiefdom's primary crop, corn, was particularly vulnerable to drought conditions, as it is estimated that 48 inches of rain were required every year to sustain crops in Mississippian societies (Bowne, 2013). The overall more positive oxygen ratios captured in the enamel from Singer-Moye may be a snapshot into a resource-stressed time, approaching the abandonment of the settlement. The archaeological deer confirm the

temperature anomaly noted by Mann et al. (2009) and increased seasonality with their stable oxygen isotope values.

Carbon

Between the modern group and archeological group, $\delta^{13}C$ pooled means in M2 molars are not detectably different at the $p < 0.05$ alpha level ($W=7$ $p = 0.28$). In contrast, $\delta^{13}C$ pooled means from M3 molars are detectably different $p < 0.05$ alpha level ($W=1$, $p = 0.02$). However, recall the use of the low-power Wilcoxon Rank Sum test for groups of different sample sizes. The result of the statistical detectability are problematic at face value. This is further compounded when the interaction of the Suess effect is considered which renders the means virtually identical. In contrast to their similar means, the spread and variation of individual curves may illuminate differences in access to foodstuffs.

$\delta^{13}C$ curves for the modern deer from the LCRV display wide spreads and varying amplitudes. For instance, D3 and D9 exhibit positive excursions upwards of – 10 ‰ in their M2 molars. Contradictory trends in D5 and D7 exhibit near horizontal curves with average values of – 18‰. D3 and D9 would indicate a higher proportion of C_4 diet, as opposed to D5 and D7, whose $\delta^{13}C$ values suggest an almost absence of C_4 plants. Morris (2015) compiled archaeological structural carbonate values for Ontario white-tailed deer. High maize consumption was interpreted from Neutral Ontario and Maya cultural complexes with average carbon values of – 10 ‰. Despite the large spread of values in modern deer curves, no seasonal trends are detected. This is consistent with the findings in Rivera-Araya and Pilaar Birch (2018) who noted there were no detectable seasonal patterns in $\delta^{13}C$ values in wild deer from Georgia. The absence of general seasonal patterns in modern $\delta^{13}C$ curves, yet high range (9.6‰), suggests-individual-specific behaviors may

be the underlying cause. Supplemented diets due to agricultural and anthropogenic sources in the LCRV, where farms and livestock are common, may explain the modern $\delta^{13}C$ values.

The $\delta^{13}C$ maxima for the archaeological specimens occur in the M3, or between late autumn and early spring. This may reflect increased ingestion of grain residue from agricultural sources as a diet supplement during winter conditions (Smith, 1991). The overall negative mean values of $\delta^{13}C$ in archaeological deer and their small ranges indicate a consistent diet intake of C_3 to C_4 ratio. A diet supplement with corn, not seasonally, but year-round could be explained by the accessibility to agricultural plots, gardens, and corn granaries common in Mississippian settlements (Scarry & Scarry, 2005). This explanation is reinforced by examples of year-round co-habitance and mutualism between deer and humans in the Neotropics. Peoples of the Pre-Columbian Neotropics were known to leave piles of maize on the outskirts of agricultural fields to bait the deer into staying nearby and minimizing disturbance to the main crops (Sugiyama et al., 2020). In the Cumberland region, garden hunting provided year-round sustenance to the late Woodland People (Peres, 2023). It is likely that the communities of the Lower Chattahoochee River Valley took advantage of similar techniques and thus deer maintained close habitation and feeding regimes near maize rich agricultural plots.

Temporal dissimilarities in scale between populations

The scalar difference in time intervals between the two groups presents challenges in comparison. The archaeological teeth are sampled from a wide interval of 100 years (1300 – 1400 C.E.) and are not directly dated. Rather, relative dating in relation to their stratigraphic positions can be inferred. However, this also presents its own suite of issues. Archaeological strata are susceptible to sediment reworking and bioturbation. Seemingly innocuous earthworms can disturb

the sediment and end up moving samples significantly (Darwin, 1892; Armour-Chelu and Andrews, 1994). With those factors considered – the midden contexts containing the archaeological deer teeth represent the period of Singer-Moye's densest occupation. The entirety of the middens contains seriated ceramics with associated production periods (Brannan, 2018). Therefore, whether the individual deer represented in midden contexts were deposited synchronously, or across long time spans, remains to be resolved.

The modern deer from the LCRV represent three succeeding years of climate signatures. Conversely, the archaeological data may represent a cluster of years, the same years, or widely dispersed years across the 1300 – 1400 C.E. interval. The $\delta^{18}O$ mean values should not be interpreted as representative of a general climate trend across the entire interval as the distribution of the archaeological deer's lifetimes across the interval of 1300 – 1400 C.E. is not known. For instance, although we observe authentic representations of the LCRV climate between 2018 – 2022 in the modern deer enamel, the three archaeological deer may offer a distorted window into three highly unusual years of climate between 1300 – 1400 CE. Still, when considering the overall $\delta^{18}O$ mean values, the archaeological samples have discernably higher values than the modern samples, by +3 ‰. Assessing whether the disparity in $\delta^{18}O$ mean values is representative of a average climatic signals at the onset of the LIA requires the addition of radiocarbon dates and more samples. Future work in this area should look to build a strong chronology of Mississippian deer enamel proxies in Georgia. Another way to remedy the dissimilarity in the temporal scale is the expansion of the modern sample population from a tightly constrained interval to one that encompasses deer from multiple decades.

Two additional modern Georgia deer enamel paleoenvironment proxy studies have been executed in the past decade (Rivera-Araya and Pilaar Birch, 2018; Malasek et al., 2023). Rivera-

Araya and Pilaar Birch used two groups of deer, wild and nonwild. The modern nonwild (n = 6) deer span birth years from 1984 to 1991. The modern wild deer represent randomly sampled individuals across Georgia over the past 50 years (n=7; Rivera-Araya and Pilaar Birch, 2018). Malasek et al. examined five known age deer from the Piedmont of Georgia, all born in the spring of 2014 (n=5). The aggregate of the three modern deer enamel isotopic datasets to this study expands the temporal sampling resolution to the order of decades. Figure 26 present a summary of modern GA deer studies and the associated lifetime distribution of deer sampled.

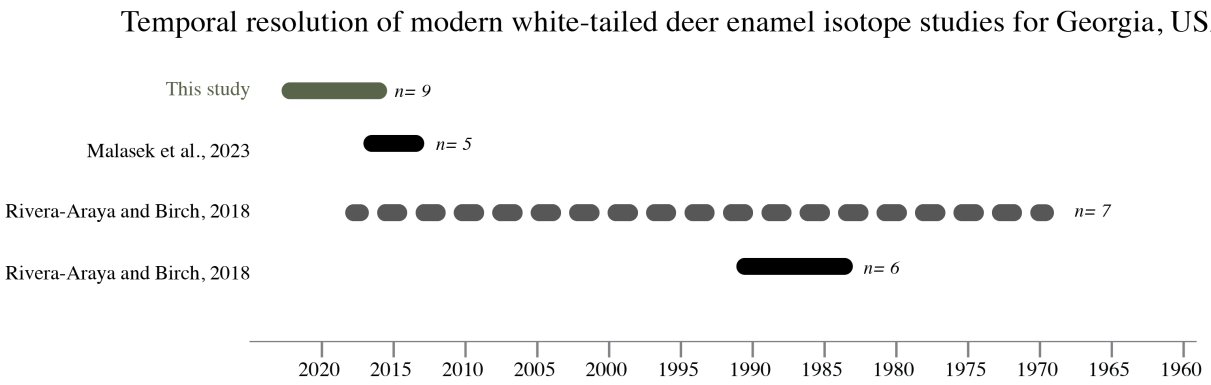

Figure 26: Summary of modern deer enamel isotope studies in Georgia, USA, and sample deer lifetimes.

The mean value of $\delta^{18}O$ across all modern deer groups including this study, Rivera-Araya and Pilaar Birch, 2018 and Malasek et al., 2023, is approximately - 3‰, even more negative than just the modern LCRV deer, whose average is -1.6‰. Henceforth, the +3 ‰ difference in $\delta^{18}O$ mean values from the modern to the archaeological likely indicates a climatic trend and is not, in fact, a product of skewed distribution and outliers,

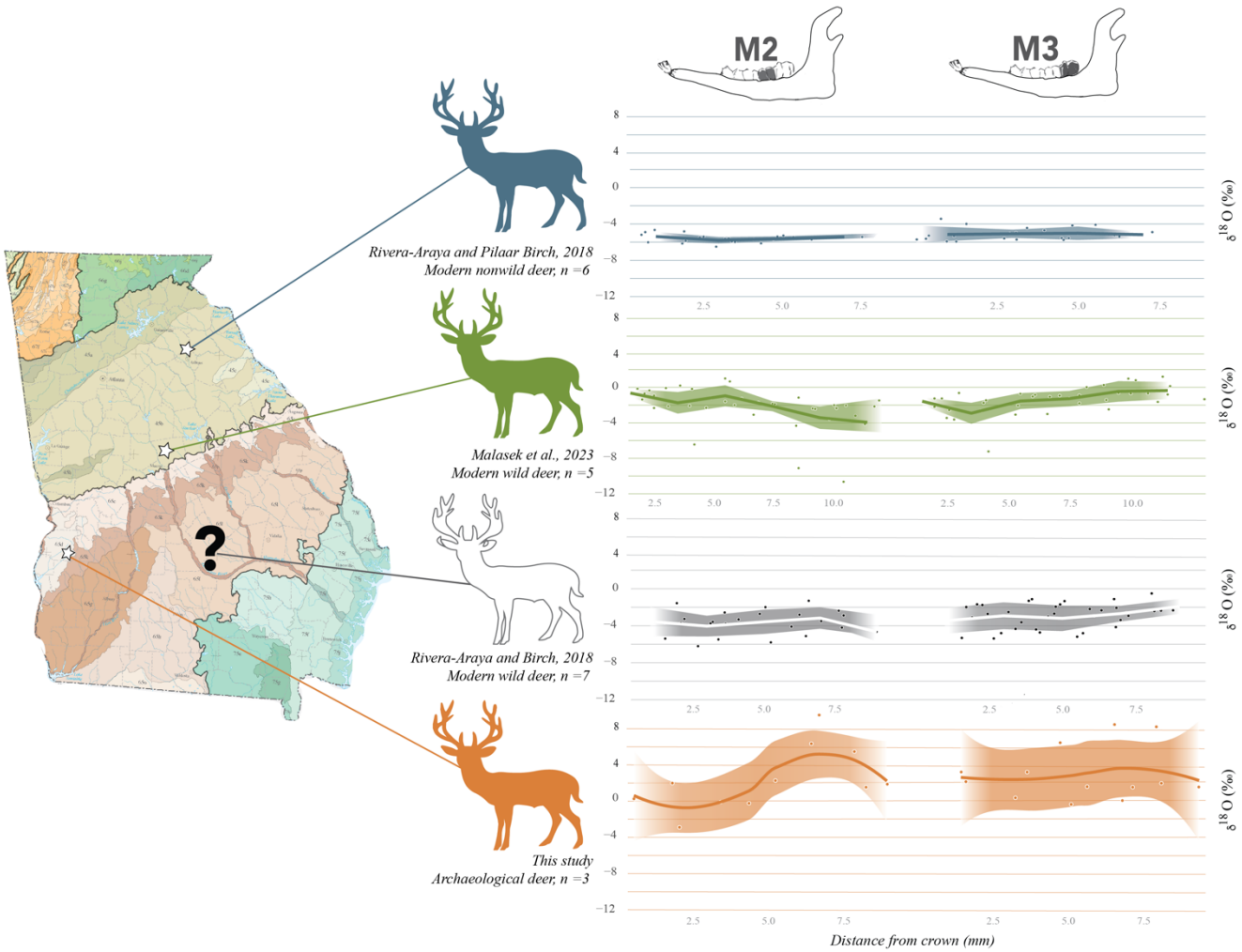

Figure 27: Comparative composite curves $\delta^{18}O$ between modern deer studies from Georgia and archaeological deer from Singer-Moye. Shaded regions represent 1-sigma of the moving average. Two groups with known localities, blue (Rivera-Araya and Birch, 2018; N=6) and green (Malasek et al., 2023; N=5) and one group with unknown provenience white (Rivera-Araya and Pilaar Birch, 2018; N=7) are represented. In blue, White-tailed deer from the Whitehall Research Facility, Athens GA. In green, wild white-tailed deer from Piedmont Wildlife Preserve Seasonal. In white, several deer from unknown provenience (Rivera-Araya & Pilaar Birch, 2018). Archaeological deer from Singer-Moye orange, N=3. All measurements in VPDB. Ecoregion map of Georgia modified from Griffith et al., 2001.

Figure 27 contextualizes $\delta^{18}O$ values from Singer-Moye against other known modern deer from Georgia. In blue, Rivera-Araya and Pilaar Birch's (2018) deer from the Whitehall Research facility in Athens, GA were nonwild, and represent a controlled population that does not reflect the true environmental variation of oxygen isotopes. The group was raised in captivity, thus given a controlled water source, resulting in no captured seasonality between the M2 and M3 intervals. The mean values of the nonwild deer are the most negative of the groups, – 7‰. This oxygen value reflects a depleted water source, potentially from a well that utilizes groundwater. Figure 28 shows groundwater values in the Piedmont region of Georgia are more depleted than enriched surface water or leaf water values that are reflected by wild deer.

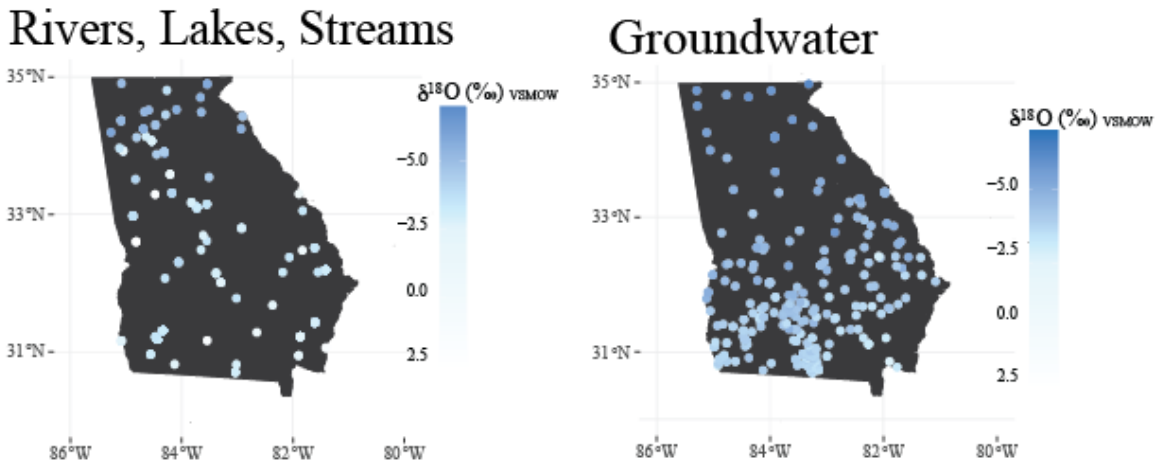

Figure 28: Physio-geographic distribution of measured $\delta^{18}O$ across Georgia for surface waters (rivers, lakes, and streams) and groundwater. Data from waterisotopes.org. Stable oxygen values were reported in VSMOW.

The group of wild deer with unknown regional provenance from the same study displays a wide spread of stable oxygen ratios that average – 4 ‰ (Rivera-Araya and Pilaar Birch, 2018). This value agrees with another wild, modern deer group from Malasek et al., (2023). The deer from the Piedmont Wildlife Preserve also exhibit peaks in late summer, middle fall, and early

spring – concomitant with the group of wild, unknown provenience deer (Rivera-Araya and Pilaar Birch, 2018). The difference between the two modern, wild groups of deer is the capture of sinusoidal nature in intra-tooth $\delta^{18}O$. Clear trends in maxima and minima in the wild, unknown provenance group (in white) are potentially masked by the variety of regional provenances. For instance, if the wild, unknown group are composed of deer from the both the northern Blue Ridge and coastal Barrier Islands of Georgia, significantly different $\delta^{18}O$ values are expected inter-geographic province. Coastal deer are expected to have enriched $\delta^{18}O$ values due to the Rayleigh rain out effect (Dansgaard, 1964).

Between all three groups of modern deer from Georgia, the range of $\delta^{18}O$ is approximately half that of the archaeological group from Singer-Moye (Figure 26). The sinusoidal pattern reflecting seasonality is much more prominent in the archaeological group than in any modern curve. Additionally, the archaeological mean value of $\delta^{18}O$ is considerably more positive than any modern group, by at minimum 2 ‰ and at higher estimates closer to 6 ‰. This discrepancy in mean $\delta^{18}O$ between the archaeological group and modern groups cannot be explained solely by sample size. The likelihood that all three deer from Singer-Moye do not represent average conditions across their associated time interval and environment is also not supported by the fact that inter-individual amplitude shape and size between the three deer varies. The presence of a higher amplitude and more positive mean value of $\delta^{18}O$ supports that it was indeed more seasonal and hotter at the time of tooth formation of the Singer-Moye deer, during the peak of the Little Ice Age.

Timing of the Medieval Warm Period and Little Ice Age

The archaeological deer teeth examined in this study are dated to the interval 1300 to 1400 C.E. This period marks the transition from the Medieval Warm Period to the Little Ice Age, according to recent estimates, placing the ending of the MWP at 1250 C.E. and the beginning of the LIA at 1400 C.E. (Mann et al., 2009). Determining whether the teeth reflect the climate patterns of the MWP or the LIA is challenging due to the poorly defined beginning and end dates for those periods. In the SE US, the warming associated with the MWP is presumed to have happened later than in other regions (Hughes & Diaz, 1994). It is notable that across both the MWP and LIA, the southeastern and mid-Atlantic US experienced significant temperature anomalies (Cronin et al., 2003; Mann et al., 2009). So, whether the teeth capture a late MWP, or early onset of the LIA, the southeastern coastal plain appears to have been anomalously warmer than its surrounding regional climate.

CHAPTER 6

CONCLUSION

White-tail deer tooth enamel archives sub-annual variation that reflects the climate and diet of their localized environments, providing a high-resolution proxy tool in climate reconstruction. In the Lower Chattahoochee River Valley, modern deer capture the humid, sub-tropical climate and precipitation amount effect in $\delta^{18}O$ values. $\delta^{13}C$ values of modern deer suggest variety in individual feeding behavior and access to C_4 foodstuffs. The tooth enamel results of archaeological deer from Singer-Moye either reflect hotter and drier conditions during the LIA or a decreased influence of the amount effect during the summer, or both. Though statistical analyses are limited due to small sample size, the archaeological specimens display discernable patterns in seasonality in the Lower Chattahoochee River Valley. Higher amplitudes and positive means in the archaeological M2 and M3 curves are characteristic of hotter, drier, and more seasonal conditions during the onset of the Little Ice Age. The LCRV's location on the Southern Atlantic Coastal Plain, where major atmospheric and oceanic streams intersect, may subject it to localized micro-climate conditions that conflict with the surrounding regional climatic trends. The prevalence of a Pleistocene Thermal Enclave in the Southeast supports the idea that amongst regional cooling, the coastal plain deviates climatically and offers refuge to warmer-tolerant biota (Russell et al., 2009).

Archaeological deer enamel from Singer-Moye provide a unique snapshot into the climate and timing of human settlement of the LCRV in the late Woodland Period. As anthropogenic climate change intensifies, looking to the past for an understanding of how this unique region will

respond will inform our predictions and actions in the future. Modern populations of deer remain ever-present on the Georgia coastal plain and local museums are repositories for zooarchaeological and comparative deer collections. With the aid of accessible modern analogs, the zooarchaeological deer offer a unique opportunity to compile robust, high-resolution paleoclimate and paleodiet reconstructions at Singer-Moye and other Mississippian mound sites.

REFERENCES

Adams, D. M., & Blanchong, J. A. (2020). Precision of cementum annuli method for aging male white-tailed deer. *PLOS ONE*, *15*(5). https://doi.org/10.1371/journal.pone.0233421

Akers, P. D., Welker, J. M., & Brook, G. A. (2017). Reassessing the role of temperature in precipitation oxygen isotopes across the eastern and central United States through weekly precipitation-day data. *Water Resources Research*, *53*(9), 7644–7661. https://doi.org/10.1002/2017WR020569

Ambrose, S. H., Buikstra, J., & Krueger, H. W. (2003). Status and gender differences in diet at Mound 72, Cahokia, revealed by isotopic analysis of bone. *Journal of Anthropological Archaeology*, *22*(3), 217–226. https://doi.org/10.1016/S0278-4165(03)00036-9

Anderson, D. G., Stahle, D. W., & Cleaveland, M. K. (1994). Paleoclimate and the Potential Food Reserves of Mississippian Societies: A Case Study from the Savannah River Valley. *American Antiquity*, *60*(2), 258–286. https://doi.org/10.2307/282140

Balasse, M. (2003). Potential biases in sampling design and interpretation of intra-tooth isotope analysis. *International Journal of Osteoarchaeology*, *13*(1–2), 3–10. https://doi.org/10.1002/oa.656

Balasse, M., & H. Ambrose, S. (2005). Distinguishing sheep and goats using dental morphology and stable carbon isotopes in C 4 grassland environments. *Journal of Archaeological Science*, *32*, 691–702. https://doi.org/10.1016/j.jas.2004.11.013

Behrensmeyer, A. K. (1978). Taphonomic and Ecologic Information from Bone Weathering. *Paleobiology*, *4*(2), 150–162.

Ben-David, M., & Flaherty, E. A. (2012). Stable isotopes in mammalian research: A beginner's guide. *Journal of Mammalogy*, *93*(2), 312–328. https://doi.org/10.1644/11-MAMM-S-166.1

Benfer, R. A. (1968). The desirability of small samples for anthropological inference. American Anthropologist, 70(5), 949-951.

Birch, J., & Brannan, S. (2015). *Summary of the 2015 Field Season at Singer-Moye (9S2W)*. *43*((1 & 2)), 95-100.

Birch, J., & Brannan, S. (2017). *Summary of the 2017 Field Season at Singer-Moye (9S2W): The Singer-Moye Achaeological settlement History (SMASH) Project*. 7.

Blitz, J. H., & Lorenz, K. G. (2006). *The Chattahoochee Chiefdoms*. University of Alabama Press. http://ebookcentral.proquest.com/lib/ugalib/detail.action?docID=547617

Blumenthal, S. A., Cerling, T. E., Smiley, T. M., Badgley, C. E., & Plummer, T. W. (2019). Isotopic records of climate seasonality in equid teeth. *Geochimica et Cosmochimica Acta*, *260*, 329–348. https://doi.org/10.1016/j.gca.2019.06.037

Bocherens, H., Mashkour, M., Billiou, D., Pellé, E., & Mariotti, A. (2001). A new approach for studying prehistoric herd management in arid areas: Intra-tooth isotopic analyses of archaeological caprine from Iran. *Comptes Rendus de l'Académie Des Sciences - Series IIA - Earth and Planetary Science*, *332*(1), 67–74. https://doi.org/10.1016/S1251-8050(00)01488-9

Bowen, G. J., & Wilkinson, B. (2002). Spatial distribution of $\delta^{18}O$ in meteoric precipitation. *Geology*, *30*(4), 315–318.

Bowne, E. E. (2013). *Mound Sites of the Ancient South: A Guide to the Mississippian Chiefdoms*. University of Georgia Press.

Brannan, S. (2018). The settlement archaeology of Singer-Moye, a large 14th-century town in the Chattahoochee Valley (Doctoral dissertation, University of Georgia).

Brannan, S., & Bigman, D. P. (2014). Ground Penetrating Radar and Resistivity Results from Mounds D and F at Singer-Moye (9SW2). *Early Georgia*, *42*(2), 14.

Brannan, S., & Birch, J. (2016a). Settlement ecology at Singer-Moye: Mississippian history and demography in the Southeastern United States. In *Settlement ecology of the ancient Americas* (pp. 69-96). Routledge.

Brannan, S., & Birch, J. (2016b). *Summary of the 2016 Field Season at Singer-Moye (9SW2): Introducing the SingerMoye Archaeological Settlement History Project (SMASH)*. *44*((1 & 2)), 101-108.

Britton, K., Grimes, V., Dau, J., & Richards, M. P. (2009). Reconstructing faunal migrations using intra-tooth sampling and strontium and oxygen isotope analyses: A case study of modern caribou (Rangifer tarandus granti). *Journal of Archaeological Science*, *36*(5), 1163–1172. https://doi.org/10.1016/j.jas.2009.01.003

Cobb, C. R., & Butler, B. M. (2002). The Vacant Quarter Revisited: Late Mississippian Abandonment of the Lower Ohio Valley. *American Antiquity*, *67*(4), 625–641. https://doi.org/10.2307/1593795

Cook Hale, J. W., & Sanger, M. (2020). Cultural spaces and climate change: Modeling Holocene archaeological settlement patterns on the coastal plain of the southeastern United States. *Journal of Anthropological Archaeology*, *59*, 101198. https://doi.org/10.1016/j.jaa.2020.101198

Cormie, A. B., & Schwarcz, H. P. (1994). Stable isotopes of nitrogen and carbon of North American white-tailed deer and implications for paleodietary and other food web studies. *Palaeogeography, Palaeoclimatology, Palaeoecology*, *107*(3–4), 227–241. https://doi.org/10.1016/0031-0182(94)90096-5

Cronin, T. M., Dwyer, G. S., Kamiya, T., Schwede, S., & Willard, D. A. (2003). Medieval Warm Period, Little Ice Age and 20th century temperature variability from Chesapeake Bay. *Global and Planetary Change*, *36*(1), 17–29. https://doi.org/10.1016/S0921-8181(02)00161-3

Dansgaard, W. (1964). Stable isotopes in precipitation. *Tellus*, *16*(4), 436–468. https://doi.org/10.1111/j.2153-3490.1964.tb00181.x

Darwin, C. (1892). The formation of vegetable mould, through the action of worms, with observations on their habits. J. Murray.

Dombrosky, J. (2019). A ~1000-year 13C Suess correction model for the study of past ecosystems. *The Holocene*, *Vol. 30*(3), 474–478.

Drucker, D., Bocherens, H., Pike-Tay, A., & Mariotti, A. (2001). Isotopic tracking of seasonal dietary change in dentine collagen: Preliminary data from modern caribou. *Comptes Rendus de l'Académie Des Sciences - Series IIA - Earth and Planetary Science*, *333*(5), 303–309. https://doi.org/10.1016/S1251-8050(01)01640-8

Dunbar, J. S. (2016). *Paleoindian Societies of the Coastal Southeast*. University Press of Florida. http://ebookcentral.proquest.com/lib/ugalib/detail.action?docID=4529738

Emerson, T. E., Hedman, K. M., Simon, M. L., Fort, M. A., & Witt, K. E. (2020). Isotopic Confirmation of the Timing and Intensity of Maize Consumption in Greater Cahokia. *American Antiquity*, *85*(2), 241–262. https://doi.org/10.1017/aaq.2020.7

Fraser, D., Kim, S. L., Welker, J. M., & Clementz, M. T. (2021a). Pronghorn (Antilocapra americana) enamel phosphate δ18O values reflect climate seasonality: Implications for paleoclimate reconstruction. *Ecology and Evolution*, *11*(23), 17005–17021. https://doi.org/10.1002/ece3.8337

Fricke, H. C., Clyde, W. C., & O'Neil, J. R. (1998). *Intra-tooth variations in del18O (PO4) of mammalian tooth enamel as a record of seasonal variations in continental climate variables*.

Fricke, H. C., & O'Neil, J. R. (1996). Inter- and intra-tooth variation in the oxygen isotope composition of mammalian tooth enamel phosphate: Implications for palaeoclimatological and palaeobiological research. *Biogenic Phosphates as Palaeoenvironmental Indicators*, *126*(1), 91–99. https://doi.org/10.1016/S0031-0182(96)00072-7

Geist, V. (1998). *Deer of the world: Their evolution, behaviour, and ecology* (1st ed). Stackpole Books.

Gilbert, F. F. (1966). Aging White-Tailed Deer by Annuli in the Cementum of the First Incisor. *The Journal of Wildlife Management*, *30*(1), 200. https://doi.org/10.2307/3797906

Goodwin, D. H., Schone, B. R., & Dettman, D. L. (2003). Resolution and fidelity of oxygen isotopes as paleotemperature proxies in bivalve mollusk shells: models and observations. Palaios, 18(2), 110-125.

Griffith, G. E., Omernik, J. M., Comstock, J. A., Lawrence, S., Martin, G., Goddard, A., Hulcher, V. J., & Foster, T. (2001). *Ecoregions of Alabama and Georgia, (color poster with map, descriptive text, summary tables, and photographs)* [Map]. U.S. Geological Survey.

Grimm, E. C., Jacobson, G. L., Watts, W. A., Hansen, B. C. S., & Maasch, K. A. (1993). A 50,000-Year Record of Climate Oscillations from Florida and Its Temporal Correlation with the Heinrich Events. *Science*, *261*(5118), 198–200. https://doi.org/10.1126/science.261.5118.198

Harrison, R. G., & Katzenberg, M. A. (2003). Paleodiet studies using stable carbon isotopes from bone apatite and collagen: Examples from Southern Ontario and San Nicolas Island, California. *Journal of Anthropological Archaeology*, *22*(3), 227–244. https://doi.org/10.1016/S0278-4165(03)00037-0

Hesselton, W. T., & Hesselton, R. M. (1982). White-tailed deer. Wild Mammals of North America, 878-901.

Hillson, S. (2005). *Teeth*. Cambridge university press.

Holland-Lulewicz, I., & Thompson, V. D. (2021). Calusa socioecological histories and zooarchaeological indicators of environmental change during the Little Ice Age in southwestern Florida, USA. The Journal of Island and Coastal Archaeology, 1-37.

Hoppe, K. (2006). Correlation between the oxygen isotope ratio of North American bison teeth and local waters: Implication for paleoclimatic reconstructions. *Earth and Planetary Science Letters*, *244*(1–2), 408–417. https://doi.org/10.1016/j.epsl.2006.01.062

Hoppe, K. A., Amundson, R., Vavra, M., McClaran, M. P., & Anderson, D. L. (2004). Isotopic analysis of tooth enamel carbonate from modern North American feral horses: Implications for paleoenvironmental reconstructions. *Palaeogeography, Palaeoclimatology, Palaeoecology*, *203*(3), 299–311. https://doi.org/10.1016/S0031-0182(03)00688-6

Hughes, M. K. (2011). Dendroclimatology in High-Resolution Paleoclimatology. In M. K. Hughes, T. W. Swetnam, & H. F. Diaz (Eds.), *Dendroclimatology: Progress and Prospects* (pp. 17–34). Springer Netherlands. https://doi.org/10.1007/978-1-4020-5725-0_2

Hughes, M. K., & Diaz, H. F. (Eds.). (1994). *The Medieval Warm Period*. Springer Netherlands. https://doi.org/10.1007/978-94-011-1186-7

Jeffries, L. (1975). *Deer Stocking Program in Georgia 1928—1974. The History of the Georgia Deer Stocking Program*. Federal aid in wildlife restoration. State Game and Fish Commission.

Julien, M.-A., Bocherens, H., Burke, A., Drucker, D. G., Patou-Mathis, M., Krotova, O., & Péan, S. (2012). Were European steppe bison migratory? 18O, 13C and Sr intra-tooth isotopic variations applied to a palaeoethological reconstruction. *The Environment and Chronology of the Earliest Occupation of North-West Europe: Current Knowledge, Problems and New Research Directions*, *271*, 106–119. https://doi.org/10.1016/j.quaint.2012.06.011

Kay, M. (1974). Dental Annuli Age Determination on White-Tailed Deer From Archaeological Sites. *Plains Anthropologist*, *19*(65), 224–227. https://doi.org/10.1080/2052546.1974.11908678

Kellett, L. C., & Jones, E. E. (Eds.). (2017). *Settlement ecology of the ancient Americas*. Routledge, Taylor & Francis Group.

Kendall, C., Eriksen, A. M. H., Kontopoulos, I., Collins, M. J., & Turner-Walker, G. (2018). Diagenesis of archaeological bone and tooth. *Palaeogeography, Palaeoclimatology, Palaeoecology*, *491*, 21–37. https://doi.org/10.1016/j.palaeo.2017.11.041

Koch, P. L. (1994). Tracing the diets of fossil animals using stable isotopes. Stable isotopes in ecology and environmental science, 63-92.

Koch, P. L., Tuross, N., & Fogel, M. L. (1997). The effects of sample treatment and diagenesis on the isotopic integrity of carbonate in biogenic hydroxylapatite. Journal of Archaeological Science, 24(5), 417-429.

Koch, P. L. (1998). Isotopic Reconstruction of Past Continental Environments. *Annual Review of Earth and Planetary Sciences*, *26*(1), 573–613. https://doi.org/10.1146/annurev.earth.26.1.573

Koch, P. L., Tuross, N., & Fogel, M. L. (1997). The Effects of Sample Treatment and Diagenesis on the Isotopic Integrity of Carbonate in Biogenic Hydroxylapatite. *Journal of Archaeological Science*, *24*(5), 417–429. https://doi.org/10.1006/jasc.1996.0126

Kohn, M. J. (1996). Predicting animal δ18O: Accounting for diet and physiological adaptation. *Geochimica et Cosmochimica Acta*, *60*(23), 4811–4829. https://doi.org/10.1016/S0016-7037(96)00240-2

Kohn, M. J. (2004). Comment: Tooth enamel mineralization in ungulates: Implications for recovering a primary isotopic time-series, by BH Passey and TE Cerling (2002). *Geochimica et Cosmochimica Acta*, *68*(2), 403–405.

Thorp, J.L, & Van der Merwe, N.J. (1987). Carbon isotope analysis of fossil bone apatite. South African Journal of Science, 83(11), 712-715.

Lund, D. C., Lynch-Stieglitz, J., & Curry, W. B. (2006). Gulf Stream density structure and transport during the past millennium. *Nature*, *444*(7119), 601–604. https://doi.org/10.1038/nature05277

Luz, B., Kolodny, Y., & Horowitz, M. (1984). Fractionation of oxygen isotopes between mammalian bone-phosphate and environmental drinking water. *Geochimica et Cosmochimica Acta*, *48*(8), 1689–1693. https://doi.org/10.1016/0016-7037(84)90338-7

Malasek, T., Barding, E., Bender, M. J., Bonham, A., Mead, A. J., Pilgrim, Z., Powers, P., Patterson, J. R., & Patterson, D. B. (2023). Evaluating the fidelity of enamel isotopic data and environmental variation in paleoecological studies: A case study in wild, known-aged, modern white-tailed deer (Odocoileus virginianus). *Palaeogeography, Palaeoclimatology, Palaeoecology*, *622*, 111587. https://doi.org/10.1016/j.palaeo.2023.111587

Mann, M. E., Zhang, Z., Hughes, M. K., Bradley, R. S., Miller, S. K., Rutherford, S., & Ni, F. (2008). Proxy-based reconstructions of hemispheric and global surface temperature variations over the past two millennia. *Proceedings of the National Academy of Sciences*, *105*(36), 13252–13257. https://doi.org/10.1073/pnas.0805721105

Mann, M. E., Zhang, Z., Rutherford, S., Bradley, R. S., Hughes, M. K., Shindell, D., Ammann, C., Faluvegi, G., & Ni, F. (2009). Global Signatures and Dynamical Origins of the Little Ice Age and Medieval Climate Anomaly. *Science*, *326*(5957), 1256–1260. https://doi.org/10.1126/science.1177303

Martínez-Polanco, M. F., & Cooke, R. G. (2019). Zooarchaeological and taphonomical study of the white-tailed deer (Cervidae: Odocoileus virginianus Zimmerman 1780) at Sitio Sierra, a pre-Columbian village in Pacific Coclé province, Panama, with an evaluation of its role in feasts. *Archaeological and Anthropological Sciences*, *11*(10), 5405–5422. https://doi.org/10.1007/s12520-019-00883-8

Martínez-Polanco, M. F., Rivals, F., & Cooke, R. G. (2020). Behind white-tailed deer teeth: A micro- and mesowear analysis from three Panamanian pre-Columbian archaeological sites. *Quaternary International*, *557*, 70–79. https://doi.org/10.1016/j.quaint.2019.09.022

Mayewski, P. A., Rohling, E. E., Curt Stager, J., Karlén, W., Maasch, K. A., Meeker, L. D., Meyerson, E. A., Gasse, F., Van Kreveld, S., Holmgren, K., Lee-Thorp, J., Rosqvist, G., Rack, F., Staubwasser, M., Schneider, R. R., & Steig, E. J. (2004). Holocene climate variability. *Quaternary Research*, *62*(3), 243–255. https://doi.org/10.1016/j.yqres.2004.07.001

Medina-Elizalde, M., Perritano, S., DeCesare, M., Polanco-Martinez, J., Lases-Hernandez, F., Serrato-Marks, G., & McGee, D. (2022). Southeastern United States Hydroclimate During Holocene Abrupt Climate Events: Evidence From New Stalagmite Isotopic Records From Alabama. *Paleoceanography and Paleoclimatology*, *37*(2). https://doi.org/10.1029/2021PA004346

Meeks, S., & Anderson, D. (2013). Drought, Subsistence Stress, and Population Dynamics Assessing Mississippian Abandonment of the Vacant Quarter. In *Soils, Climate and Society: Archaeological Investigations in Ancient America* (pp. 61–83).

Menne, M. J., Durre, I., Korzeniewski, B., McNeill, S., Thomas, K., Yin, X., Anthony, S., Ray, R., Vose, R. S., Gleason, B. E., & Houston, T. G. (2012). *Global Historical Climatology Network—Daily (GHCN-Daily), Version 3* [Data set]. NOAA National Centers for Environmental Information. https://doi.org/10.7289/V5D21VHZ

Miller, H., Chenery, C., Lamb, A. L., Sloane, H., Carden, R. F., Atici, L., & Sykes, N. (2018). The relationship between the phosphate and structural carbonate fractionation of fallow

deer bioapatite in tooth enamel. *Rapid Communications in Mass Spectrometry*, *33*(2). https://doi.org/10.1002/rcm.8324

Morris, Z. H. (2015). Reconstructing subsistence practices of southwestern Ontario Late Woodland Peoples (AD 900-1600) using stable isotopic analyses of faunal material (Doctoral dissertation, The University of Western Ontario (Canada)).

Munro, L. E., Longstaffe, F. J., & White, C. D. (2008). Effects of heating on the carbon and oxygen-isotope compositions of structural carbonate in bioapatite from modern deer bone. *Palaeogeography, Palaeoclimatology, Palaeoecology*, *266*(3–4), 142–150. https://doi.org/10.1016/j.palaeo.2008.03.026

Napora, K. G., Jantzi, S. (2020). Five and a half millennia of environmental change on the Georgia Coast, USA: A tree-ring based analysis [Unpublished doctoral thesis]. University of Georgia.

Nesje, A., & Dahl, S. O. (2003). The 'Little Ice Age' – only temperature? *The Holocene*, *13*(1), 139–145. https://doi.org/10.1191/0959683603hl603fa

Noble, E. J., McManus, J. G., Mead, A. J., Mead, H., Seminack, C., Balco, W., Bennett, T., Crain, N. M., Duckworth, C., Malasek, T., Pearson, J. Z., Rhinehart, P., Ussery, M. E., Sun, Y., Patterson, J. R., & Patterson, D. B. (2020). Enamel isotopes reveal late Pleistocene ecosystem dynamics in southeastern North America. *Quaternary Science Reviews*, *236*, 106284. https://doi.org/10.1016/j.quascirev.2020.106284

Passey, B. H., & Cerling, T. (2002). Tooth enamel mineralization in ungulates: Implications for recovering a primary isotopic time-series. *Geochimica et Cosmochimica Acta*, *66*, 3225–3234. https://doi.org/10.1016/S0016-7037(02)00933-X

Pederzani, S., & Britton, K. (2019). Oxygen isotopes in bioarchaeology: Principles and applications, challenges and opportunities. *Earth-Science Reviews*, *188*, 77–107. https://doi.org/10.1016/j.earscirev.2018.11.005

Pellegrini, M., Donahue, R. E., Chenery, C., Evans, J., Lee-Thorp, J., Montgomery, J., & Mussi, M. (2008). Faunal migration in late-glacial central Italy: Implications for human resource exploitation. *Rapid Communications in Mass Spectrometry*, *22*(11), 1714–1726. https://doi.org/10.1002/rcm.3521

Peres, T. M. (2023). Garden Hunting and Food Sharing during the Mississippian Period in the American South. Food Provisioning in Complex Societies: Zooarchaeological Perspectives, 171.

Pilaar Birch, S. E., Miracle, P. T., Stevens, R. E., & O'Connell, T. C. (2016). Late Pleistocene/Early Holocene Migratory Behavior of Ungulates Using Isotopic Analysis of Tooth Enamel and Its Effects on Forager Mobility. *PLOS ONE*, *11*(6), e0155714. https://doi.org/10.1371/journal.pone.0155714

Pompeani, D. P., Bird, B. W., Wilson, J. J., Gilhooly, W. P., Hillman, A. L., Finkenbinder, M. S., & Abbott, M. B. (2021). Severe Little Ice Age drought in the midcontinental United States during the Mississippian abandonment of Cahokia. *Scientific Reports*, *11*(1), 13829. https://doi.org/10.1038/s41598-021-92900-x

Purdue, J. R. (1983). Methods of determining sex and body size in prehistoric samples of white-tailed deer (Odocoileus virginianus). *Transactions of the Illinois State Academy of Science*, *76*(3/4), p 351-357. ill.

Rees, J. W. (1969). Morphologic variation in the mandible of the white-tailed deer (Odocoileus virginianus): A study of populational skeletal variation by principal component and

canonical analyses. *Journal of Morphology*, *128*(1), 113–130. https://doi.org/10.1002/jmor.1051280106

Rees, J. W. (1971). Mandibular Variation with Sex and Age in White-Tailed Deer in Canada. *Journal of Mammalogy*, *52*(1), 223–226. https://doi.org/10.2307/1378456

Rivera-Araya, M., Emery, K. F., Arnauld, M. C., & Pilaar Birch, S. (2019). Stable isotope analysis of white-tailed deer teeth as a paleoenvironmental proxy at the Maya site of La Joyanca, northwestern Petén, Guatemala. *Isotopes in Environmental and Health Studies*, *55*(4), 344–365. https://doi.org/10.1080/10256016.2019.1636047

Rivera-Araya, M., & Pilaar Birch, S. (2018). Stable isotope signatures in white-tailed deer as a seasonal paleoenvironmental proxy: A case study from Georgia, United States. *Palaeogeography, Palaeoclimatology, Palaeoecology*, *505*, 53–62. https://doi.org/10.1016/j.palaeo.2018.05.025

Russell, D. A., Rich, F. J., Schneider, V., & Lynch-Stieglitz, J. (2009). A warm thermal enclave in the Late Pleistocene of the South-eastern United States. *Biological Reviews*, *84*(2), 173–202. https://doi.org/10.1111/j.1469-185X.2008.00069.x

Sauer, P. (1984). Physical Characteristics. In *White-tailed Deer, Ecology and Management* (pp. 73–90). Stackpole Books.

Scarry, C. M., & Scarry, J. F. (2005). Native American 'garden agriculture' in southeastern North America. *World Archaeology*, *37*(2), 259274 https://doi.org/10.1080/00438243500095199

Schultz, V., & Flyger, V. (1965). Relationship of Sex and Age to Strontium-90 Accumulation in White-Tailed Deer Mandibles. *The Journal of Wildlife Management*, *29*(1), 39–43. https://doi.org/10.2307/3798629

Severinghaus, C. W. (1949). Tooth Development and Wear as Criteria of Age in White-Tailed Deer. *The Journal of Wildlife Management*, *13*(2), 195. https://doi.org/10.2307/3796089

Smith, C. K., & McGrath, D. A. (2011). The Alteration of Soil Chemistry through Shell Deposition on a Georgia (U.S.A.) Barrier Island. *Journal of Coastal Research*, *27*(1), 103–109. https://doi.org/10.2112/JCOASTRES-D-09-00086.1

Smith, W. P. (1991). Odocoileus virginianus. *Mammalian Species*, *388*, 1–13. https://doi.org/10.2307/3504281

Sponheimer, M., & Lee-Thorp, J. A. (1999). Oxygen Isotopes in Enamel Carbonate and their Ecological Significance. *Journal of Archaeological Science*, *26*(6), 723–728. https://doi.org/10.1006/jasc.1998.0388

Stahle, D. W., & Cleaveland, M. K. (1994). Tree-Ring Reconstructed Rainfall Over the Southeastern U.S.A. During the Medieval Warm Period and Little Ice Age. *The Medieval Warm Period*, 199–212. https://doi.org/10.1007/978-94-011-1186-7_5

Sugiyama, N., Martínez-Polanco, M. F., France, C. A. M., & Cooke, R. G. (2020). Domesticated landscapes of the neotropics: Isotope signatures of human-animal relationships in pre-Columbian Panama. *Journal of Anthropological Archaeology*, *59*, 101195. https://doi.org/10.1016/j.jaa.2020.101195

Thompson, D. R. (1958). Field Techniques for Sexing and Aging Game Animals. *Wisconsin Conservation Department's Special Wildlife Report*, *no. 1*.

Thomson, M. T. (1960). *Streamflow Maps of Georgia's Major Rivers* [Information circular]. United States Geological Survey.

Van Der Merwe, N. J., & Vogel, J. C. (1978). ^{13}C Content of human collagen as a measure of prehistoric diet in woodland North America. *Nature*, *276*(5690), 815–816. https://doi.org/10.1038/276815a0

Williams, S. (1980). Armorel: A very late phase in the lower Mississippi valley. In *Southeastern Archaeological Conference Bulletin* (Vol. 22, pp. 105-110).

Willoughby, L. (2012). *Flowing Through Time: A History of the Lower Chattahoochee River*. University of Alabama Press.

Zazzo, A., Balasse, M., & Patterson, W. P. (2005). High-resolution $\delta^{13}C$ intratooth profiles in bovine enamel: Implications for mineralization pattern and isotopic attenuation. *Geochimica et Cosmochimica Acta*, *69*(14), 3631–3642. https://doi.org/10.1016/j.gca.2005.02.031

Zazzo, A., Lécuyer, C., Sheppard, S. M. F., Grandjean, P., & Mariotti, A. (2004a). Diagenesis and the reconstruction of paleoenvironments: A method to restore original $\delta^{18}O$ values of carbonate and phosphate from fossil tooth enamel. *Geochimica et Cosmochimica Acta*, *68*(10), 2245–2258. https://doi.org/10.1016/j.gca.2003.11.009

APPENDIX A: MODERN MANDIBLES


5
Jaw 5: L Buccal

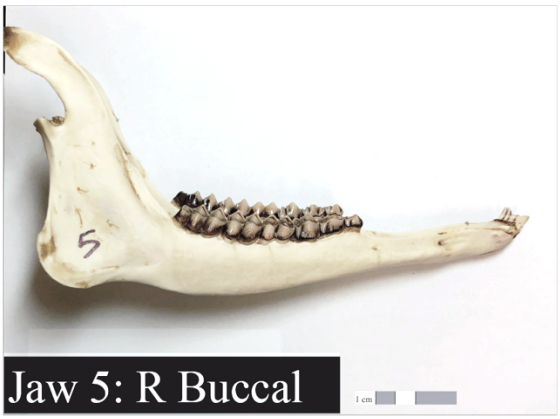
5
Jaw 5: R Buccal


Length: 21.6 cm
Jaw 5: Planview


6
Jaw 6: L Buccal


6
Jaw 6: R Buccal


Length: 20.8 cm
Jaw 6: Planview

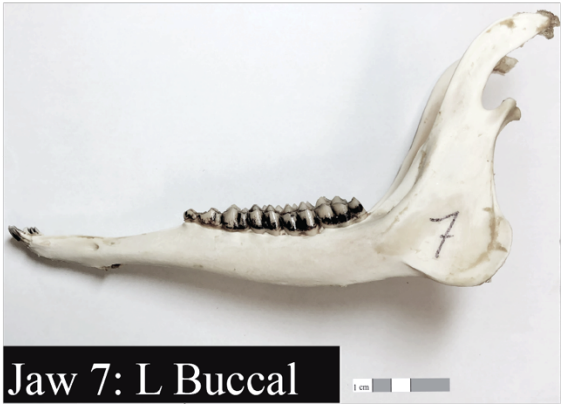
7
Jaw 7: L Buccal

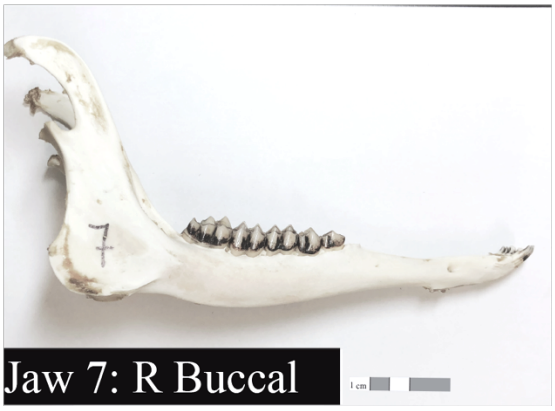
7
Jaw 7: R Buccal


Length: 21.8 cm
Jaw 7: Planview

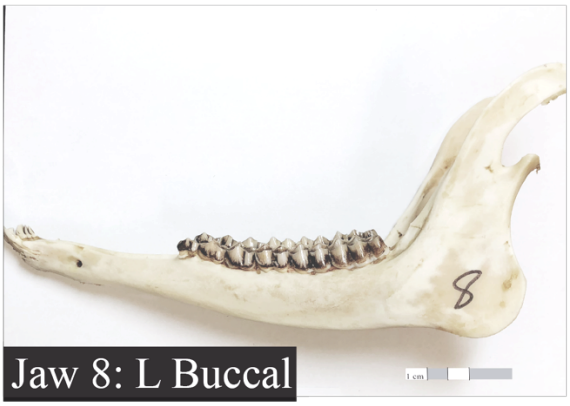
Jaw 8: L Buccal


Jaw 8: R Buccal


Length: 22.1 cm
Jaw 8: Planview


Jaw 9: L Buccal


Jaw 9: R Buccal


Length: 21.8 cm
Jaw 9: Planview

APPENDIX B : ARCHAEOLOGICAL TEETH, SINGER-MOYE - PRESAMPLING

SM1: top, lingual, buccal

SM2: top, lingual, buccal

SM3: top, lingual, buccal

SM4: top, lingual, buccal

SM5: top, lingual, buccal

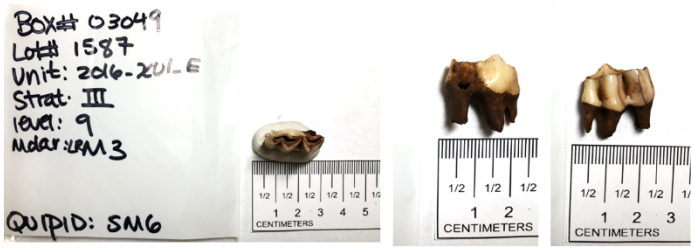

SM6: top, lingual, buccal

APPENDIX C : MODERN DEER M1 THIN SECTION FOR CEMENTUM ANNNULI ANALYSIS

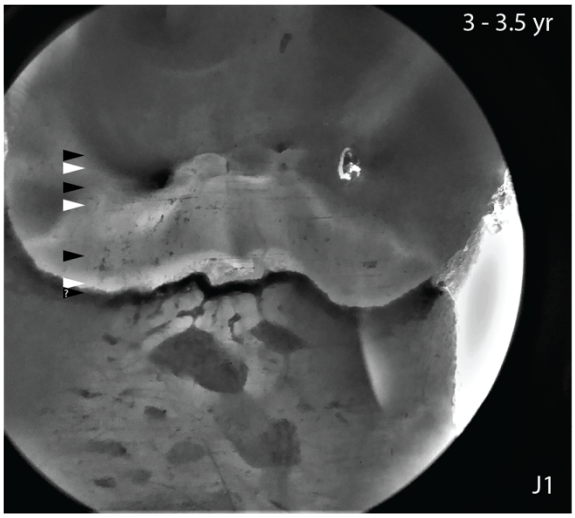

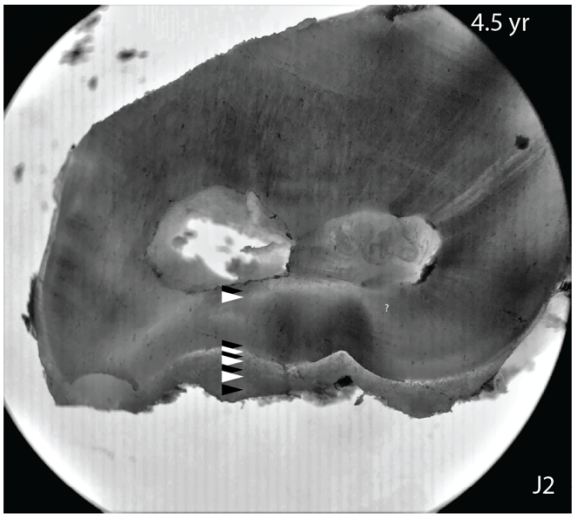

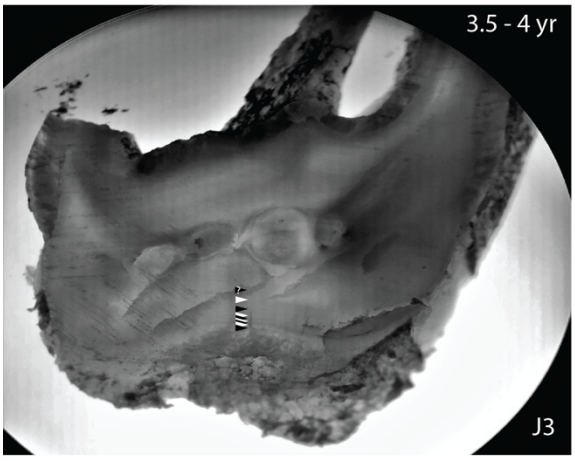

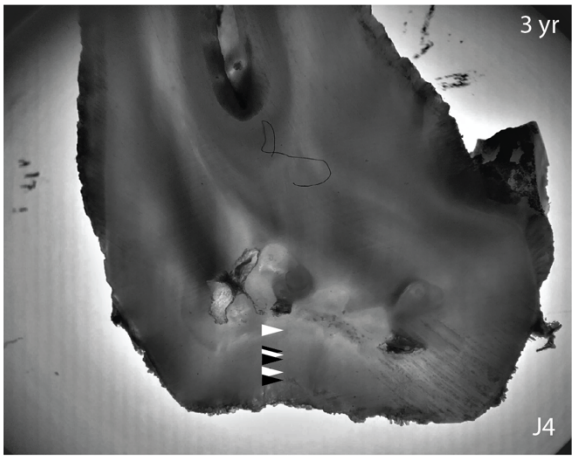

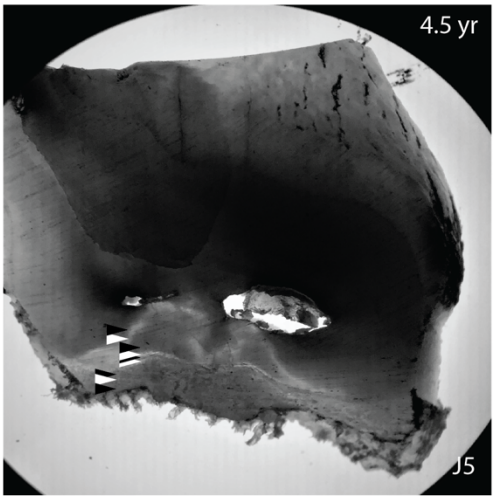

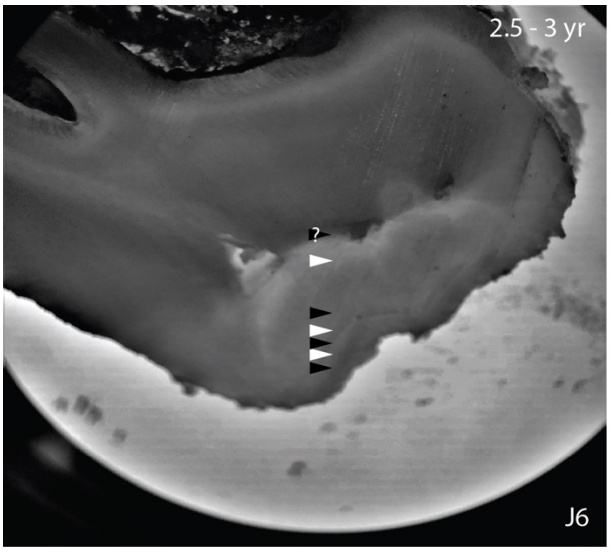
2.5 - 3 yr
J6

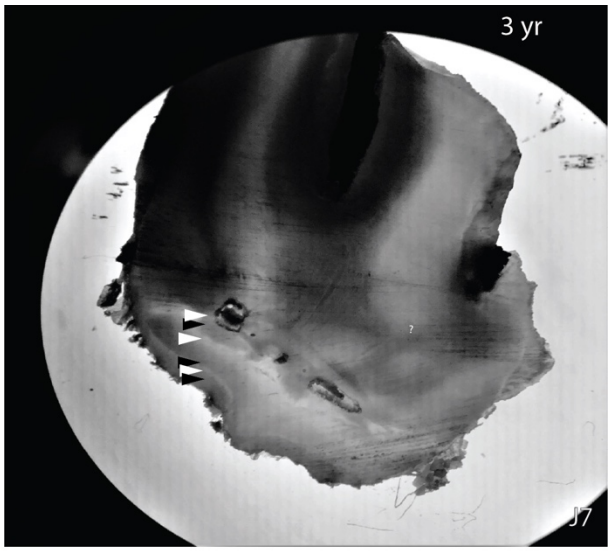
3 yr
J7

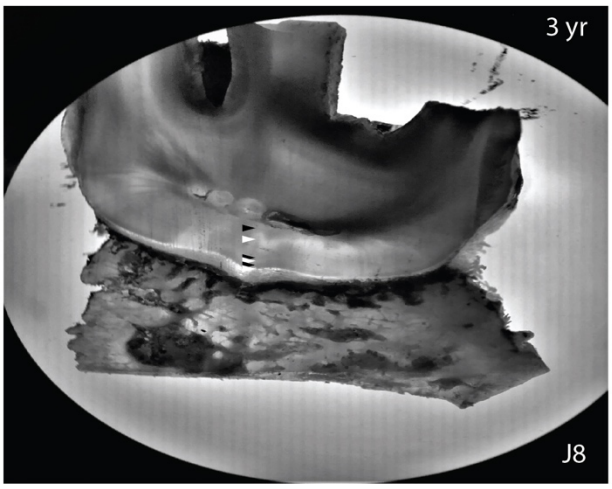
3 yr
J8

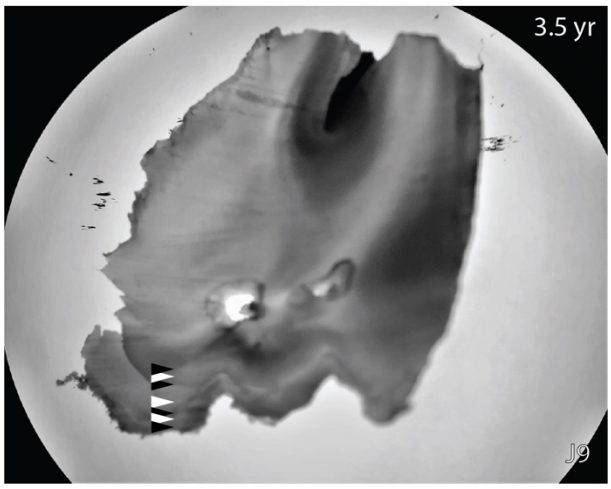
3.5 yr
J9